European Journal of Biomedical and Life Sciences

№ 4 2021

PREMIER Publishing

Vienna
2021

European Journal of Biomedical and Life Sciences

Scientific journal

№ 4 2021

ISSN 2310-5674

Proofreading Kristin Theissen
Cover design Andreas Vogel
Additional design Stephan Friedman
Editorial office Premier Publishing s.r.o.
Praha 8 – Karlín, Lyčkovo nám. 508/7, PSČ 18600
E-mail: pub@ppublishing.org
Homepage: ppublishing.org

European Journal of Biomedical and Life Sciences is an international, German/English/Russian language, peer-reviewed journal. It is published bimonthly with circulation of 1000 copies.

The decisive criterion for accepting a manuscript for publication is scientific quality. All research articles published in this journal have undergone a rigorous peer review. Based on initial screening by the editors, each paper is anonymized and reviewed by at least two anonymous referees. Recommending the articles for publishing, the reviewers confirm that in their opinion the submitted article contains important or new scientific results.

Premier Publishing s.r.o. is not responsible for the stylistic content of the article. The responsibility for the stylistic content lies on an author of an article.

Instructions for authors

Full instructions for manuscript preparation and submission can be found through the Premier Publishing s.r.o. home page at: http://www. ppublishing.org.

Material disclaimer

The opinions expressed in the conference proceedings do not necessarily reflect those of the Premier Publishing s.r.o., the editor, the editorial board, or the organization to which the authors are affiliated.

Premier Publishing s.r.o. is not responsible for the stylistic content of the article. The responsibility for the stylistic content lies on an author of an article.

Included to the open access repositories:

The journal has the GIF impact factor .562 for 2018.

Typeset in Berling by Ziegler Buchdruckerei, Linz, Austria.
Printed by Premier Publishing s.r.o., Vienna, Austria on acid-free paper.

Section 1. Clinical Medicine

https://doi.org/10.29013/ELBLS-21-4-3-7

Du Mingxin,
American Heritage School, FL, US
E-mail: pl250791@ahschool.com;
xxjnicole@hotmail.com

RECOVERY AMONG COVID-19 PATIENTS IN KOREA

Abstract

Aim: This study aimed to build a predictive model for the days for recovery among COVID-19 patients in Korea in 2020.

Method: A public data was used in this study. All the records were randomly assigned into 2 groups: training sample (50%) and testing sample (50%). A linear regression model was built to predict the Days for recovery in 2016 using the training sample and then was applied in the testing sample for performance assessment.

Results: The average days for recovery was 21.2 for the full sample, 21.4 in the training sample, and 21.1 in the testing sample.

According to the linear regression, age and month were significant for the recovery duration from COVID-19 in Korea in 2020.

Multiple R-squared was 0.04 and the adjusted R-squared was 0.03. The average mean squared error for the linear model in the testing sample was 66.9. The correlation between the predicted and the observed was 0.21. The min-max accuracy was 0.74. Mean absolute percentage deviation is 0.44.

Conclusions: In this study, we identified important of predictors for the days for recovery among COVID-19 patients in Korea in 2020, for example age and month.

Keywords: Covid19, recovery, linear regression, R-Square, predictive model.

1. Introduction

The World Health Organization (WHO) declared COVID-19 a pandemic on March 11, pointing to >118.000 cases of coronavirus pneumonia worldwide [1].

Among adults, the risk for severe illness from COVID-19 increases with age, with older adults at highest risk. Severe illness means that the person with COVID-19 may require hospitalization, intensive care, or a ventilator to help them breathe, or they may even die.

There are also other factors that can increase your risk for severe illness, such as having underlying medical conditions. By understanding the factors that put you at an increased risk, you can make decisions about what kind of precautions to take in your daily life [2].

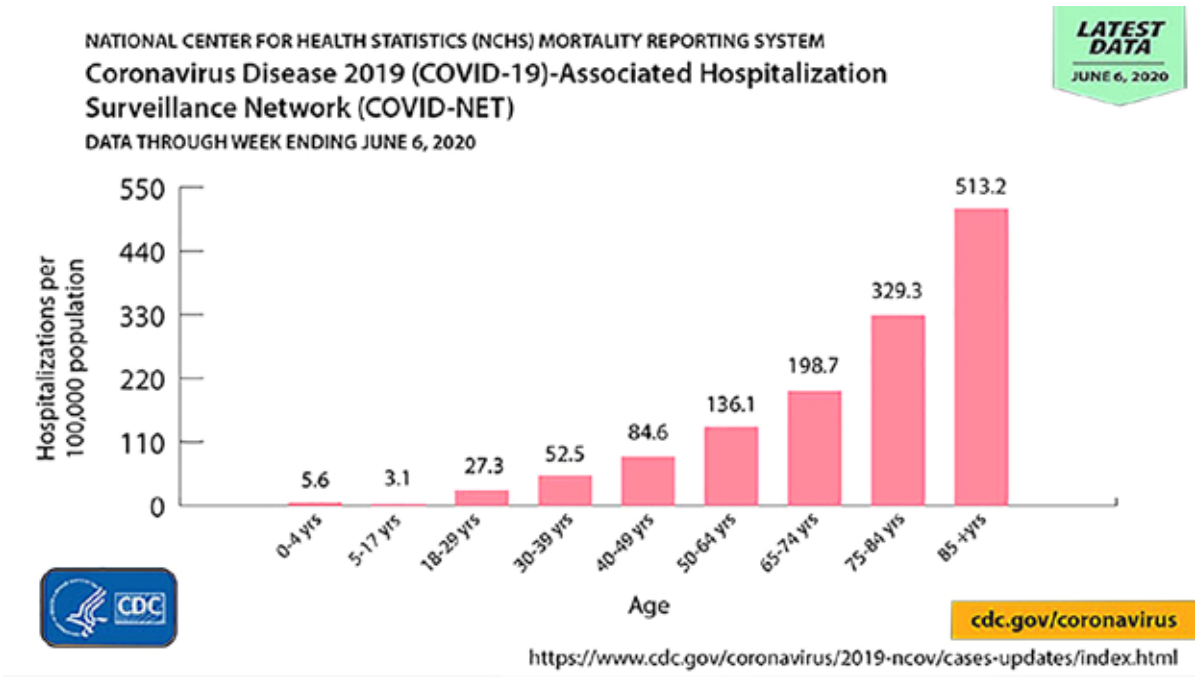

Korea's very effective model has been based on a "TRUST" strategy – an acronym for "Transparency, Robust screening and quarantine, Unique but universally applicable testing, Strict control, and Treatment." South Korea's ability to test, trace, and treat infected people has allowed the nation's leaders in Seoul to control the spread of the virus without imposing the aggressive lockdowns or complete travel bans that other countries have adopted [3].

This study aimed to build a predictive model for the days for recovery among COVID-19 patients in Korea in 2020.

2. Data and Methods:

Data

This dataset is public available for research.

All the records were randomly assigned into 2 groups: training sample (50%) and testing sample (50%).

R-squared is a statistical measure of how close the data are to the fitted regression line. It is also known as the coefficient of determination, or the coefficient of multiple determination for multiple regression. The definition of R-squared is fairly straight-forward; it is the percentage of the response variable variation that is explained by a linear model.

Or:

R-squared = Explained variation / Total variation

R-squared is always between 0 and 100%: 0% indicates that the model explains none of the variability of the response data around its mean. 100% indicates that the model explains all the variability of the response data around its mean.

Mean squared errors (MSE) were calculated and compared between both models. Min-Max Accuracy is defined as mean (min(actual, predicted)/ max(actual, predicted)). The mean absolute percentage error (MAPE), also known as mean absolute percentage deviation (MAPD), is a measure of prediction accuracy of a forecasting method in statistics, for example in trend estimation, also used as a loss function for regression problems in machine learning.

3. Results:

The random sample size is 469 in the testing sample and 468 in training sample, a total of 937 records.

The random sample size is 469 in the testing sample and 468 in training sample, a total of 937 records. The average days for recovery was 21.2 for the full sample, 21.4 in the training sample, and 21.1 in the testing sample.

Table 1.

	min	Q_1	Median	Mean	Q_3	Max
Full sample	0.0	15.0	20.0	21.2	26.0	50.0
Training sample	0.0	15.0	20.0	21.4	26.0	45.0
Testing sample	3.0	15.0	20.0	21.1	26.0	50.0

Figure 1 is to display the pattern of correlations in terms of their signs and magnitudes using visual thinning and correlation-based variable ordering. Moreover, the cells of the matrix can be shaded or colored to show the correlation value. The positive correlations are shown in blue, while the negative correlations are shown in red, the darker the hue, the greater the magnitude of the correlation.

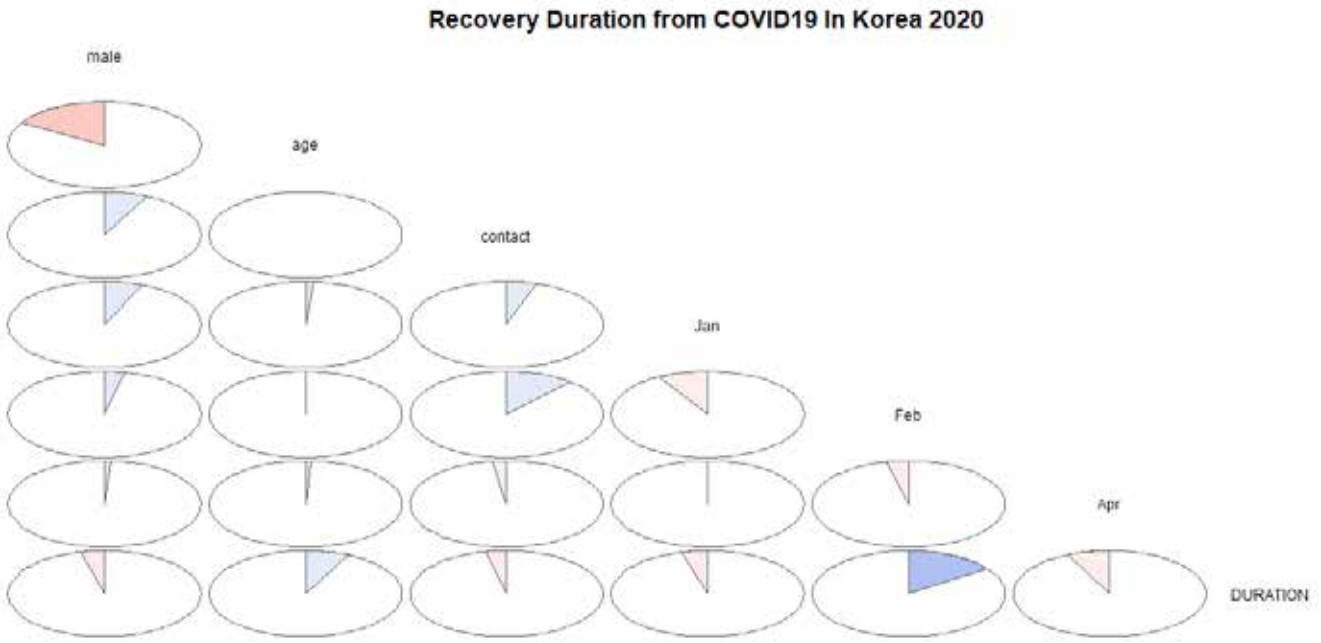

Figure 1. Pearson correlation coefficient across all the variables

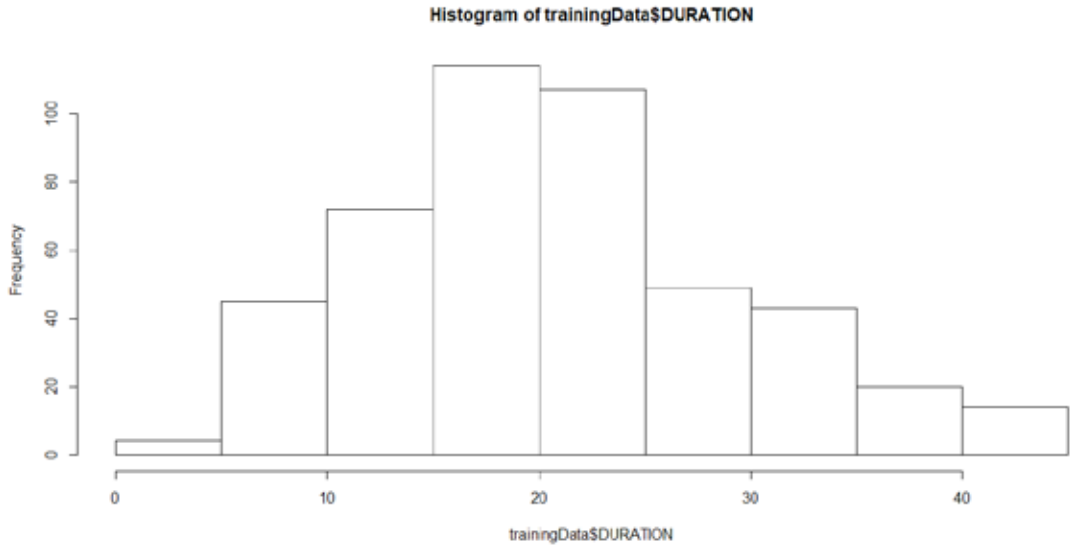

Figure 2. Distribution of Days for recovery in Training Sample

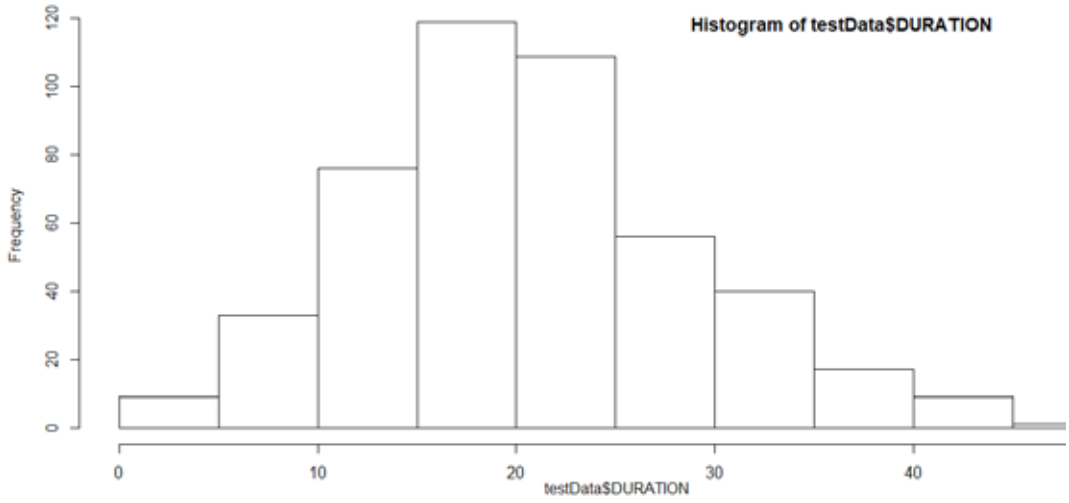

Figure 3. Distribution of Days for recovery in Test Sample

According to the linear regression, age, month were significant for the recovery duration from COVID-19 in Korea in 2020.

The age increases by 1 year, the duration of recovery increases by 0.03 days. Patients diagnosed in the Feb took 2.66 days longer to recover compared to patients diagnosed in March. Patients diagnosed in the April took 12.50 days shorter to recover compared to patients diagnosed in March.

Table 1.– Linear Regression to Predict Days for recovery

	Estimate	**Std. Error**	**t value**	**Pr(>|t|)**	
(Intercept)	19.232	0.803	23.940	< 2e-16	***
male	–0.470	0.574	–0.819	0.413	
age	0.032	0.015	2.145	0.032	*
contact	–1.055	0.687	–1.535	0.125	
Jan	–2.331	2.705	–0.862	0.389	
Feb	2.662	0.569	4.676	0.000	***
Apr	–12.501	5.984	–2.089	0.037	*

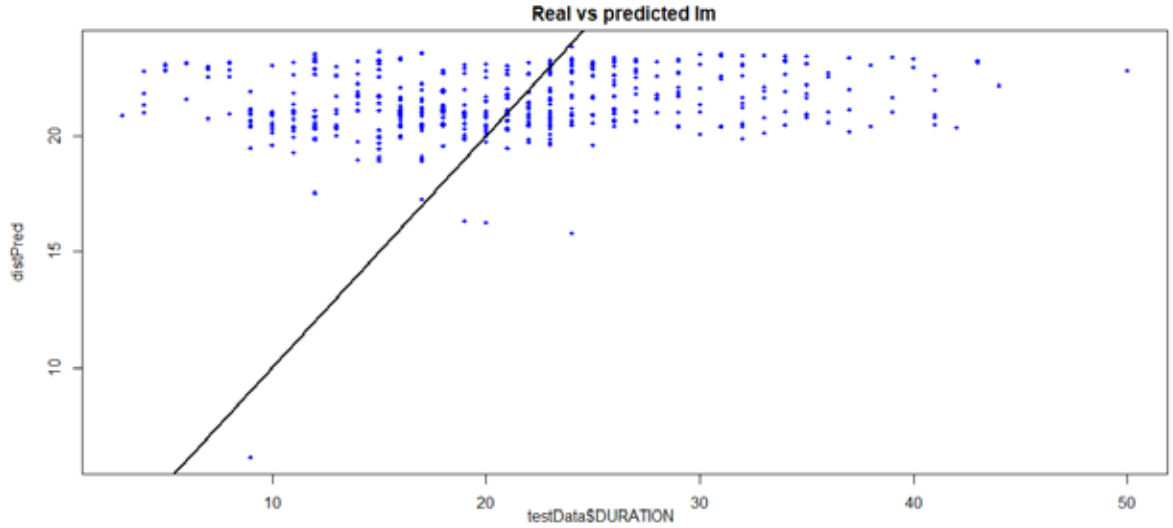

Figure 4. Predicted versus Observed Days for recovery

Multiple R-squared was 0.04 and the adjusted R-squared was 0.03. The average mean squared error for the linear model in the testing sample was 66.9. The correlation between the predicted and the observed was 0.21. The min-max accuracy was 0.74. Mean absolute percentage deviation is 0.44.

4. Discussion

The average days for recovery was 21.2 for the full sample, 21.4 in the training sample, and 21.1 in the testing sample.

According to the linear regression, age and month were significant for the recovery duration from COVID-19 in Korea in 2020. Multiple R-squared was 0.04 and the adjusted R-squared was 0.03. The average mean squared error for the linear model in the testing sample was 66.9. The correlation between the predicted and the observed was 0.21. The min-max accuracy was 0.74. Mean absolute percentage deviation is 0.44.

In another study, while men and women have the same prevalence, men with COVID-19 are more at risk for worse outcomes and death, independent of age. older age and a high number of comorbidities were associated with higher severity and mortality in patients with both COVID-19 and SARS. Age was comparable between men and women in all data sets. In the case series, however, men's cases tended to be more serious than women's (P = 0.035). In the public data set, the number of men who died from COVID-19 is 2.4 times that of women (70.3 vs. 29.7%, P = 0.016). In SARS patients, the gender role in mortality was also observed. The percentage of males were higher in the deceased group than in the survived group (P = 0.015) [4].

In this study, we identified important of predictors for the days for recovery among COVID-19 patients in Korea in 2020, for example age and month. It helps to predict the duration of recovery from COVID-19 and help predict the burden on health care system.

References:

1. WHO director-general's opening remarks at the media briefing on COVID-19. World Health Organization website. URL: https://www.who.int/dg/speeches/detail/who-director-general-s-opening-remarks-at-the-media-briefing-on-covid-19–11-march-2020/ Published March 11, 2020.
2. CDC. URL: https://www.cdc.gov/coronavirus/2019-ncov/need-extra-precautions/older-adults.html
3. South Korea's Success Against COVID-19. URL: https://www.theregreview.org/2020/05/14/oh-south-korea-success-against-covid-19
4. Gender Differences in Patients With COVID-19: Focus on Severity and Mortality. Front. Public Health, 29. April, 2020. URL: https://doi.org/10.3389/fpubh.2020.00152
5. Tabachnick B. and Fidell L. Using Multivariate Statistics (4th Ed.). Needham Heights, MA: Allyn & Bacon, 2001.
6. Stat Soft. Electronic Statistics Textbook. URL: http://www.statsoft.com/textbook/stathome.html.

https://doi.org/10.29013/ELBLS-21-4-8-11

Mabrouk Ben Othmen,
PhD student
Nechytailo Yuriy,
Professor, doctor of medical science
Bukovinian State Medical University, Chernivtsi, Ukraine
E-mail: nechitailo.yuri@bsmu.edu.ua

SOME INDICATORS OF CARDIOVASCULAR SYSTEM FUNCTIONS IN CHILDREN WITH ACUTE OBSTRUCTIVE BRONCHITIS

Abstract. The study includes assessment of cardiorespiratory data in children hospitalized with acute bronchitis with and without obstructive syndrome. In cases with bronchial obstruction decrease of blood pressure and signs of pulmonary hypertension observed.

Keywords: children, acute bronchitis, obstructive syndrome, blood pressure, echocardiography.

Introduction. Acute bronchitis (AB) is the leading types of respiratory tract pathology and hospitalization among children of all age worldwide. Among the diseases of the respiratory system, the incidence of AB in different countries reaches 20–28% [2]. In general, term of AB refers to a clinical syndrome characterized by the presence of cough, lower respiratory tract symptoms in the absence of acute pneumonia, bronchiolitis, chronic pathology or other established cause of cough [2, 8]. Bronchitis is not only the most common separate form of diseases of the lower respiratory tract but also it could be a part of the combined forms of pathology such as laryngotracheobronchitis and tracheobronchitis. In addition, bronchitis as a clinical syndrome is a component in bronchiolitis and pneumonia [4]. According to studies of etiological causes, bronchitis is mostly caused by viral agents such as influenza viruses, parainfluenza, adenoviruses, respiratory syncytial virus, coronaviruses and others [1, 3]. Bacterial flora, which can cause primary infection or be an agent of viral-bacterial inflammation, also plays a role in the etiological factors of acute bronchitis [6, 9].

Significant role in the pathogenesis and clinical picture of acute bronchitis played manifestation of bronchoobstruction, which depend on many factors, such as genetic predisposition, previous chronic diseases of the respiratory tract, etiology of disease, etc. [11]. Bronchial obstructive syndrome includes a number of pathogenic mechanisms – edema of the mucous membrane and submucosa, destruction of epithelial cells, impaired mucociliary clearance, accumulation of thick mucus, bronchial hyperreactivity and more.

Cardiovascular involvement in patients with respiratory diseases is well known and increased risk of severe complications and may be related to multiple pathophysiological factors including baseline compromised cardiorespiratory function, changed mechanisms of pulmonary regulation, ventilation-perfusion, pulmonary hypertension and myocardial dysfunction [5, 8]. The pandemic caused by coronavirus infection COVID-19 has completely transformed assessment of cardiac manifestations and related complications in respiratory pathology. In AB cases cardiovascular complications (arrhythmias, extreme bradycardia etc) reported in 1–5% and constitute the most common extrapulmonary manifestations [3]. Therefore, the cardiovascular evaluation of children with AB based mostly on the physical examination and it could be better assessed by other methods like echocardiography (ECHO). In adult

ECHO in many cases of pulmonary diseases shows increased pressure in the small circle of blood circulation, which is an important mechanism for changing the electromechanical activity of the myocardium, central and peripheral hemodynamics, diastolic function of the heart etc [7, 10]. But data regarding ultrasound cardiac imaging in children with AB have not yet been systematically collected.

The aim was to study circulation system disorders in children with obstructive and nonobstructive forms of AB.

Material and methods: In total 39 children aged 7–14 years (mean age 8.4 ± 0.53 years) hospitalized in a children's hospital with acute bronchitis were examined: 20 of them (first group) had obstructive syndrome and 19 (second group) without its signs. The study includes, except clinical features, assessment of nutrition, physical activity habits, anthropometric data, blood pressure measurement by oscilometric device, spirometry and pulse oximetry, ECHO. Statistical analysis conducted with program Statistica (StatSoft Inc.). Data were expressed as mean ± standard error for quantitative variables. All p-values were two-tailed and $p<0.05$ was considered statistically significant.

Results and discussion. The diagnosis of acute bronchitis was established on the basis of clinical and anamnestic data and laboratory parameters. X-ray examination of the chest was performed in only 3 children to exclude pneumonia. According to the degree of severity at hospitalization, the condition was moderate in 13 children (43.3%), severe – in 17 (56.7%). Due to the indicators of general clinical blood tests, a differential diagnosis was made between the viral and bacterial nature of the disease at the time of hospitalization. The presence of leukocytosis with a predominance of neutrophils and a shift of the leukocyte formula to the left, which indicated in favor of the bacterial nature of the disease, was in 12 children. In some children, this result was confirmed by determining the level of C-reactive protein and procalcitonin.

The heart rate (HR) at hospitalization was affected by body temperature, the degree of intoxication, the stage of gas exchange violation, the emotional reaction of the child. The average HR in the first group patients was 101.8 ± 3.54 beats/min, and in children of the second group – 92.1 ± 2.63 beats/min ($p <0.05$). At admission systolic blood pressure (SBP) in children of the first group was – 84.3 ± 1.6 mm Hg, in the second group SBP was higher – 90.6 ±1.5 mm Hg ($p<0.05$). Level of diastolic blood pressure (DBP) was nearly the same – in obstructive patients – 52.4 ± 0.9 mm Hg, in second group – 54.2 ± 0.9 mm Hg ($p > 0.05$). During first four days oxygen saturation and vital signs were measured intermittently at a frequency of every 4 hours during daytime. In children of the first group during pulse oximetry level of saturation was in range between 92–97%, in second – 95–98%.

On the 4-th day in the hospital, stabilization of the general condition, reduction of body temperature to normal values and lower level of intoxication were obtained. The level of HR in this period in children of the first group was 85.3 ± 0.78 beats/min, in children of the second group – 83.5 ± 0.78 beats/min ($p > > 0.05$). There were no significant difference in blood pressure level: in first group SBP – 93.1 ± 1.06 mm Hg, DBP – 57.1 ± 0.61, in second – SBP – 94.6 ± ± 1.5 mm Hg, DBP – 58.4 ±0.8 mm Hg.

The children of both group passed ECG recording and echocardiography. According to ECHO in children from the first group HR was 97.6 ± ± 4.37 beats/min (with range from 56 to 127), in persons from the second group HR was lower – 86.5 ± 2.65 beats/min (from 54 to 114 beats/min) ($p < < 0.05$). In the patients with AB without obstruction following ECHO results were registered: ejection fraction (EF) – 69.9 ± 1.25%, fractional shortening (FS) – 38.9 ± 1.0, end systolic volume (ESV) – 17.8 ± ± 1.23, end diastolic volume (EDV) – 53.5 ± 4.01, gradient of velocity on mitral valve (GVMV) – 3.5 ± ± 0.15, gradient of velocity on pulmonary valve (GVPV) – 3.6 ± 0.2, proportion GVPV/GVMV –

103.4 ± 5.79%. In the children from the first group with obstructive AB the data of ECHO was different: EF- 65.6±1.42%, FS – 39.2±1.72, ESV – 19.2 ± ± 1.55, EDV – 52.8 ± 2.59, GVMV – 3.6 ± 0.23, GVPV – 3.9 ± 0.32, GVPV/GVMV – 115.2 ± 13.0%. The last digit could be assessed as sign of pulmonary hypertension.

The duration of inpatient treatment in average was 7.4 ± 0.53 days with subsequent outpatient treatment and rehabilitation. Depending on the clinical manifestations and severity were used several groups of medications recommended by appropriate guidelines – antibiotics, suspected bacterial disease, antipyretics, antihistamines and corticosteroid hormones, mucolytic. The supplemental oxygen was not use. Correction of water-electrolyte metabolism disorders and measures to improve mucociliary clearance were also performed.

An important issue of our study is that systemic and pulmonary hemodynamics depend on the clinical course of acute bronchitis – with or without obstructive syndrome. It was established that in children with obstructive phenomena signs revealed specific changes in gradient of velocity on pulmonary valve as of pulmonary hypertension, which was associated with some decrease of systemic blood pressure and in gas exchange.

There are many publications about cardiovascular involvement in pathophysiology of such respiratory diseases as bronchial asthma, bronchiolitis and chronical obstructive bronchitis [8, 10]. In the situation of Coronavirus disease outbreak established influence of acute respiratory syndrome with pulmonary lesions on other organs, including heart with cardiovascular symptoms [3]. Therefore, the use of echocardiography, could be useful for assessing and monitoring cardiovascular complications in severe cases of obstructive bronchitis in children too.

Conclusion. Due to the close functional relationship between the respiratory and circulatory system, the course of obstructive bronchitis in children accompanied by changes in the cardiovascular system with hemodynamic disorders in the small circle of blood circulation and reducing of the gas exchange function.

Conflicts of interests: The authors declared no conflict of interest.

Refences:

1. Barssoum K., Victor V., Salem A., Kumar A. et al. Echocardiography, lung ultrasound, and cardiac magnetic resonance findings in COVID-19: A systematic review. Echocardiography. 2021. Aug; – 38(8).– P. 1365–1404.
2. Boldy D. A., Skidmore S. K., Ayres J. G. Acute bronchitis in the community: clinical features, infective factors, changes in pulmonary function and bronchial reactivity to histamine. Respir Med. 2008.– 84(5).– P. 377–385. Published online, 2008. Feb, 8. Doi: 10.1016/S0954-6111(08)80072-8
3. Cameli M., Pastore M. C., Aboumarie H. S., Mandoli G. E. et al. Usefulness of echocardiography to detect cardiac involvement in COVID-19 patients. Echocardiography. 2020.– 12 p. URL: http://10.1111/echo.14779. Doi: 10.1111/echo.14779
4. Karunanayake C. P., Rennie D. C., Ramsden V. A. et al. The first nations lung health project research team bronchitis and its associated risk factors in first nations children. Children (Basel) 2017. Dec; – 4(12).– 103 p. Doi: 10.3390/children4120103
5. Monahan K., Lenihan M., Brittain E., Saliba L. et al. The relationship between pulmonary artery wedge pressure and pulmonary blood volume derived from contrast-echocardiography: a proof-of-concept study. Echocardiography. 2018. Sep.– 35(9).– P. 1266–1270. Published online 2018. May 14. Doi: 10.1111/echo.14023

6. Park J. Y., Park S., Lee S. H. et al. Microorganisms causing community-acquired acute bronchitis: the role of bacterial infection. PLoS One. 2016.– 11(10).– e0165553. Doi: 10.1371/journal.pone.0165553
7. Schneider M., Ran H., Pistritto A. M., Gerges C. et al. Pulmonary artery to ascending aorta ratio by echocardiography: A strong predictor for presence and severity of pulmonary hypertension. PLoS One. 2020.– 15(7).– e0235716. Doi: 10.1371/journal.pone.0235716
8. Kimura D., McNamara I.F., Wang J., Fowke J. H. et al. Pulmonary hypertension during respiratory syncytial virus bronchiolitis: a risk factor for severity of illness. Cardiol Young. 2019. May.– 29(5).– P. 615–619. Doi:10.1017/S1047951119000313.
9. Smith S. M., Fahey T., Smucny J., Becker L. A. Cochrane Acute Respiratory Infections Group. Antibiotics for acute bronchitis. Cochrane Database Syst Rev. 2017.– 6. CD000245. Doi: 10.1002/14651858. CD000245.pub4
10. Sobolev V. A. (Specific features of intracardiac relationships according to echocardiographic data in patients with obstructive or restrictive ventilation disorders). Ter Arkh. 2002.– 74(12).– P. 60–3. Russian. PMID: 12577844.
11. Sullivan M. J., Phung T-K.N., Park J-A. Bronchoconstriction: a potential missing link in airway remodelling. Open Biol. 2020.–10. 2002.– 54 p. URL: http://dx.doi.org/10.1098/rsob.200254

https://doi.org/10.29013/ELBLS-21-4-12-14

Badashkeev Mikhail Valeryevich,
candidate of pedagogical sciences, psychologist
OGBUZ "Bokhansky RB"
E-mail: badashkeevm@mail.ru
Shoboev Andrey Eduardovich,
neurologist, OGBUZ "Bokhansky RB"
E-mail: shoboev.87@mail.ru

POST STROKE REHABILITATION: NEUROPLASTICITY PROCESSES IN RECOVERY TREATMENT AFTER ISCHEMIC STROKE

Abstract. This article discusses various aspects of neuroplasticity in patients who have undergone ischemic stroke; we attribute the dynamics and ambiguity of this process to certain features. We emphasize the process of dynamism, its ambiguity of involving the structures of the opposite hemisphere of the brain in the process of recovery. Terms from the moment of stroke and activation of various parts of the brain in the post-stroke period are considered. The authors pay attention to neurorehabilitation and a multidisciplinary approach in the restorative treatment of patients who have undergone ischemic stroke. It is also noted that rehabilitation measures should be started in the early period of stroke, immediately after confirming this diagnosis and stabilizing the condition of the patient.

Keywords: ischemic stroke, functional recovery, acute cerebral circulation disorder, post-stroke rehabilitation, neuroplasticity, neurorehabilitation.

The problem of ischemic strokes today is global for medical and social services, this problem is more associated with a high percentage of disability, and complete social maladaptation of patients. There are 16 million cases of cerebral circulation disorders (hereinafter, MMC) in the world every year, with an average of 70–75% of patients showing residual events. Often, even with intensive treatment using a full range of rehabilitation measures, 30–40% of patients have low dynamics, which certainly leads to incapacity, therefore, a person becomes disabled for 40–50 years.

In recent decades, ideas about the neurofunctional features of the CNS have been rapidly changing. According to the electronic database PubMed, the number of publications devoted to this problem is growing exponentially. Until 1990, 2 works were published, from 1990 to 2000–43, and over the next 10 years – more than 600 publications [5, 134–143].

For the first time, the concept of plasticity of the nervous system was introduced by A. Bethe when he described the operation to suture the tendon of the wrist flexor with the peripheral ends of the paralyzed extensor of the fingers, i.e. two parts of one split muscle, usually functioning as a whole, were given two antagonistic purposes. By the plasticity of the nervous system, the author understood its adaptability to changed conditions due to a change in peripheral afferentization [4, 82–93].

Well-planned rehabilitation measures are important in the management of patients after a stroke. They can be of varying degrees effective for 80% of

patients after PMC, 10% have complete spontaneous recovery of impaired functions, and only 10% of patients have rehabilitation measures that are unpromising [6]. The concept of neuroplasticity plays a key role in the rehabilitation of patients with neurological diseases. Various methods and technologies of restorative treatment are based on knowledge about mechanisms and processes of plastic restructuring [7; 8]. Experimental studies of recent years have made it possible to postulate one of the important principles of the biological phenomenon of neuroplasticity, which is subsequently actively used in determining the program of rehabilitation treatment of patients with diseases of the central nervous system (CNS): the emergence, existence and effective use of neuronal connections directly depend on their functional activity [9].

Thus, the concept of neuroprotection involves the continuous adaptation of a neuron to new functional conditions, which is the sum of all mechanisms directed against damaging factors. These processes are regulated by hormones, neurotrophic growth factor (BDNF), neurotransmitters, cytokines, electrophysiological activity, stress, etc. An example of neuroplasticity in early ontogenesis is the fact that in children under 10 years of age the dominant hemisphere (in 85% of cases) in the formation of speech and figurative functions is the right hemisphere, and later these functions go to the left [6].

Thus, in the process of ontogenesis, not only the structure of mental functions changes, but also their anatomical organization. At the same time, if normal lateralization is disrupted when one of the hemispheres is affected, then the speech function moves to a healthy hemisphere, which becomes dominant in verbal function. In adults, an example of neuroplasticity is an increase in certain brain structures associated with professional activities. In professional translators, this is an increase in the left temporal lobe, in musicians – the primary motor zone, the temporal lobe and the anterior part of the corpus call sum, in taxi drivers whose professional activities are associated with spatial orientation, the size of the hippocampus. It was established that neuronal plasticity is accompanied by changes in the structure of astroglia and astrocytes, an increase in contact zones between astrocytes and synapses, an increase in the number and area of dendrite processes, an increase in the number of synapses, in addition, it is accompanied by other activating effects both in nervous and glial tissues [6].

We, in turn, put hope in the neuroplasticity of the brain, which is critical for functional recovery and therefore a significant reduction in disability. In general, by neuroplasticity, we mean a certain ability of the cells of the nervous system to regenerate anatomically and functionally change. At the same time, neuroplasticity processes are associated not only with the neurons themselves, but also qualitative, quantitative changes in neuronal connections and glial elements, the development of new sensorimotor pathways and integrations in the central nervous system in the recovery period of treatment [1; 2].

In our particular case, Citicolin plays an important role due to good tolerability and combinability, as well as neuroprotective exposure. In earlier scientific papers, we described a combined combination of Citicolin and Cortexin, which undoubtedly gave positive dynamics to the process of functional recovery after ischemic stroke [3]. In this study with Citikolin monotherapy, we observed the following pattern: all patients tolerated Citikolin well, all patients showed positive dynamics. That, in principle, is confirmed by other researchers on this issue [8, 1390].

Thus, the use of knowledge of the features of neuroplasticity leads to a significant effectiveness of rehabilitation therapy during the recovery period. The determining factor is the integrity of the white matter or damage to the descending motor pathways, and not the motor cortex itself, since no significant dynamics were observed when the motor cortex sections were affected. Which in principle indicates a sufficiently high neuroplastic potential of white matter of the conducting structures of the

CNS even with severe damage compared to large cortical lesions, and the prognostic significance of the functional activity of the corticospinal tract for subsequent recovery of post-stroke deficiency.

References:

1. Badashkeev M. V. Neuroplasticity processes in the recovery period after ischemic stroke // mat. междунар. науч.– prakt.konf. "Breakthrough Research: Challenges, Limits and Opportunities" / Rev. ed. A. A. Sukiasyan.– Voronezh, 2020.– P. 264–265.
2. Badashkeev M. V. Neuroplasticity as the basis for recovery from ischemic stroke // mat. междунар. науч.– prakt.konf. "The development of integration processes as a goal and condition for increasing the competitiveness of science" / otv. ed. A. A. Sukiasyan – Orenburg, 2020.– P. 172–175.
3. Badashkeev M. V. Combined neuroprotection in recovery cognitive functions // Materials in the International Scientific Conference "Science and innovations 2021: development directions and priorities" / "Auspublishers" publishing house – Australia, Melbourne. 2021.– P. 186–189.
4. Bethe A. Plasticity (adaptability) of the nervous system // journal. The successes of modern psychology.– T. 3.– No. 1. 1934.– P. 82–93.
5. Galanin I. V., Naryshkin A. G., Gorelik A. L., Tabulina S. D., Mikhailov V. A., Skormets T. A., Lobzin S. V. Current state of the problem of neuroplasticity in psychiatry and neurology // Bulletin of the Northwest State Medical University named after I.I.– Vol. 7.– No. 1. 2015.– P. 134–143.
6. Damulin I. V., Ekusheva E. V. Clinical significance of the phenomenon of neuroplasticity in ischemic stroke. Annals of Clinical and Experimental Neurology.– No. 10(1). 2016.– P. 57–64.
7. Yekusheva E. V. Sensomotor integration in central nervous system damage clinical and pathogenetic aspects. Autoreferat diss. Doc. honey. sciences.– Moscow, 2016.– 48 p.
8. Kadykov A. S., Shakhparonova N. V. Rehabilitation after a stroke. Russian Medical Journal – Moscow,– No. 11(25). 2003.– 1390 p.
9. Wasaka T., Kakigi R. Sensorimotor Integration. In: Magneto encephalography. From signals to dynamic cortical networks. Eds. S. Supek, C. J. Aine / Berlin, Heidelberg: Springer-Verlag, 2014.– P. 727–42.

Section 2. Life Sciences

https://doi.org/10.29013/ELBLS-21-4-15-26

Zixi Gao,
The experimental high school
attached to Beijing Normal University, Beijing, China
E-mail: 1193004899@qq.com

SYSTEMATIC ANALYSIS OF TRPM8'S POLYMORPHISM AND THE PREDICTION OF ITS ASSOCIATION WITH DISEASES

Abstract

Introduction: TRPM8, Transient Receptor Potential Cation Channel Subfamily M Member 8, is located on the chromosome 2. TRPM8 is known for its ability to sense cold temperature or other cooling agents at the body level, including menthol, icilin, cold temperature. At the cellular level, TRPM8 is the non-selective cation channel that can control the movement of calcium ions. There has been enough research investigating TRPM8's function as a sensitive temperature receptor, but seldom research has examined its polymorphism and amino acids change.

Objective: Since TRPM8's SNPs (Single Nucleotide Polymorphisms) have not been fully analyzed, we hope to systematically identify and verify the SNPs that affect TRPM8's transmembrane structure and function, so that the polymorphism of the TRPM8 gene can be mapped to the changes in the structure and function of the protein it encodes. Also, we aim to use SNPs to investigate the relationship between TRPM8 and several diseases.

Methods: The dbSNP database is first used to download all SNPs of TRPM8, and wANNOVAR is used later to do the annotation. Then all SNPs are gathered, and Uniprot is used to find their corresponding exon and amino acids. The aforementioned steps are used to investigate TRPM8 systematically. In terms of pathological research, by setting the p-value at 0.01 as our filter condition, we use GWAS (Genome-Wide Association Study) Central to find the connection between TRPM8 and diseases. Ultimately, UCSC Genome Browser, UCSC Cell Browser, and Gene Expression Omnibus are used to verify the connection.

Results: There are, in general, 870 exonic nonsynonymous SNPs, which is 62.77% of all SNPs. At the amino acid level, 70 of the transmembrane amino acids can be affected by exonic SNPs. Among the 70 SNPs found related to amino acids, 34 of them are dangerous SNPs, making these dangerous SNPs potential, pathogenic sites. Interestingly, 61 intronic SNPs of TRPM8 are found related to diseases, such as monoclonal gammopathy, epilepsy, and so on. when the p-value is smaller than or equal to 0.0001, two intronic SNPs including rs11563199 and rs17869077 are related to psychiatric disorders. The upregulation of TRPM8 when psychiatric disorders occur was also investigated to try

to explain the possible mechanism. This connection is first discovered, suggesting an important role of TRPM8 as a possible biological marker of psychiatric disorders.

Keywords: TRPM8, SNP, non-selective cation channel, psychiatric disorders.

Introduction

TRPM8 is the last member of TRP's largest subfamily. TRPM8 mostly permeates calcium ions and is crucial in maintaining calcium homeostasis. All TRPM8, known for sensing cold, exists in a wide range of animals, including chicken, mouse, lizard, and human, showing its early existence.

As a transmembrane protein, TRPM8 serves to non-selectively transport cations, especially calcium ions. When activated by cooling agents, like menthol, or cold temperature, TRPM8 shows strong outward rectification and generates more negative electronic potential, so that depolarization occurs and increases the possibility of opening the TRPM8 cation channel (1–3). In addition to cold and menthol, TRPM8 is sensitive to voltage and phosphatidylinositol-4,5-biphosphate (PIP2) which hydrolysis can make TRPM8 desensitize [4].

Since TRPM8 can sense cold, it is widely distributed in the sensory neurons of the trigeminal ganglion and the dorsal root. Both the cold temperature and cooling agents, including menthol, can switch the activation curve to physiological membrane potentials while TRPM8 is activated [5]. N-Glycosylation is used to modulate TRPM8's sensitivity to cold temperature and cooling agents, and the loss of N-Glycosylation may reduce TRPM8 sensitivity [6].

In addition to sensory neurons, TRPM8 also exists in the prostate, testis, heart, taste papillae, human lung epithelial cells, and other sites [7; 8; 9]. Since TRPM8 is widely distributed in the prostate cell, the relationship between TRPM8 and the cancer is widely investigated. Past research showed that, compared to normal prostate cell, in the prostate cancer cell, TRPM8, served as the calcium cation channel, will decide oncogenic status, dependent calcium ions signatures, that is important in prostate cell proliferation and apoptosis. TRPM8's expression will increase in cancerous human prostate tissue, and decrease in cancerous human prostate [9]. There is also research showing TRPM8's existence in the bladder: TRPM8's agonists, including menthol, can activate TRPM8, and reduce the interval of micturition, and vice versa [10]. Except for prostate cancer, TRPM8 is also believed as the therapeutic target of migraine. Existing research showed that one of the TRPM8 nonsynonymous SNPs, rs10166942, can lower the risk of suffering from migraines. Having depression or anxiety disorder could lead to a higher risk of having a severe migraine. Although rs10166942's SNPs is related to migraine, the possibility of using TPRM8 agonists or antagonists as treating migraine still needs more investigation [11].

Past research analyzed how TRPM8 can sense cold from either the angle of SNP or amino acids, but none of them have compared and examined both in order to reach a more continuous and comprehensive level. Also, very little research has used TRPM8 SNPs to try to explain certain, relating diseases. Therefore, our goal is to 1) annotate all possible exonic, nonsynonymous SNPs change and all pathogenic SNPs systematically, 2) identify the corresponding amino acids in relation to exonic nonsynonymous SNPs, 3) predict and analyze certain pathogenic SNPs or amino acids that can lead to certain diseases and try to explain the process and outcome.

Methods

SNP analysis

SNPs extraction

The dbSNP database (https://www.ncbi.nlm.nih.gov/snp/), which is a system used to store and analyze biology, especially molecular biology, genetics, and others. It is also used to help scientists investigating the structure and function of molecules online, instead of doing experiments themselves [12]. This website has been used to

extract all TRPM8 SNPs. The data was saved as a VCF file.

SNP annotation and classification

We use wANNOVAR (https://wannovar.wglab.org) to annotate all TRPM8 SNPs, including the starting and ending point; the original and changeable nucleotide of SNPs; SNP's location: exonic, intronic, 5'-UTR region (UTR represents for untranslated region), 3'-UTR region, upstream, downstream, splicing site, intergenic region; SNPs type (synonymous, nonsynonymous, frameshift, etc.); and so on.

Amino acids analysis

Identify exons and amino acids affected by TRPM8 SNPs

By using data from Uniprot, a database containing a protein's size, function, changes in amino acids, protein subcellular localization in a cell, and other annotated data related to protein. We used the the reference mRNA transcript ENST00000324695 to show TRPM8 gene structure. Then we generate and analyzes figures of place these amino acids locate.

Relating diseases analysis

Identify certain diseases connected with TRPM8 SNPs

By using GWAS Central database (https://www.gwascentral.org/), a database including the experiments related to a certain gene, always about a gene's location (mainly from SNP sites) related to certain diseases, we obtain TRPM8's relating diseases. First search the keyword, 'TRPM8', and then set the p-value equal to or smaller than 0.01, because we aim to identify diseases that show quite a strong relation with TRPM8. Then databases of certain diseases are compared to TRPM8 genome annotation in order to find out TRPM8 SNPs in those diseases.

The connection between TRPM8 and diseases

UCSC cell browser (https://cells.ucsc.edu) was used to examine TRPM8's expression at single cell level in body organs of patients compared with TRPM8 expression in organs of normal people. In addition, data sets related to differential TRPM8 in normal human and patient tissues were downloaded from Gene Expression Omnibus (GEO) database (https://www.ncbi.nlm.nih.gov/geo/) in order to show TRPM8 expression upregulation or downregulation is related to diseases found by GWAS.

Results

TRPM8 function and distribution

TRPM8 appears in many body organs, including the brain, prostate, the trigeminal ganglion dorsal root. The Figure down below, shows TRPM8 distribution in cell and body. TRPM8 is in the dorsal root and trigeminal ganglion to carry out its function: while depolarization, sensing cold to change its activation curve to control calcium influx.

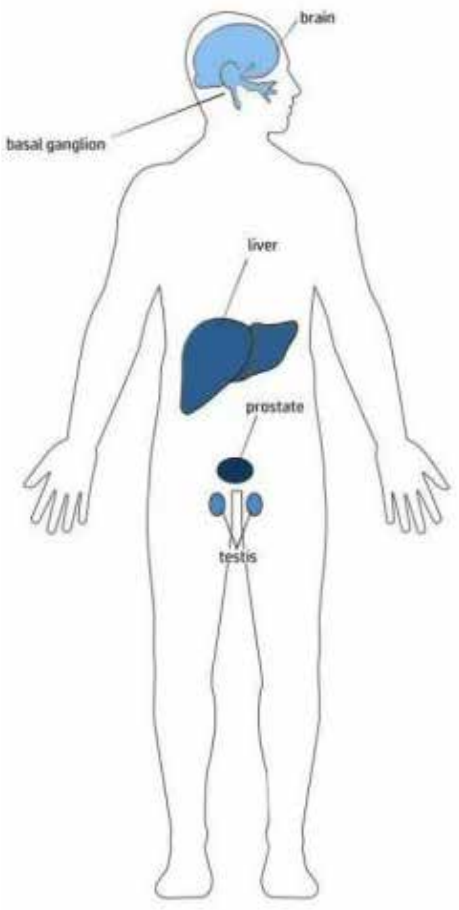

Figure 1. TRPM8 distribution in the human body. In the figure, TRPM8 is widely distributed in the nervous system, reproductive system, and digestive system, which corresponds to the human brain, basal ganglion, prostate, and testis. The data is downloaded from Cell expression Atlas

The identification and categorization of TRPM8 SNPs

SNPs are nucleotide changing on one single locus, and the rate is at least one percent among all human populations. TRPM8 has 102,181 bases, 22.404 of which are SNPs. A part of this research focused on investigating analyzing TRPM8 SNPs and their relation with exons and amino acids.

Among all 22.404 SNPs, this part of the research focuses more on the 1.386 exonic SNPs and 18.225 intronic SNPs located on the coding region. Only 402 are synonymous SNPs, SNPs that can change their nucleotide but do not affect amino acids' type, in these 1386 SNPs (Figure 2). Among all, nonsynonymous SNPs account for the highest portion, reaching 62.77%, meaning over half of the exonic SNPs in the coding region can affect TRPM8 gene coding the protein.

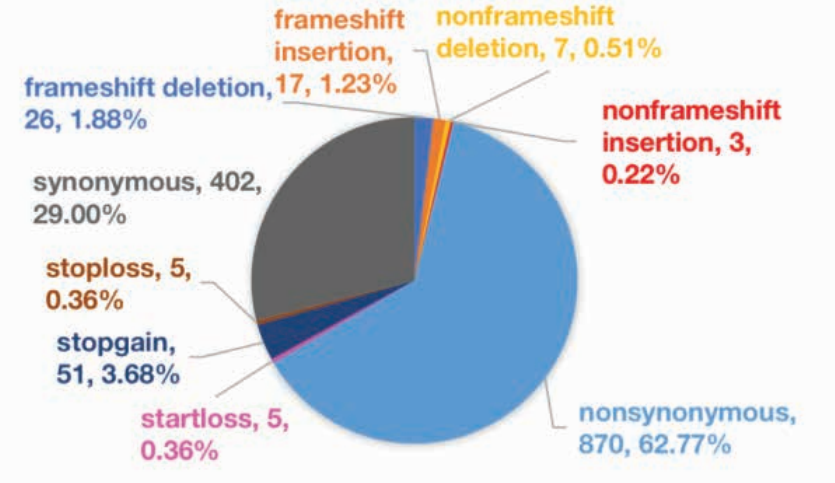

Figure 2. TRPM8 exonic SNPs classification. In the figure, take 'nonsynonymous, 870, 62.77%' as an example. 'nonsynonymous' represents the type of SNP, '870' represents the number of SNPs, and '62.77%' represents the ratio of the specific type of SNPs to all SNPs. As can be seen from the figure, only 29% of exonic SNPs are synonymous SNPs. Nonsynonymous SNPs are the most common SNPs among all exonic SNPs, with the ratio reaching 62.77%

TRPM8 exons and amino acids' relation with its functions

Another part is to find changeable exons and the corresponding region in TRPM8's transmembrane region. First, I divide the SNPs into 21% synonymous SNPs, 62.77% nonsynonymous SNPs, and 8.23% other SNPs. In 8.23% of all other SNPs, there is three nonframeshift insertion; five startloss SNPs that cause changes on exon 1, exon 2, exon 3; five stoploss SNPs which change on exon 9; seven nonframeshift deletion; seventeen frameshift insertion that change exon 1 to exon 10; 26 frameshift deletion that mianly focus on exon9, 17, 20; and 51 stopgain SNPs that mainly focus on exon11, 12, 16, 17, 22. All TRPM8's nonsynonymous SNPs in the coding region appear on exon 2 to exon 25. Exon 12 and exon 20 are exons that can mutate the most, with 92 and 91 SNPs, respectively.

TRPM8 protein is a homotetramer including one pore helix, one ascending loop, and a transmembrane region. S1 to S6, representing helix 1 to helix 6, are interrelated to form a channel hole in the center; thus generating an ion channel (6). At the micro level, TRPM8 has 1,104 amino acids, and amino acid 692–712 (S1), 735–755 (S2), 760–780 (S3), 795–815 (S4), 830–850 (S5), and 959–979 (S6) are served as the six transmembrane helices. Each of the six helices has its unique function: S2 and S3 have binding sites for cooling chemicals such as menthol, the S4 fragment, and the intermediate part of S4 and S5 can sense voltage change, making TRPM8 the voltage-gated calcium channels, and

the channel hole is formed between S5 and S6. Therefore, the six transmembrane regions of S1-S6 are closely related to the function of TRPM8 [13; 14], and investigating these transmembrane region's changes can be important to understand how TRPM8's function is being affected.

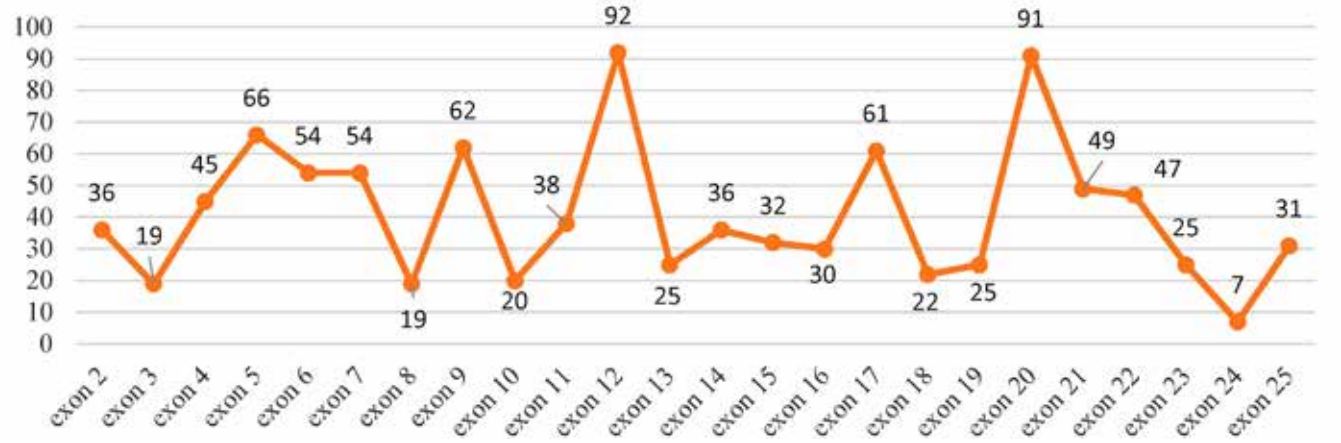

Figure 3. We sort out all TRPM8 exon's nonsynonymous SNPs on the translated region. Exon 12 and exon 20 have the most SNPs, and exon 24 has the least SNPs. Most of the exons have SNPs in the range 20–60, and the average is 41.083. The peak-like occurrence was frequent

At the TRPM8 SNPs level, some researches have shown that, nonsynonymous SNP rs11562975 turning from GG to GC will lead to changes in sensitivity of TRPM8 to cold and cooling agents [15]. TRPM8 has 22.404 SNPs that can mutate, which is 21.94% of the total TRPM8 bases. Among the 22.404 SNPs, 19611, that is 87.53% of SNPs located on the coding area, which can directly affect the coding of TRPM8 protein. Among these SNPs, rs7577262 is considered the most closely related to cold adaption [16].

At the protein level, existing research shows that TRPM8 amino acids change can make a severe influence on TRPM8 function as the cation channel. For example, the absence of Y908, a side chain of Y908, results in almost complete loss of TRPM8 stimulation of cold and menthol [17]. The change from asparagine to glutamine in 934 amino acids will lead to N-Glycosylation loss, which causes TRPM8 to lose its sensitivity to cold and menthol, and reduces expression [18]. The leucine to proline change of amino acid 1089 at the site was also found to reduce TRPM8 expression and channel activity [16]. Mutations Y1005A and L1009R, as scientists researched, can block the activation of menthol, and changes in LYS-995, ARG-998, and ARG-1008 will reduce the sensitivity of TRPM8 to PIP 2 [19].

We hope to summarize all amino acids that can change the sensitivity of TRPM8 as a cation channel. Therefore, we use TRPM8's annotation and selected all transmembrane amino acids and SNPs and exons.

70 SNPs were concluded to be linked to amino acids in the transmembrane region, corresponding to exon 16, 17, 18, 19, and exon21. Excluding the repeated 15 amino acids corresponding to several SNPs, there are a total of 55 amino acids that could mutate. The average possible changeable amino acid is 9.17, indicating that nearly half of the amino acids are likely to change their types and mutate in the transmembrane region. S1, S3, and S6 have 10–12 amino acids, accounting for about 50%-57% of all amino acids, while S2, S4, and S5 account for about 33%-38% of the amino acids in the transmembrane region. Such a high proportion indicates that the amino acids of TRPM8 have a very high possibility of changing the structure of the protein. Moreover, in combination with previous experiments, changes in amino acid types may seriously affect the channel function of TRPM8, and even be associated with related diseases [10, 18].

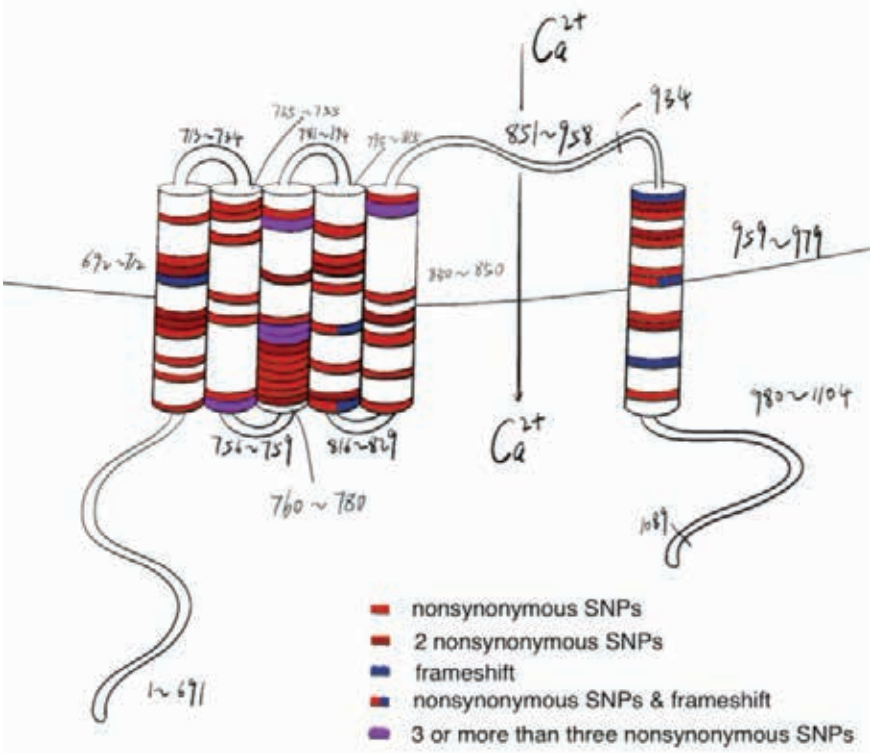

Figure 4. The distribution of SNPs locates on TRPM8 amino acids of the transmembrane region. S6 has the most SNPs among all six transmembrane regions. S3 and S6 are helices with the most SNPs; S2 and S4 are helices with the least SNPs. Existing researches have shown that the change of amino acids 934 will lower the cold sensitivity function of TRPM8, and the change of amino acids 1089 will lower TRPM8's expression [6, 18]

Table 1.– Brief information of TRPM8 SNPs *

SNP	Reference	Alteration	Function	Exon	Amino acids change
1	*2*	*3*	*4*	*5*	*6*
rs762170786	A	T	nonsynonymous	exon 16	N692Y
rs767999589	T	A	nonsynonymous	exon 16	I696N
rs1422384639	T	A	stopgain	exon 16	C698X
rs200853140	T	C	nonsynonymous	exon 16	I701T
rs1407748410	T	C	nonsynonymous	exon 16	I702T
rs766440724	A	G	nonsynonymous	exon 16	I702M
rs1350887877	C	A/G	nonsynonymous	exon 16	P703T/P703A
rs1411533847	T	-	frameshift deletion	exon 16	V705Gfs*
rs1273059733	G	C/T	nonsynonymous	exon 16	G706R/G706C
rs1219957101	G	A	nonsynonymous	exon 16	C707C
rs1280983305	G	A	nonsynonymous	exon 16	V710I
rs200217624	G	A	nonsynonymous	exon 17	V736M
rs779488832	G	A	nonsynonymous	exon 17	V737I
rs377385182	T	C	nonsynonymous	exon 17	S739P
rs778493522	C	A	stopgain	exon 17	Y745X

1	*2*	*3*	*4*	*5*	*6*
rs200649506	G	A	nonsynonymous	exon 17	A747T
rs1286988090	T	C	nonsynonymous	exon 17	Y754H
rs199991435	G	A	nonsynonymous	exon 17	V755M
rs763131949	T	C/G	nonsynonymous	exon 17	V755A/V755G
rs1350788437	C	T	nonsynonymous	exon 17	H761Y
rs149382347	A	G	nonsynonymous	exon 17	H761R
rs201939575	C	T	nonsynonymous	exon 17	S762L
rs1464646092	G	A	nonsynonymous	exon 17	V763M
rs1172210298	C	T	nonsynonymous	exon 17	P764S
rs770879940	–	C	frameshift insertion	exon 17	E768Rfs*1
rs991220444	A	G	nonsynonymous	exon 17	H765R
rs774214043	C	–	frameshift deletion	exon 17	E768Sfs*1
rs201204922	C	A	nonsynonymous	exon 17	H765Q
rs201080817	C	A/G	nonsynonymous	exon 17	P766T/P766A
rs778608904	C	A/T	nonsynonymous	exon 17	P766H/P766L
rs202105112	C	A/G/T	nonsynonymous	exon 17	P767T/P767A/ P767S
rs148846269	C	A/G	nonsynonymous	exon 17	P767H/P767R
rs749366311	G	A	nonsynonymous	exon 17	E768K
rs200296802	C	A	stopgain	exon 17	S773X
rs200296802	C	T	nonsynonymous	exon 17	S773L
rs199516053	G	A/C	nonsynonymous	exon 17	V777I/V777L
rs766286039	T	C	nonsynonymous	exon 17	V777A
rs753818944	C	T	nonsynonymous	exon 17	L778F
rs1156234321	G	A	stopgain	exon 18	W798X
rs1430954187	A	G	nonsynonymous	exon 18	D802G
rs777936976	A	G	nonsynonymous	exon 18	T803A
rs200017552	C	T	nonsynonymous	exon 18	T803M
rs1293814216	G	A	nonsynonymous	exon 18	G805R
rs771167003	G	A	nonsynonymous	exon 18	G805E
rs761976363	-	T	frameshift insertion	exon 18	Y808Lfs*13
rs560346678	T	C	nonsynonymous	exon 18	Y808H
rs201621223	G	A	nonsynonymous	exon 18	A811T
rs769614714	G	A/T	nonsynonymous	exon 18	V814I/V814L
rs1235983967	–	A	frameshift insertion	exon 18	F815Ifs*6
rs200252660	T	A	nonsynonymous	exon 18	F815I
rs201483334	T	C	nonsynonymous	exon 19	V830A
rs867129706	C	A	nonsynonymous	exon 19	L834M
rs1286708460	T	C	nonsynonymous	exon 19	I838T
rs1235272940	A	C/T	nonsynonymous	exon 19	T840P/T840S

1	*2*	*3*	*4*	*5*	*6*
rs1305952489	A	G	nonsynonymous	exon 19	R842G
rs1278968434	G	A	nonsynonymous	exon 19	V849I
rs765594459	T	C/G	nonsynonymous	exon 19	V849A/V849G
rs148696315	G	T	nonsynonymous	exon 19	S850I
rs752284591	T	–	frameshift deletion	exon 21	L959Rfs*66
rs781648773	G	A/C	nonsynonymous	exon 21	V960M/V960L
rs1250600746	G	A	nonsynonymous	exon 21	C961Y
rs556646442	A	G/T	nonsynonymous	exon 21	Y963C/Y963F
rs1042643351	G	T	nonsynonymous	exon 21	M964I
rs1335105286	A	C	nonsynonymous	exon 21	T967P
rs923789976	CCAA-CAT	–	frameshift deletion	exon 21	N968Cfs*55
rs756513083	A	C	nonsynonymous	exon 21	N968H
rs751406672	C	A	nonsynonymous	exon 21	L971M
rs780680561	T	C/G	nonsynonymous	exon 21	V972A/V972G
rs1490992389	-	T	frameshift insertion	exon 21	L975Afs*16
rs1450467773	A	G	nonsynonymous	exon 21	M978V

** Not synonymous, exonic SNPs and their relating amino acids are selected. There are, in general, 70 SNPs that can change amino acids. SNPs mainly locate on exon16, 17, 18, 19, and exon 21, and exon 17 has the most SNPs. Nonsynonymous SNPs are 82.86% of all 70 SNPs, meaning amino acid changing type is a common way of TRPM8's structural change*

Among all the changing forms, the proportion of nonsynonymous SNVs is 82.86%; while in TRPM8 exonic SNPs annotation, the proportion of nonsynonymous SNVs is 88.41%. This indicates that the types and number of SNPs changes in the transmembrane region of TRPM8 are not significantly different from that of TRPM8 as a whole, but the number of other missense changeable SNPs except nonsynonymous SNPs is slightly reduced.

TRPM8 changeable SNPs and amino acids cause diseases

Some of TRPM8 exonic, nonsynonymous SNPs can be pathogenic. We first use TRPM8 annotation to select 34 dangerous SNPs. Dangerous SNPs of S6 accounted for 71.43% of all not synonymous SNPs showing its danger of changing SNPs. Based on the fact that S6 and S5 constitute the channel pore, it can be inferred that the variation of S6 may cause the channel to flood with too many or too little calcium ions, making it pathogenic. In contrast, there are only 20% dangerous SNPs in the S3 region, and changes in SNPs and amino acids do not significantly affect the function of the amino acid, i.e. their ability to bind to specific agonists or antagonists. Dangerous SNPs of the six helices accounted for 40.96% of the total, indicating that the variation of SNPs was likely to have a significant impact on TRPM8 functionality.

Since TRPM8's change its amino acids can lead to its functional change, and it is widely distributed, TRPM8 has been considered several diseases' potential targets. According to data from GWAS, when setting a p-value smaller than or equal to 0.01, eight diseases are related with 43 TRPM8 SNPs. The diseases are psychiatric disorders, rheumatoid arthritis, and type II diabetes, astigmatism, monoclonal gammopathy, coronary artery disease, epilepsy, and migraine, and the body indicators are blood glucose, blood pressure, hearing, and so on. Although there are eight diseases relate to 43 SNPs, there is no diseases is related with exonic SNPs, meaning currently

there are no SNPs that can directly affect the type of amino acids to lead to diseases.

There are eight diseases that have been found related to psychiatric disorders, while few research has researched the relationship between psychiatric disorders and TRPM8. Actually, like mental disorders, psychiatric disorders' biological causes have not been yet discovered, let alone finding pathogenic sites. Eventually, instead of the systematic study on the relationship between the SNPs of TRPM8 and these 8 diseases, we will focus on the relationship between TRPM8 and psychiatric disorders, to provide new opinion on the cause of psychiatric disorders.

According to incomplete statistics, thirty hundred million people all over the world are affected by psychiatric disorders. Although the trend is getting stronger, scientists still have not found the cause of psychiatric disorders and their biological marker in the body.

Currently, very few research has been found on investigating the relationship between the TRPM8 gene and psychiatric disorders. Therefore, we examine the relationship between TRPM8 and psychiatric disorders thoroughly. we show that two TRPM8 intronic SNPs, rs11563199 and rs17869077, are related to psychiatric disorders.

We also try to testify how TRPM8 is related to psychiatric disorders. First, we use UCSC cell browser to investigate TRPM8 expression in autism patients and normal human. In the control group, which is the normal human's nervous system, there are 732 TRPM8-expressed cells were found. In the nervous system of people with ASD, 608 TRPM8 proteins were found, which is only 83.06% of the normal amount. However, ASD patients has more cells expressing TRPM8 2.19–5.02 (the highest expression amount). Therefore, in most ASD patients' cells, TRPM8 expression is diminished or disappeared. The downregulation of TRPM8 in most ASD patients' cells is likely to lead to unsatisfied cell demand for calcium ions.

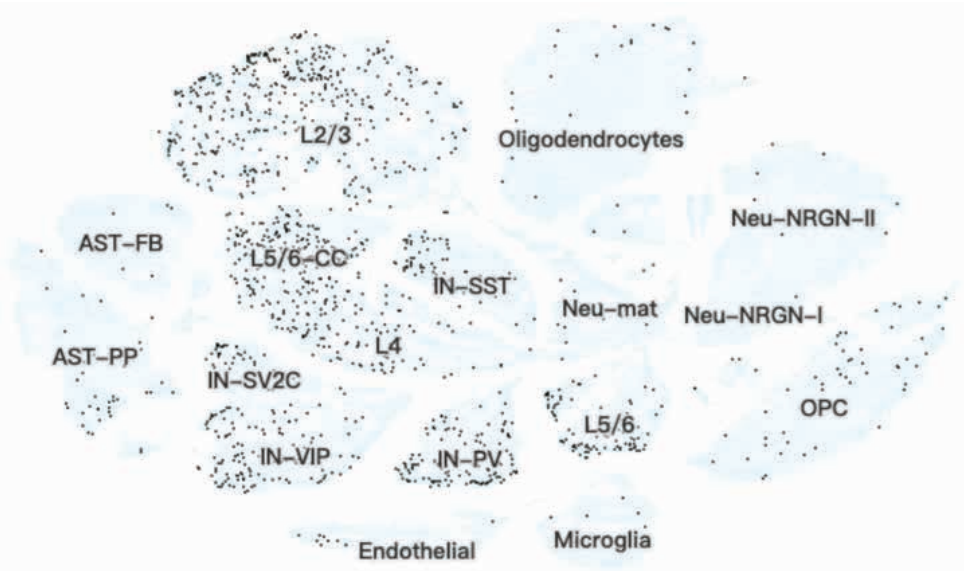

Figure 5. Differential expression of TRPM8 in different cell types of human autistic-spectrum disorder brain tissue. L2/3, L4 represents layer2/3, layer4, and served as excitatory neurons, and many cells express TRPM8 here, showing its function in basal ganglion root. L5/6-CC are deep layer cortico-cortical excitatory projection neurons. Neu-NRGN-II and Neu-NRGN-I represent Neurogranin expressing neurons. OPC represents Oligodendrocytes precursor cells and has cells showing high TRPM8 expression. Neu-mat is immature cells that do not contain many cells expressing TRPM8, showing TRPM8 does not appear significantly while the early stages. IN-SST is somatostatin interneurons. IN-PV represents Parvalbumin interneurons that have many cells expressing TRPM8. IN-SV2C and IN-VIP are interneurons. AST-FB and AST-PP are astrocytes

The data of GEO also showed that compared with the control group, the expression of TRPM8 in schizophrenia was generally down-regulated, leading to the decreased expression of TRPM8 in neurons.

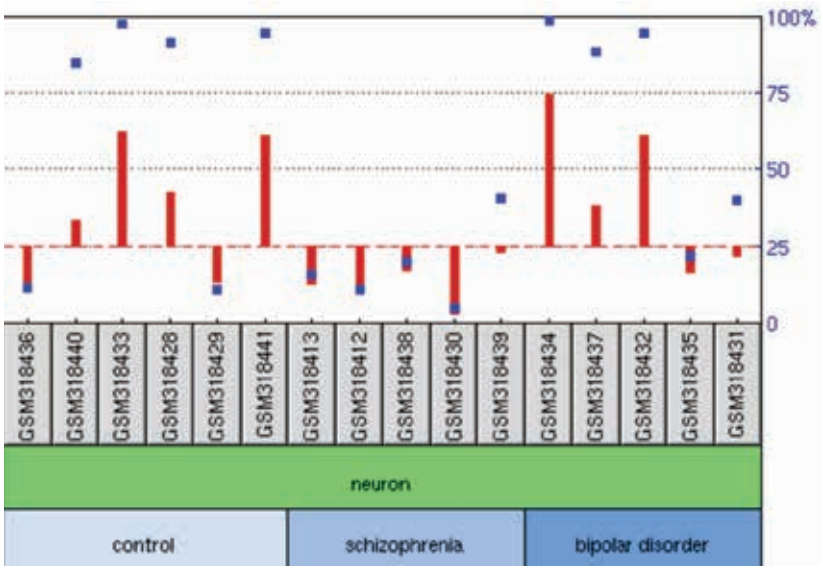

Figure 6. GEO data shows TRPM8 expression in neuron. The red lines represent the relative expression level of TRPM8, and blue dots show TRPM8's rank among all genes in the version. Compared to the control group, TRPM8 expression in neurons with schizophrenia is attenuated [20]

Discussion

Based on the result, we try to find out the relation between TRPM8 downregulation expression in neurons and psychiatric disorders. Since TRPM8 served as cation channels, the reduced TRPM8 expression in neurons can lead to less calcium ions influx into neurons. Existing study showed that although psychiatric disorders' relating channel protein-coding genes (TRPM8 in this research) may show relative low expression, these genes and relating calcium pathways can still play important though transient role in the developing process [21].

We also try to explain how rs11562199 and rs17869077's nucleotide change can lead to changes at the cell level. By using data from genome UCSC, we find out that rs11563199 can transform from cytosine to thymine. Since DNA methylation is common on cytosine, changing from cytosine to thymine may lead to the lost of DNA methylation. The possibility of switching from cytosine to thymine is 14.584%. The same change occur on rs17869077. The nucleotide of rs17869077 changes from C to T, which may lead to not only DNA methylation lost on cytosine but also histone modification. Existing researches also show that DNA methylation is necessary to mediate memory consolidation in hippocampus [22]. And connections between memory and psychiatric disorders have also been investigated. Among many stress-associated diseases, including major depressive disorder, memory capacity seemed to be disrupted [23].

Since patients with major depression disorder may have trouble in recalling, and DNA methylation plays important role in long-term memory solidification, the lost of DNA methylation, which occurs when rs11563199 or rs17869077 change their nucleotides from cytosine to thymine, shows strong link with long-term memory loss, even to depression. We try to explain the relations between TRPM8 two intronic SNPs, rs11563199 and rs17869077, from two angles: the reduction of voltage-controlled calcium channel and the lost of DNA methylation.

Conclusion

Through the above studies, we summarize 986 TRPM8 exonic, not synonymous SNPs, accounting for 79% among all TRPM8 exonic SNPs. To be

broader, exon 12 and exon 20 become exons that have the most exonic, nonsynonymous SNPs, and TRPM8's sixth helix become the helix that have the most exonic SNPs affecting amino acids, having 11 changeable amino acids. By examining TRPM8 SNPs' relation with certain diseases, a total of 43 SNPs are found to be associated with asthma, astigmatism, diabetes, psychiatric disorders, coronary artery disease, epilepsy, migraine, monoclonal gammopathy, and rheumatoid arthritis. Specifically, the change of rs11563199 and rs17869077 nucleotide from cytosine to thymine may lead to changes in TRPM8 expression, which may affect the absorption of calcium ions or influence on long-term memory solidification, and be associated with schizophrenia, depression, or other types of psychiatric disorders.

For the next step, we will: 1) identify one amino acids SNPs from the dangerous SNPs and use experiments to testify how the SNPs change can affect TRPM8's function, making it a confirmed pathogenic site, 2) create the wild-type and mutant of TRPM8 to verify whether the changes of rs11563199 and rs17869077 nucleotide will lead to the upregulation or downregulation of TRPM8 expression, thereby reducing/ increasing the inflow of calcium ions into the cell, and become pathogenic sites.

References:

1. Mc Kemy D. D., Neuhausser W. M., and Julius D. Identification of a cold receptor reveals a general role for TRP channels in thermosensation. Nature,– 416. 2002.– P. 52–58.
2. Peier A. M., Moqrich A., Hergarden A. C., Reeve A. J., Andersson D. A., Story G. M., Earley T. J., Dragoni I., McIntyre P., Bevan S. and Patapoutian A. A. TRP channel that senses cold stimuli and menthol. Cell – 108. 2002.– P. 705–715.
3. Voets T., Droogmans G., Wissenbach U., Janssens A., Flockerzi V. and Nilius B. Theprinciple of temperature-dependent gating in cold and heat-sensitive TRP channels. Nature – 430. 2004.– P. 748–754.
4. Liu B., Qin F. Functional control of cold- and menthol-sensitive TRPM8 ion channels by phosphatidylinositol 4,5-bisphosphate. J Neurosci. Feb.– 16.– 25(7). 2005.– P. 1674–81. Doi: 10.1523/JNEUROSCI.3632–04.2005. PMID: 15716403; PMCID: PMC6725927.
5. Bidaux G., Beck B., Zholos A., Gordienko D., Lemonnier L., Flourakis M., Roudbaraki M., Borowiec A. S., Fernandez J., Delcourt P., Lepage G., Shuba Y., Skryma R., Prevarskaya N. J. "Regulation of activity of transient receptor potential melastatin 8 (TRPM8) channel by its short isoforms". Biol. Chem.– 287. 2012.– P. 2948–2962.
6. Erler I., Al-Ansary D. M., Wissenbach U., Wagner T. F., Flockerzi V., Niemeyer B. A. Trafficking and assembly of the cold-sensitive TRPM8 channel. J Biol Chem. Dec. 15.– 281(50). 2006.– P. 38396–404. Doi: 10.1074/jbc.M607756200. Epub 2006. Oct 25. PMID: 17065148.
7. Sabnis A. S., Shadid M., Yost G. S. and Reilly C. A. Human lung epithelial cells express a functional cold-sensing TRPM8 variant. Am. J. Respir. Cell Mol. Biol.– 39. 2008.– P. 466–474.
8. Gkika D., Lemonnier L., Shapovalov G., Gordienko D., Poux C., Bernardini M., Bokhobza A., Bidaux G., Degerny C., Verreman K., Guarmit B., Benahmed M., de Launoit Y., Bindels R. J., Fiorio Pla A. & Prevarskaya N. zTRP channel-associated factors are a novel protein family that regulates TRPM8 trafficking and activity. The Journal of cell biology,– 208(1). 2015.– P. 89–107. URL: https://doi.org/10.1083/jcb.201402076
9. Dussor G., Cao Y. Q. TRPM8 and Migraine. Headache. Oct.– 56(9). 2016.– P. 1406–1417. Doi: 10.1111/head.12948. Epub 2016 Sep 16. PMID: 27634619; PMCID: PMC5335856.
10. Francesco A. Mistretta, Andrea Russo, Fabio Castiglione, Arianna Bettiga, Giorgia Colciago, Francesco Montorsi, Laura Brandolini, Andrea Aramini, Gianluca Bianchini, Marcello Allegretti, Silvia Bovolenta,

Roberto Russo, Fabio Benigni and Petter Hedlund TRPM8 as a Drug Target in Models for Bladder Overactivity. Journal of Pharmacology and Experimental Therapeutics January – 1.– 356(1). 2016.– P. 200–211. DOI: https://doi.org/10.1124/jpet.115.228684

11. Ling Y. H., Chen S. P., Fann C. S., Wang S. J., Wang Y. F. TRPM8 genetic variant is associated with chronic migraine and allodynia. J Headache Pain. Dec.– 16.– 20(1). 2019.– 115 p. Doi: 10.1186/s10194–019–1064–2. PMID: 31842742; PMCID: PMC6916225.
12. Sherry S. T.1, Ward M. H., Kholodov M., Baker J., Phan L., Smigielski E. M., Sirotkin K. Nucleic Acids Res. Jan 1.– 29(1). 2001.– P. 308–11. URL: https://www.ncbi.nlm.nih.gov/home/about/mission/ (the NCBI database of genetic variation).
13. Yin Y., Wu M., Zubcevic L., Borschel W. F., Lander G. C., Lee S. Y. Structure of the cold- and menthol-sensing ion channel TRPM8. Science. Jan – 12.– 359(6372). 2018.– P. 237–241. Doi: 10.1126/science.aan4325. Epub 2017 Dec 7. PMID: 29217583; PMCID: PMC5810135.
14. Pedretti A., Marconi C., Bettinelli I., Vistoli G. Comparative modeling of the quaternary structure for the human TRPM8 channel and analysis of its binding features. Biochimica et Biophysica Acta. May.– 1788(5). 2009.– P. 973–982. DOI: 10.1016/j.bbamem.2009.02.007.
15. Kozyreva T. V., Tkachenko EIa, Potapova T. A., Romashchenko A. G., Voevoda M. I. (Relationship of single-nucleotide polymorphism rs11562975 in thermo-sensitive ion channel TRPM8 gene with human sensitivity to cold and menthol). Fiziol Cheloveka. Mar-Apr.– 37(2). 2011.– P. 71–6. Russian. PMID: 21542321.
16. Igoshin A. V., Gunbin K. V., Yudin N. S., Voevoda M. I. Searching for Signatures of Cold Climate Adaptation in TRPM8 Gene in Populations of East Asian Ancestry. Front Genet. Aug.– 23.– 10. 2019.– 759 p. Doi: 10.3389/fgene.2019.00759. PMID: 31507633; PMCID: PMC6716346.
17. Bidaux G., Sgobba M., Lemonnier L., Borowiec A. S., Noyer L., Jovanovic S., Zholos A. V., Haider S. Functional and Modeling Studies of the Transmembrane Region of the TRPM8 Channel. Biophys J. Nov. 3.– 109(9). 2015.– P. 1840–51. Doi: 10.1016/j.bpj.2015.09.027. PMID: 26536261; PMCID: PMC4643257.
18. Pertusa M., Madrid R., Morenilla-Palao C., Belmonte C., Viana F. N-glycosylation of TRPM8 ion channels modulates temperature sensitivity of cold thermo-receptor neurons. J Biol Chem. May – 25.– 287(22). 2012.– P. 18218–29. Doi: 10.1074/jbc.M111.312645. Epub 2012 Apr 5. PMID: 22493431; PMCID: PMC3365712.
19. Phelps C. B., Gaudet R. The role of the N terminus and transmembrane domain of TRPM8 in channel localization and tetramerization. J Biol Chem. Dec.– 14.– 282(50). 2007.– P. 36474–80. Doi: 10.1074/jbc.M707205200. Epub 2007. Oct 1. PMID: 17908685.
20. Harris L. W., Wayl M. and Lan M., Ryan M. et al. A search of the GEO Profiles database revealed that TRPM8 is upregulated in schizophrenia and downregulated in bipolar disorder patient. (GEO accession GSE12679).
21. Heyes S., Pratt W. S., Rees E., Dahimene S., Ferron L., Owen M. J., Dolphin A. C. Genetic disruption of voltage-gated calcium channels in psychiatric and neurological disorders. Prog Neurobiol. Nov. 134. 2015.– P. 36–54. Doi: 10.1016/j.pneurobio.2015.09.002. Epub 2015 Sep 16. PMID: 26386135; PMCID: PMC4658333.
22. Sweatt J. D. Dynamic DNA methylation controls glutamate receptor trafficking and synaptic scaling. J Neurochem. May.– 137(3). 2016.– P. 312–30. Doi: 10.1111/jnc.13564. Epub 2016 Mar 3. PMID: 26849493; PMCID: PMC4836967.
23. Pittenger C. Disorders of memory and plasticity in psychiatric disease. Dialogues Clin Neurosci. Dec.– 15(4). 2013.– P. 455–63. Doi: 10.31887/DCNS.2013.15.4/cpittenger. PMID: 24459412; PMCID: PMC38

https://doi.org/10.29013/ELBLS-21-4-27-33

Tamar Gvazava,
University of Georgia
MD, PhDc in Public Health,
the School of Health Sciences
E-mail: tamar.gvazava@ug.edu.ge
Vasil Tkeshelashvili,
University of Georgia
MD, JD, PhD, ScD, Professor
E-mail: v.tkeshelashvili@ug.edu.ge

THE BURDEN OF BREAST CANCER IN TBILISI IN 2015–2019

Abstract: According to the GLOBOCAN estimated 2,261,419 cases of breast cancer incidence and 684 996 breast cancer related deaths were registered worldwide in 2020. Epidemiological study on clarification of the burden of breast cancer in Tbilisi has been carried out at the University of Georgia. Primary data on 3,743 cases of breast cancer incidence during the years 2015–2019 was obtained from the population-based cancer registry of National Center for Disease Control and Public Health (NCDC). Based on descriptive data analyses, it was identified that the burden of breast cancer in female population in Tbilisi, represents the important problem of medical and social character and ranks 1st place in the structure of cancer in the female population in Tbilisi. Recommendations have been developed based on the results of the study.

Keywords: breast cancer, incidence, mortality, disease burden, epidemiological study, Tbilisi, Georgia.

Problem statement: In the modern world, the burden of diseases is significantly defined by the chronic non- contagious disease, with cancer on its leading position. It is widely recognized that breast cancer has passed the frames of the healthcare sphere and gained the importance of social problem.

According to the Global Cancer Statistics (GLOBOCAN) 2020 report, which estimates the incidence and mortality for 36 types of cancer in 185 countries, the global burden of cancer has been identified in 20 world regions. In both sexes combined, the second most frequently diagnosed and most common cause after lung cancer is female breast cancer (2,261,419 cases, 11.7% of the total number of cases). Breast cancer among women is the most commonly diagnosed cancer and is the leading cause of cancer death. In both sexes combined, breast cancer is the 5th leading cause of death (684,996 cases, 6.9% of the total number of cases) after lung cancer (18%), colorectal cancer (9.4%), liver cancer (8.3%) and stomach cancers (7.7%).

A large proportion of breast cancers come from developing countries. Therefore, it is necessary to develop a cancer control policy in order to implement cancer advocacy and alleviate the global burden of the disease in developing countries.

Using the burden of breast cancer and socio-economic indicators may determine the financial losses or gains associated with improving or deteriorating women's health, which is so important for a developing country like Georgia.

The establishment of the Population-based cancer registries in NCDC since 2015 has made it possible to further study the epidemiological features of breast cancer.

According to the NCDC, 29,303 cases of cancer were registered in Georgia in 2015–2019, of which 9,298 cases of breast cancer, which ranks first in the structure of cancer. The second most common is thyroid cancer, and the third is the gynecological cancer (cervix, cervix and ovary).

Therefore, the burden of breast cancer is the actual problem for most of the world countries. Considering the social importance of the problem, it is actual to study incidence and death rates of breast cancer, risks of cancer progression and the burden of breast cancer in the female population of Tbilisi.

Goals and objectives of the study: The aim of the research is to clarify the structure of breast cancer incidence and death in Tbilisi based on the data of the Georgian Cancer Registry, to determine its burden, and to develop preventive recommendations.

Objectives set up considering the design of the study: To determine the frequency and peculiarities of breast cancer incidence and death in the population of women in Tbilisi according to standardized indicators in 2015–2019 years, to determine the burden of breast cancer in the population of women in Tbilisi and develop preventive recommendations for health advocacy for breast cancer patients.

Target groups and methodology of research: Electronic databases of the Population-based cancer registries for 2015–2019 were studied (NCDC). Registry data analysis was performed.

A descriptive epidemiological study was conducted using the method recommended by the International Agency for Research on Cancer (IARC, Lyon), the International Association of Cancer Registers (IACR, Lyon), the European Network of Cancer Registries (ENCR, Lyon) and the Union for International Cancer Control (UICC, Geneva). The following gross and standardized rates were calculated: Crude Morbidity and Mortality rate; Age-Specific Rate; Age-Standardized Rate (ASR); 95% confidence interval for age standardized rate (95% CI ASR); Truncated Age Standardized Rate (TASR); 95% confidence interval for Truncated Age Standardized Rate (95% CI TASR); Age-Adjusted Rate (AAR); 95% confidence interval for age-adjusted rate (95% CI AAR); Standardized Rate Ratio (SRR); 95% confidence interval for standardized ratio ratios (95% CI SRR); Cumulative Risk (Cumulative Risk- CR64, CR74,); 95% confidence interval for cumulative risk (95% CI CR); Standardized Incidence Ratio (SIR); 95% confidence interval for standardized incidence ratio (95% CI SIR). Disability-adjusted life years (DALYs) in breast cancer patients were studied.

The obtained statistical rates were presented in the form of tables, represented graphically and analyzed.

Results of the research:

The burden of breast cancer incidence in Tbilisi: In 2015–2019, 11,695 cases of cancer were registered in Tbilisi, out of which 3,743 cases of breast cancer, which ranks first in the structure of cancer. Thyroid cancer ranks second, and gynecological cancer ranks third (cervix, uterine body and ovary).

The incidence structure of 10 major sites of cancers in Tbilisi is given in crude and ASR figures in Tables 1, while the descriptive statistics of breast cancer (crude, ASR, AAR, CR0–64, CR0–74) in Tbilisi and Georgia are given in Table 2.

Table 1. – Incidence structure of 10 major women cancer sites in Tbilisi in 2015–2019 according to crude and age standardized rates

#	Tumor sites	Absolute number	Crude rate	ASR	95%CI
1	*2*	*3*	*4*	*5*	*6*
1	Breast	3743	123,6	85,3	82.5–88.1

1	*2*	*3*	*4*	*5*	*6*
2	Thyroid	1942	64,1	52,4	50.1–54.8
3	Cervix	648	18,6	16,0	14.7–17.3
4	Uterine body	714	18,5	15,2	14.1–16.4
5	Colorectum	775	25,6	14,9	13.8–16.0
6	Ovary	496	15,1	11,0	10.0–12.0
7	Skin	604	19,9	10,5	9.6–11.5
8	Blood	455	15,0	10,4	9.3–11.5
9	Lymph system	228	7,5	5,7	4.9–6.5
10	Stomach	286	9,4	5,5	4.8–6.1

Table 2. – Descriptive statistics of breast cancer incidence in Georgia and Tbilisi (2015–2019)

#	Region	Crude rate per 100,000 women	ASR	95%CI ASR	AAR	95%CI AAR	CCR0–64	95%CI CR0–64	CR0–74	95%CI CR0–74
1	Georgia	95,7	62,9	61,8–64,5	95,7	94,3–97,0	4,8	4,7–4,9	7,0	6,8–7,1
2	Tbilisi	123,6	85,3 *	82,5–88,1	123,6 *	120,7–126,4	6,2 *	6,0–6,5	9,5 *	9,1–9,8

* *p<0.001*

As can be clearly seen from Tables 1 and 2, according to all statistical rates (crude, ASR, AAR, CR0–64, CR0–74) breast cancer ranks 1st, both in Georgia and in Tbilisi.

Comparing the GLOBOCAN (2020) data to age standardized rates (ASR), the incidence of breast cancer in Georgia is 1.3 times lower than the level of Southern Europe ranked five (79,6%000) and is 1.1 times higher than the level in Polynesia which is ranked six (58,2%000). The incidence level of breast cancer in Tbilisi is 1.1 times higher than the level of Southern Europe and is identical to the level of Northern Europe (86,4%000) (SRR = 1.1).

According to the Age Standardized rate (ASR), in 1988–1992 years 35.7 women per 100,000 were diagnosed with breast cancer in Tbilisi (95% CI ASR, 33.9–37.5). According to the Age Standardized Rate (ASR), in 2015–2019, 85.3 women per 100,000 had breast cancer in Tbilisi (95% CI ASR 82.5–88.1).

According to the SRR, in 2015–2019 in Tbilisi, compared to 1988–1992 (27-year interval), the incidence of breast cancer increased 2.4 times (Table 3).

Table 3. – Comparison of the ASR rate of breast cancer in Tbilisi (ratio) in 1988–1992 and 2015–2019: SRR

Years	ASR	SE	95% CI ASR	SRR
1988–1992	35,7	0,9	33,9–37,5	2,4
2015–2019	85,3	1,4	82.5–88.1	

In Tbilisi, the age-specific incidence of breast cancer is high in the 40–74 age category and the peak is in the 65–69 age category (Figure 1).

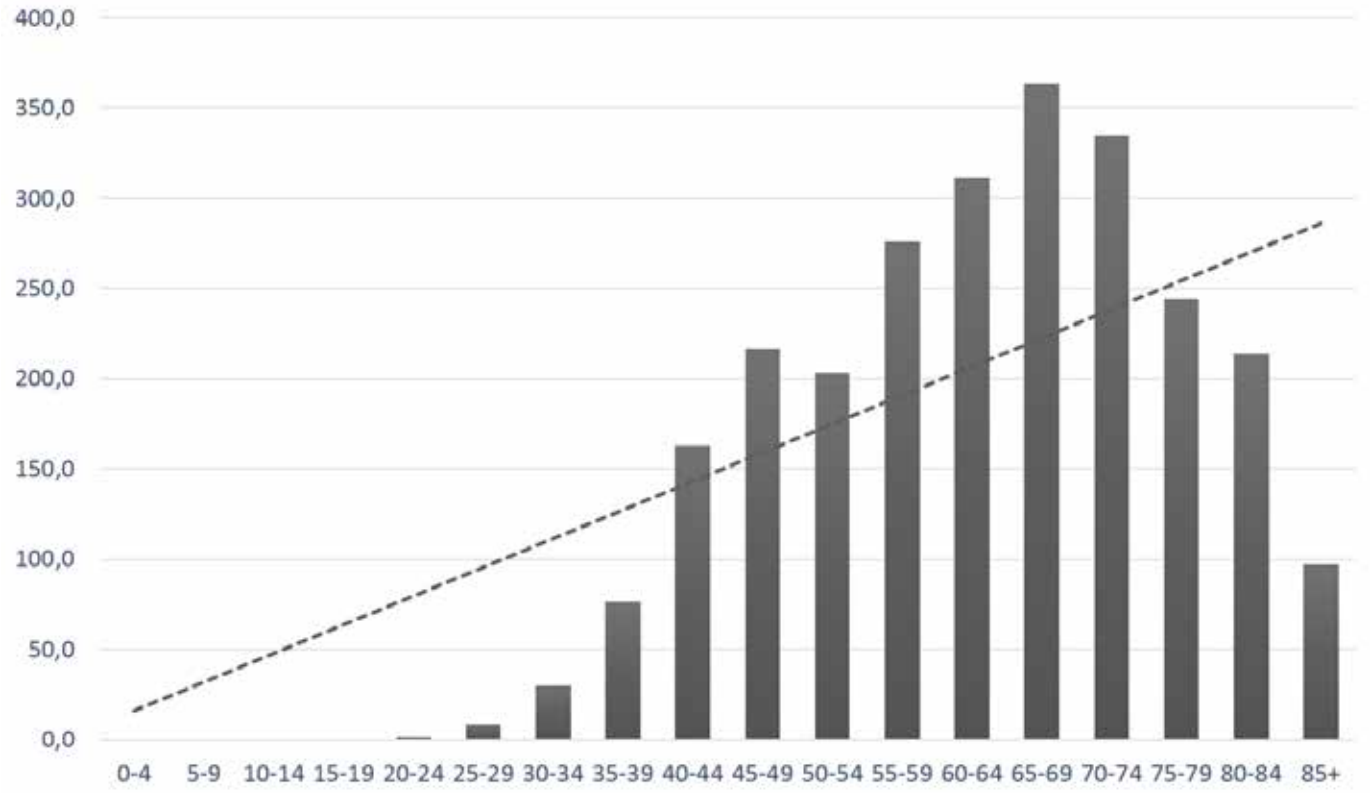

Figure 1. Age-specific rates for breast cancer incidence in Tbilisi in 2015–2019 per 100,000 women (ai)

In order to prepare a correct recommendation, the truncated age-standardized rate (TASR) in different age categories in Georgia and Tbilisi was studied. The obtained results are given in Table 4.

Table 4. – Truncated age-standardized rate (TASR) of breast cancer in Georgia and Tbilisi

Age group	Georgia			Tbilisi		
	TASR	95%CI		TASR	95%CI	
30–79	123,6	119,4	127,8	575,4	559,2	591,6
35–79	140,0	135,6	144,4	658,0	640,7	675,4
40–79	156,9	152,3	161,6	751,0	732,5	769,4
30–74	122,3	118,1	126,5	562,8	546,5	579,0
35–74	138,9	134,4	143,3	645,6	628,2	663,0
40–74	156,2	151,5	160,9	739,2	720,6	757,7

Table 4 clearly shows that in 2015–2019, 156 women (156% 000) were diagnosed with breast cancer per 100,000 women aged 40–74 in Georgia. According to truncated age-standardized rate in Tbilisi (TASR40–74), for every 100,000 women aged 40–74, 739 women (739%000) were diagnosed with breast cancer every year, which is 4.7 times higher (TASR40–74=156%000) than the similar finding in Georgia.

According to the Age Standardized Mortality Rate (ASMR), in 2002–2004, there were 33.2 deaths per 100,000 women with breast cancer in Tbilisi. According to the Age Standardized Mortality Rate (ASMR), in 2015–2019, 112.2 deaths due to breast

cancer per 100,000 women were reported in Tbilisi (Table 5).

Table 5. – Age Standardized Mortality (ASMR) rates in Tbilisi and Georgia in 2015–2019

	ASMR	ASMR
year	Georgia	Tbilisi
2016	84,6	88,1
2017	104	95
2018	129,7	129,1
2019	134,9	136,4

Source: Research results

According to the SRR, the age-standardized mortality rate (ASMR) of breast cancer in Tbilisi increased by 3.4 times in 2015–2019 compared to 2002–2004 (SRR = 3.4; 95% CI SRR = 3.2–3.6).

The global burden of breast cancer was assessed with the (Disability Adjusted Life Years) DALYs index. In 2015–2019, breast cancer in Tbilisi accounted for 17,946 disability-adjusted life years (DALYs), of which 56% (10,070) were years life-lost (YLL) and 44% (7,876) were years of life with disability (YLD). The absolute number of patients was 3,743, and the number of DALYs per woman with breast cancer averaged 4.8 years (Table 6).

Table 6. –Disability adjusted life years (DALYs) due to breast cancer in 2015–2019 in Tbilisi

Site	**YLD**				**YLL**				**DALY**			
ICD-10	**TOTAL years**	**n=**	**Mean**	**SD**	**TOTAL years**	**n=**	**Mean**	**SD**	**TOTAL years**	**n=**	**Mean**	**SD**
Tbilisi	7876	3743	2.1	1.2	10070	662	15.2	10.8	17946	3743	4.8	7.9
50.0	161.0	81	2.0	1.2	208	14	14.9	12.5	369	81	4.6	7.9
50.1	348	190	1.8	1.1	398	31	12.8	12.2	747	190	3.9	7.3
50.2	429	245	1.8	1.1	248	21	11.8	9.3	677	245	2.8	4.6
50.3	201	101	2.0	1.2	249	15	16.6	12.6	450	101	4.5	8.2
50.4	1515	867	1.7	1.2	1330	85	15.6	11.8	2845	867	3.3	6.3
50.5	262	144	1.8	1.3	62	12	5.2	8.1	324	144	2.2	3.2
50.6	18	5	3.5	1.5	8	2	4.0	5.7	26	5	5.1	4.7
50.8	310	148	2.1	1.3	580	38	15.3	10.8	890	148	6.0	9.2
50.9	4634	1962	2.4	1.2	6987	444	15.7	10.5	11621	1962	5.9	8.7

In malignant neoplasm of overlapping sites of breast (ICD-10-C50.8), the disability-adjusted life years (DALYs) due to breast cancer for each woman were a maximum of 6 years lost, with a total loss of 890 women/year. In upper lateral quadrant location of the breast cancer (ICD-10-C50.4) although the mean DALYs are low (3.3), the number of lost women / years is also high due to the high rate of this location (2,845). All this shows the need to improve the quality of diagnostics and indicates the need to raise the awareness of clinic oncologists and family doctors, pathologists, registers in the form of training webinars to ensure the registration of these variables and their consideration in clinical epidemiological monitoring.

It should be noted that the YLL and YLD percentages differ from the global YLL and YLD percentages, and in the case of Georgia, the YLL and YLD percentages play an almost equal role in the formation of DALY, which we cannot say globally about DALY due to breast cancer (worldwide study), the formation of which accounted for 88% of YLL and 12% of YLD.

Such a percentage difference between YLL and YLD is due to the duration of the indicated worldwide study and the observations of our study in Georgia. The global study lasted from 1990 to 2015. In our case this period is from 2015 to 2019. It is clear that YLL will not be fully represented in this short period of time.

Summary: Breast Cancer Burden in Tbilisi

In 2015–2019, breast cancer ranks first in the overall incidence structure of the female population in Georgia and Tbilisi. Age-standardized (ASR, world standard) and age-adjusted (AAR, Georgian and Tbilisi standards, 2014) rates per year, respectively, in Georgia – 62,9%000 (ASR = 62.9, 95% CI ASR = 61.8–64.5) / 95,7%000 (AAR = 95.7; 95% CI AAR = 94.3 97.0), in Tbilisi — 85.3%000 (ASR = 85.3; 95% CI ASR = 82.5–88.1) / 123,6%000 (AAR = 123.6; 95% CI AAR = 120.7–126.4). According to the Standardized Rate Ratio (SRR), the incidence of breast cancer in Tbilisi was 1.4 times higher (SRR = 1.4) than the overall cancer incidence rate in Georgia.

Comparing the GLOBOCAN (2020) data to age standardized rates (ASR), the incidence level of breast cancer in Tbilisi is 1.1 times higher than the level of Southern Europe and is identical to the level of Northern Europe (86,4%000) (SRR = 1.01).

According to the Standardized Rate Ratio (SRR), the incidence of breast cancer (SRR = 2.4, 95% CI SRR = 2.2–2.5) in Tbilisi increased 2.4 times in 2015–2019, compared to 1988–1992, ie in the 27-year dynamics.

The peak of breast cancer in Tbilisi falls on the age group of 40–74 years, ie in the late reproductive and premenopausal periods, and especially in the postmenopausal period. According to truncated age-standardized rate in Tbilisi (TASR40–74), for every 100,000 women aged 40–74, 739 women (739%000) were diagnosed with breast cancer every year, which is 4.7 times higher (TASR40–74=156%000) than the similar finding in Georgia.

With age-standardized (ASR) rates per 100,000 women, the death rate due to breast cancer in Tbilisi in 2015–2019 was 112.2 per year. According to the SRR, the incidence of breast cancer deaths in Tbilisi increased by 3.4 times in 2015–2019 compared to 2002–2004 (SRR = 3.4; 95% CI SRR = 3.2–3.6). According to the Standardized Mortality Ratio (SMR), the incidence of breast cancer deaths increased by 238% in 13-year dynamics (SMR = 338.0, 95% CI SIR = 275.4–400.5).

According to the DALYs index, 17,946 women/life year were lost due to breast cancer in Tbilisi in 2015–2019, each patient lost an average of 4.8 years.

Conclusions: The Burden of breast cancer in female population in Tbilisi represents the important problem of medical and social character.

The incidence level of breast cancer in Tbilisi is 1.1 times higher than the level of Southern Europe and is identical to the level of Northern Europe.

Breast cancer incidence in Tbilisi increased by 2.4 in 27-year period.

For every 100,000 women aged 40–74, 739 women were diagnosed with breast cancer every year in Tbilisi, which is 4.7 times higher than the similar finding in Georgia.

The incidence of breast cancer deaths in Tbilisi increased by 3.4 times in 13-year period.

According to the DALYs index, 17,946 women/life years were lost due to breast cancer in Tbilisi in 2015–2019, each patient lost an average of 4.8 years.

Recommendations:

To ensure comprehensive control of breast cancer to increase the effectiveness of early detection and screening-programs of breast cancer, to reduce the burden of cancer and hypo diagnostics, as well as to approach international guidelines, it is recommended to establish a breast cancer screening guideline for Georgia.

For more in-depth study of the burden of breast cancer, in the post-treatment period, continuous (before the patient's death) data collection and registration in the follow-up mode (ECOG scale) recommended by the Georgian Population-based Cancer Register will allow us to assess the cancer burden according to both DALYs and QALYs.

Academic substantiation of women's health advocacy and education of women population, breast self-examination training and periodic screening habits will help to optimize breast cancer prevention management.

References:

1. Breast cancer facts & figures (2019–2020) American Cancer Society https://www.cancer.org/content/dam/cancer-org/research/cancer-facts-and-statistics/breast-cancer-facts-and-figures/breast-cancer-facts-and-figures-2019–2020.pdf
2. Population based cancer registry, three-year results (2015–2017) NCDC; https://www.ncdc.ge/Handlers/GetFile.ashx? ID=8d23d768-d885–4756-b631–33f3c623057a
3. Breast Cancer: Statistics; (2020) American Society of Clinical Oncology; (Jan 2020) https://www.cancer.net/cancer-types/breast-cancer/statistics
4. Cancer Incidence in Five Continents, volume X; (2014) International Agency for Research on Cancer (IARC), Chapter 5 https://ci5.iarc.fr/CI5I–X/old/vol10/CI5vol10.pdf
5. Tkeshelashvili V. (2007). Epidemiological Features of Cancer Incidence in Tbilisi in the Period of 1988–1992. www.cancernet.ge, Biennial 2007–2008: 2nd Annual, 4th quarter, Tbilisi, 2007
6. Ferlay J, Colombet M, Cancer incidence and mortality patterns in Europe: Estimates for 40 countries and 25 major cancers in 2018. https://www.ncbi.nlm.nih.gov/pubmed/30100160
7. Fitzmaurice Christina (2019), Global, Regional, and National Cancer Incidence, Mortality, Years of Life Lost, Years Lived with Disability, and Disability-Adjusted Life-Years for 29 Cancer Groups, 1990 to 2017A Systematic Analysis for the Global Burden of Disease Study, 27 Sep 2019; JAMA Oncol. 2019;5(12):1749–1768. doi:10.1001/jamaoncol.2019.2996 https://jamanetwork.com/journals/jamaoncology/fullarticle/2752381
8. Global, Regional, and National Cancer Incidence, Mortality, YLL, YLD, and DALI for 32 Cancer Groups, 1990 to 2015. A systematic Analysis for the GBD Study. JAMA Oncol. 2017; 3 (4):524–548 https://pubmed.ncbi.nlm.nih.gov/27918777
9. Siegel RL, Miller KD, Jemal A. (2019) Cancer statistics, 2019; CA Cancer J Clin. 2019 Jan. 69 (1):7–34 https://acsjournals.onlinelibrary.wiley.com/doi/epdf/10.3322/caac.21583

Section 3. General Biology

https://doi.org/10.29013/ELBLS-21-4-34-43

Ou Rachel,
Bridgewater-Raritan High School
Bridgewater, NJ 08807, USA
E-mail: rachelo1500@gmail.com

IDENTIFICATION OF AUTISM SPECTRUM DISORDER RELEVANT GENES USING GENE EXPRESSION AND GENETIC INFORMATION

Abstract. Autism Spectrum Disorder (ASD) refers to a broad range of neurodevelopmental conditions that cause significant communication and behavioral issues. It is mostly a heritable condition, with multiple genes playing pathogenic roles. Although extensive studies have been conducted to establish the genic connections in ASD patients, some gene connections may have been overlooked due to the vast number of genes and the vast amount of information available. In this research, we used statistical tools to analyze public databases in an effort to discover novel genes associated with autism. By comparing DNA and RNA from autistic population and the general population, we identified 31 down-regulated and up-regulated genes in the cerebellum, frontal cortex, and temporal cortex which have a positive connection with ASD. Of these genes, 6 genes GGNBP2, TUBGCP5, ZDHHC8, DHRS11, RABL2B, and PANX2 have been identified to be tightly associated with ASD at RNA and genetic levels. All six genes are novel and they may play a role in the development of ASD.

Keywords: Autism Spectrum Disorder (ASD), differentially expressed genes (DEGs), up-regulated, down-regulated, cerebellum, frontal cortex, temporal cortex.

Introduction:

Autism Spectrum Disorder (ASD) refers to a broad range of neurodevelopmental conditions that cause significant communication and behavioral issues. Symptoms include abnormal facial expressions, repetitive behavior, and delayed language skills. ASD is a heritable condition, with multiple genes playing pathogenic roles. Compared with normal individuals, those that display phenotypes associated with ASD have different genes which have abnormal regulations.

The occurrence of ASD is 62/10,000. Males are four times more likely to suffer than females. A large number of de novo copy-number variations and single-base-pair mutations have been found in ASD patients. In addition to genetic influences, many environmental risk factors have been connected to ASD, such as various pharmaceutical drugs and toxicants. In recent years, ASD research has progressed beyond genes and molecules to circuits and neural connectivity. Structural neuroimaging studies have revealed differences in brain volume and connectivity in those with ASD and those without [1].

Although there is no cure for ASD, many interventions have been developed. These interventions

seek to improve behavioral, cognitive, and social skills. Since each individual with ASD has his/her unique strengths and weaknesses, treatment plans are specific to an individual's needs. Some examples of treatments include behavior analysis, speech therapy, social skills training, and the use of assistive technology [2].

This study seeks to: 1. Identify novel differentially expressed genes (DEGs), which are dysregulated in terms of gene expression in brain tissues of ASD patients; 2. Identify the brain regions in which these DEGs are expressed; and 3. Identify the cell types in which these DEGs are expressed. By understanding the function of these genes, their expression in different brain regions, researchers will be better able to address the genes' roles in ASD, and new methods for diagnosing ASD early on may be revealed. In addition, these abnormal genes may be used as targets for drug development.

Methods:

Data was collected from public databases and analyzed using statistical tools. First, preliminary data was collected from the Gene Expression Omnibus (GEO) database (GSE28521) [3], which is a public functional genomics data repository. Next, a list of the down-regulated and up-regulated DEGs was compiled based on statistical significance (P) and fold change (FC) value. Then, in order to identify key pathways and biological processes involved in ASD, we performed functional enrichment analysis for the up-regulated and down-regulated genes using the Database for Annotation, Visualization and Integrated Discovery (DAVID) [4], a database including functional annotation tools for large lists of genes. Next, the Genotype-Tissue Expression (GTEx) Portal [5], a public resource for the study of tissue-specific gene expression and regulation, was utilized in order to investigate the brain regions in which these genes are expressed. Then, expression profile analysis using single cell RNA sequencing data was performed to investigate what cell types are mainly associated with the DEGs. Finally, data was compared to the Clinvar database [6], a public archive of reports of the relationships among human variations and phenotypes, to identify overlapping DEGs in order to correlate the data with genetic evidence.

Final DEGs were annotated using annotation tool SOURCE by Princeton (https://source-search.princeton.edu/). The annotations include the gene symbol, full name, Entrez Gene ID, chromosome number, protein subcellular localization, UniProt ID, and a brief functional description.

Results:

Dataset and Workflow

To identify genes tightly associated with ASD, we performed analyses according to the workflow chart shown in Figure 1. Briefly, we used GEO database to retrieve the dataset with GEO accession number GSE28521. The dataset consists of RNA from approximately 100mg of postmortem brain tissue, including cerebellum, frontal cortex, and temporal cortex of autistic and control groups. We identified DEGs in these tissues and selected all down-regulated and up-regulated genes for further enrichment analysis. The purpose of this analysis is to identify potential signaling pathway, metabolic pathway and other enriched physiological processes or molecular functions that are tightly associated with the DEGs. Because differential expression analysis is based on a microarray dataset of which cross-hybridization might cause false-positive results, we further used RNA-sequencing (RNA-seq) data to confirm the expression of DEGs in human brain regions.

Besides gene expression analysis mentioned above, we also used the ClinVar database to investigate ASD relevant genes that were altered by gene variation such as mutation and SNP (Single Nucleotide Polymorphism). Genes that were common from both genetic analysis (ClinVar) and expressional analysis are more likely to be connected to ASD. Therefore, we paid more attention to these genes and made detailed annotations.

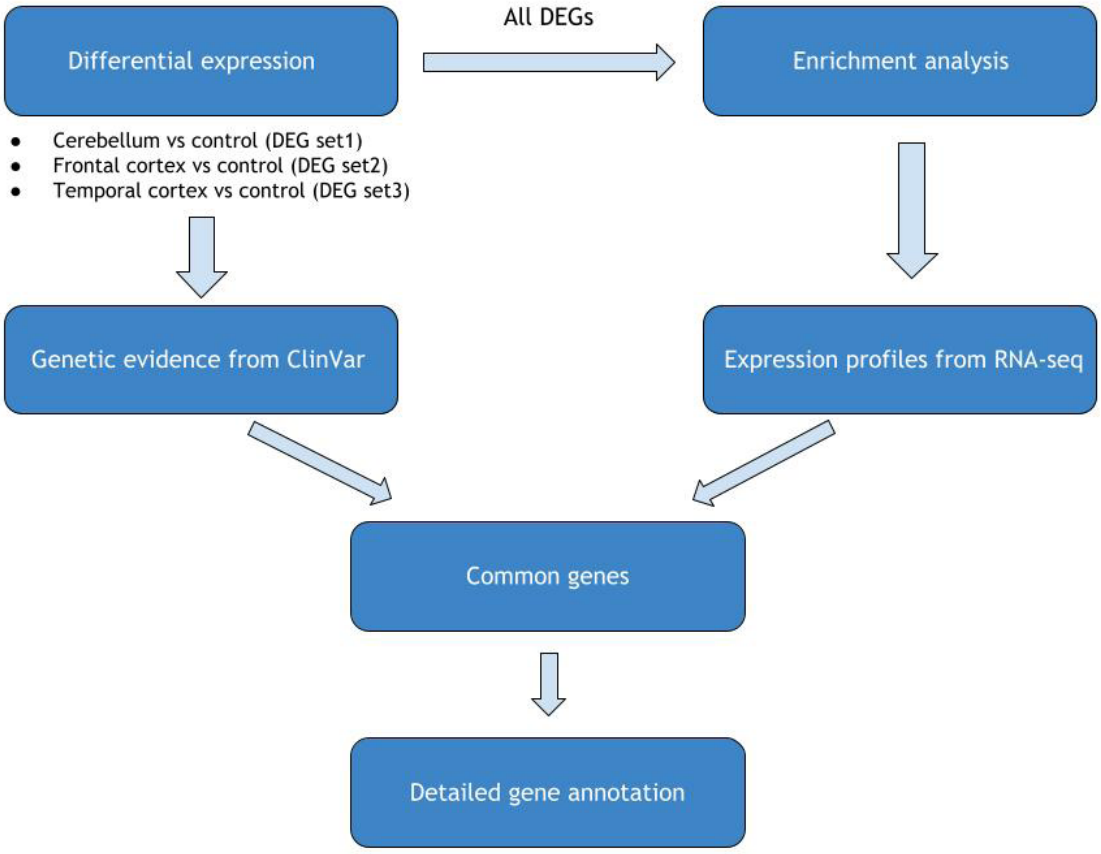

Figure 1. Workflow of the current study

Identification of DEGs Using Micro Arraying Data

A total of 31 down-regulated and up-regulated genes were identified in the cerebellum, frontal cortex, and temporal cortex. For all analyses, the P-value was <= 0.05, indicating statistical significance. The criteria for up-regulated genes is Fold Change (FC) value >= 1.5, which means that the average gene expression level of a gene in ASD group is at least 1.5 times higher than that in the control group. For down-regulated genes, the FC value was set <= 0.6. All the DEGs are listed in Table 1 (cerebellum), Table 2 (frontal cortex) and Table 3 (temporal cortex).

Table 1 lists DEGs in cerebellum of ASD patents. Cerebellum is a brain region that coordinates voluntary movements such as posture, coordination, speech, and smooth muscular activity. A total of 9 DEGS were identified: 7 up-regulated genes, and 2 down-regulated genes.

Table 1.– DEGs of cerebellum in ASD patients

Gene Symbol	Gene Title	Fold Change	P value	Direction
1	*2*	*3*	*4*	*5*
EPHB6	EPH receptor B6	1.616	0.00227	Up
NES	Nestin	1.502	0.00456	Up
BCHE	Butyrylcholinesterase	1.583	0.0102	Up
LRRC37A4P	leucine rich repeat containing 37 member A4, pseudogene	1.661	0.0114	Up
NDRG2	NDRG family member 2	1.641	0.0173	Up

1	*2*	*3*	*4*	*5*
FAM181B	family with sequence similarity 181 member B	1.641	0.0230	Up
NTM	Neurotrimin	1.510	0.0321	Up
MYH11	myosin, heavy chain 11, smooth muscle	0.562	0.0180	Down
CPLX3	complexin 3	0.577	0.0276	Down

Table 2 lists the down regulated DEGs in the frontal cortex of ASD patients. Frontal cortex is a brain region in control of memory, emotions and impulse control. 10 down-regulated genes were identified.

Table 2.– Down-regulated DEGs of frontal cortex in ASD patients

Gene Symbol	Gene Title	Fold Change	P value
STAT4	signal transducer and activator of transcription 4	0.504	0.000116
HAPLN4	hyaluronan and proteoglycan link protein 4	0.489	0.000119
VAMP1	vesicle associated membrane protein 1	0.582	0.000436
PVALB	Parvalbumin	0.424	0.000691
TUBGCP5	tubulin, gamma complex associated protein 5	0.510	0.000810
SCN1B	sodium voltage-gated channel beta subunit 1	0.563	0.00273
GABRG2	gamma-aminobutyric acid type A receptor gamma2 subunit	0.599	0.00397
GAD2	glutamate decarboxylase 2	0.594	0.0122
RTN4	reticulon 4	0.572	0.0319
RTN1	reticulon 1	0.525	0.0362

Table 3.– Down-regulated DEGs of temporal cortex in ASD patients

Gene Symbol	Gene Title	Fold Change	P value
NEFH	neurofilament heavy polypeptide	0.441	0.0000916
PCSK1	proprotein convertase subtilisin/kexin type 1	0.533	0.000108
HAPLN4	hyaluronan and proteoglycan link protein 4	0.407	0.000110
CCDC184	coiled-coil domain containing 184	0.575	0.000206
VAMP1	vesicle associated membrane protein 1	0.585	0.00113
ADCYAP1	adenylate cyclase activating polypeptide 1	0.589	0.00159
STAT4	signal transducer and activator of transcription 4	0.539	0.00267
VGF	VGF nerve growth factor inducible	0.558	0.00302
NGEF	neuronal guanine nucleotide exchange factor	0.592	0.00360
PVALB	Parvalbumin	0.340	0.00433
SCN1B	sodium voltage-gated channel beta subunit 1	0.438	0.00560
NSG1	neuron specific gene family member 1	0.551	0.00619
CRH	corticotropin releasing hormone	0.493	0.0189
GAD1	glutamate decarboxylase 1	0.536	0.0194
GAD2	glutamate decarboxylase 2	0.226	0.0200

In the temporal cortex, a brain region responsible for auditory stimuli, memory, and speaking, 15 down-regulated genes were identified (Table 3).

These results suggest that different brain regions of ASD patients are affected and the dysregulated genes are not exactly the same in different brain regions, which further suggests the complexity of

the disease. On the other hand, we found that there are six co-downregulated genes *STAT4*, *HAPLN4*, *VAMP1*, *PVALB*, *SCN1B* and *GAD2* in the frontal cortex and temporal cortex regions. These genes should play an important role in the development of ASD disease.

Functional Enrichment Analysis of DEGs

Next, we performed functional enrichment analysis using the DAVID tool on the up- and down-regulated DEGs to reveal the key pathways and biological processes associated with the genes. We did not obtain any significant enrichment results based on the up-regulated genes in Table 1 when p value was set less than or equal to 0.05. This may be the result from the limited gene counts. However, when we used all of the down-regulated genes for analysis, we found that a lot of biological processes and pathways are involved in these genes (Figure 2). For example, the most significant process is neurogenesis, which is the process in which new neurons are formed in the brain. This process is crucial for brain development in embryos, but it also continues after birth in certain brain regions. The involved genes related to neurogenesis include ADCYAP1, RTN4 and NGEF, and so on. Therefore, the enriched process reveals that the ability to form new neurons in ASD patients is damaged because of down-regulation of relevant genes.

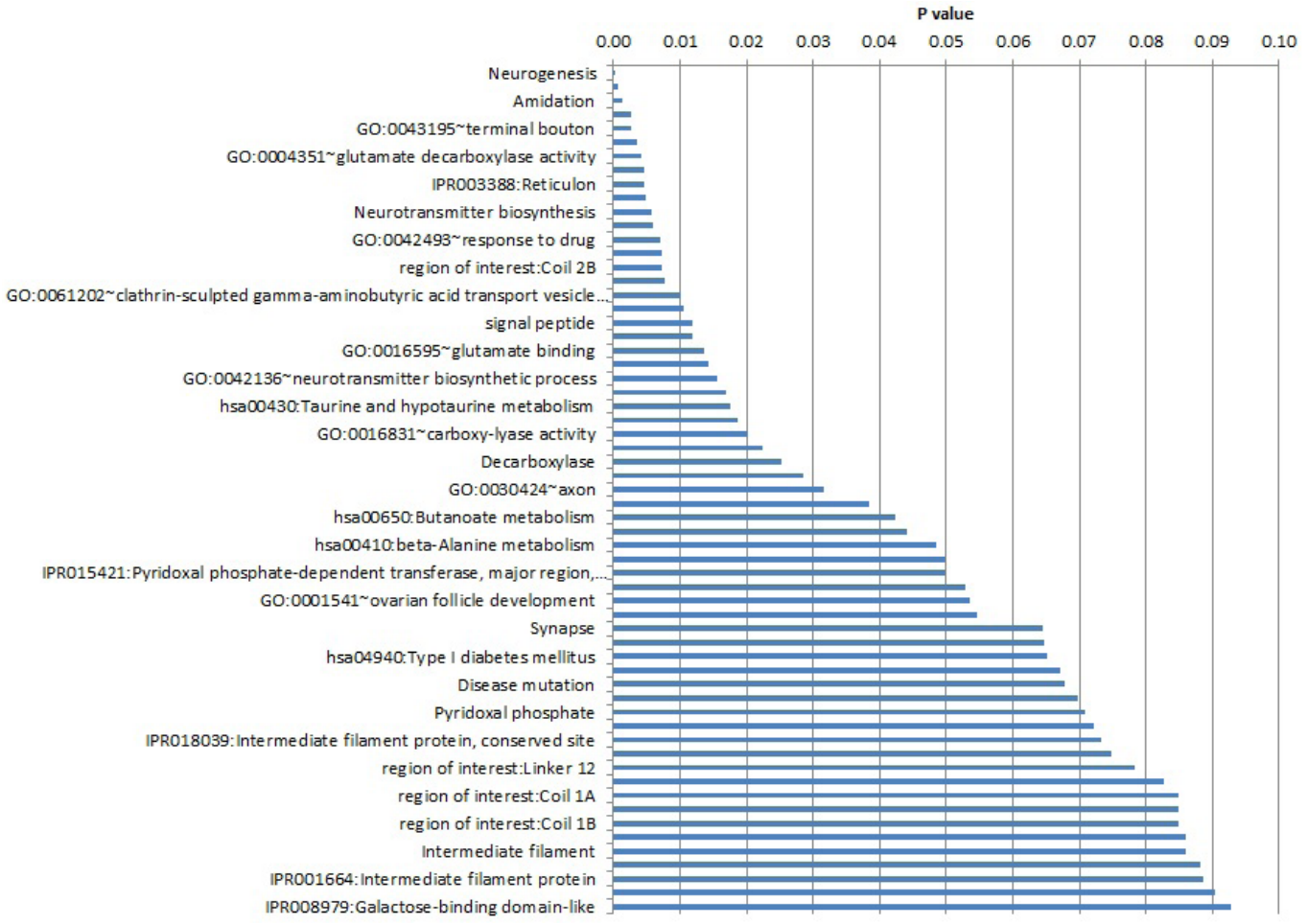

Figure 2. Functional enrichment analysis using DAVID tool.

Besides neurogenesis, another important process is amidation, which represents a type of protein modification. The decreased process indicates that a decreased neuropeptide amidation could occur in ASD patients. The third process is terminal bouton, also known as axon terminal or synaptic bouton. It is

the far end of a neuron's axon and is crucial for neural communication. This process may also be damaged in ASD patients. Other processes such as reticulon, neurotransmitter biosynthesis and glutamate binding, and so on, are also enriched in the downregulated genes, suggesting an extensive affection of brain function in ASD patients.

Expression Profile of DEGs Using RNA Sequencing Data

The above DEGs were identified using microarray data. Next, RNA sequencing data was analyzed to validate the expression of DEGs in human tissue. In particular we wanted to see whether these genes show specific expression in human brain regions. Results from analyzing the data using the GTEx portal reveal the brain regions in which these DEGs are expressed: cerebellum, cerebellar hemipster, hypothalamus, anterior cingulate cortex, frontal cortex, and so on. As shown in Figure 3, we can see all of these genes can be expressed in human brain tissue. However, DEGs vary in their expression levels. For example, NDRG2, RNT4 and RNT1 are highly expressed in all regions compared with other DEGs. However, we found that MYH11, BCHE, CRH and ADCYAP1 show very low expression levels in the brain tissues. BCHE is upregulated in the cerebellum of ASD patients (Table 1), whereas the other three genes are further downregulated. The mechanism and significance still await further investigation.

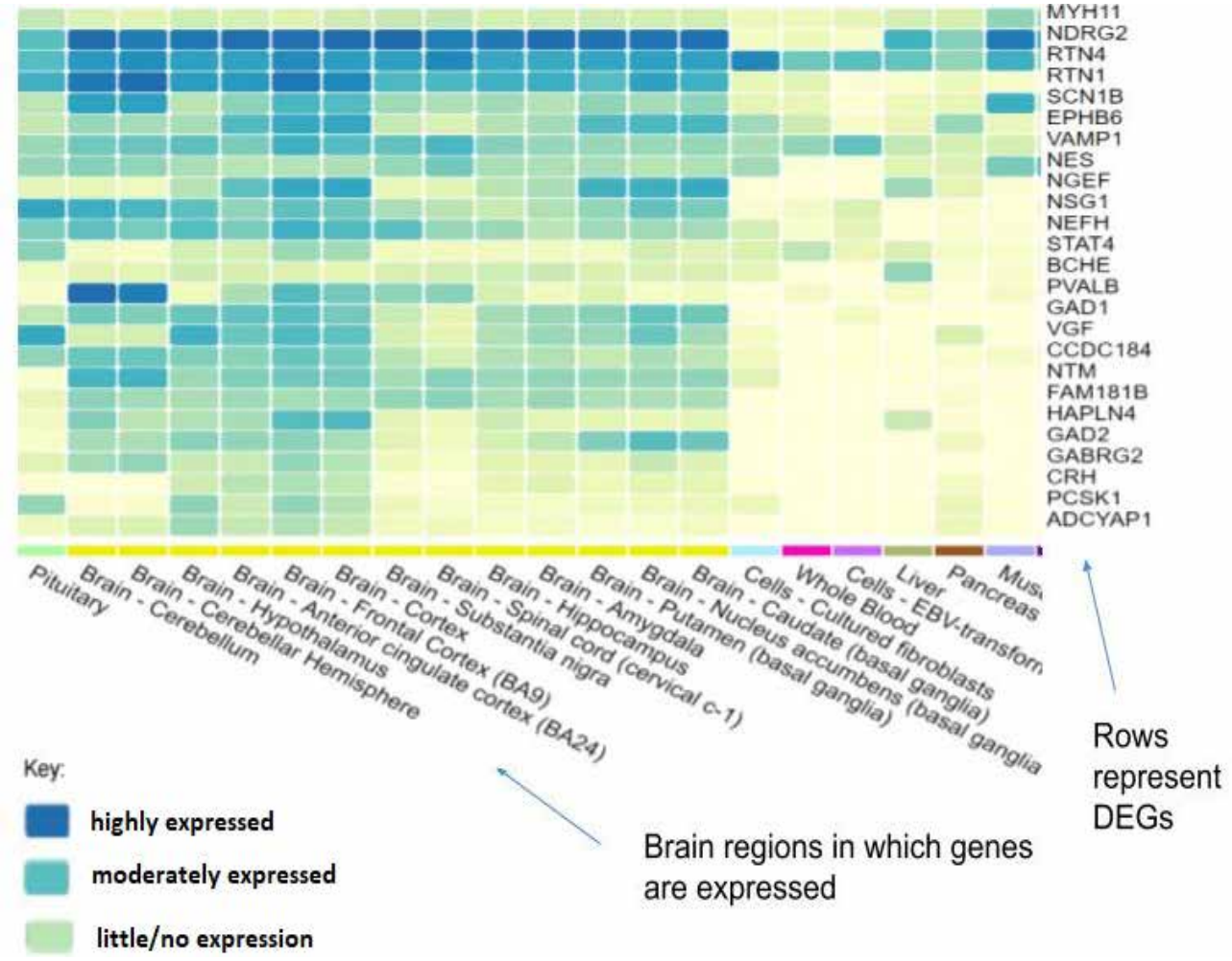

Figure 3. Expression levels of selected DEGs in brain regions using GTEx RNA-seq data. Each block represents gene expression level indicated by the color bar

Identification of gene variation relevant to ASD

The above analyses were based on gene expression at RNA level, and we don't know whether there is genetic change of these genes that also represents the potential mechanism to cause ASD. Therefore, we searched the ClinVar database, a public archive of reports of the relationships among human variations and phenotypes, to find genomic variations related to ASD. If a gene mutation happens to be located on the above differential genes, it means that the likelihood of this gene playing a more important role in the etiology of ASD is strong based on both the heredity factor and the gene expression factor. Consequently, we compared data used in this research and data from ClinVar. We found that there are 184 non-redundant genes and several chromosome regions recorded in the database to be associated with ASD. Surprisingly, there was no overlap between these genes and the DEGs in Tables 1, 2 and 3. The count of DEGs mainly depends on filter condition, such as fold change. If we change the filter conditions during DEG identification, some differential genes may have genetic changes at the same time.

As shown in Table 4, 6 downregulated genes including *GGNBP2, TUBGCP5, ZDHHC8, DHRS11, RABL2B, PANX2* (Table 4) were identified to be overlapped when only p value was used as filter condition. The gene *TUBGCP5* showed the maximum reduction with a fold change 0.51.

Table 4. – Down-regulated DEGs with simultaneous genetic variation in ASD.

Gene Symbol	Gene Title	Fold Change	P value	Region	Protein subcellular localization	Functional description
GGNBP2	gametogenetin binding protein 2	0.788	0.000174	frontal cortex	cytoplasmic vesicle; associated with vesicular structures	may be involved in spermatogenesis
TUBGCP5	tubulin, gamma complex associated protein 5	0.51	0.00081	frontal cortex	cytoplasm, cytoskeleton, microtubule organizing center, centrosome.	gamma-tubulin complex is required for microtubule nucleation at the centrosome.
ZDHHC8	zinc finger, DHHC-type containing 8	0.722	0.00792	frontal cortex	cytoplasmic vesicle membrane; multi-pass membrane protein	palmitoyltransferase involved in glutamatergic transmission. mediates palmitoylation of abca1
RABL2B	RAB, member of RAS oncogene family-like 2B	0.732	0.00757	temporal cortex	secreted	oxidoreductase activity, oxidation-reduction process
PANX2	pannexin 2	0.987	0.00446	temporal cortex	intracellular	GTP Binding, GTPase activity, Rab protein signal transduction, intracellular protein transport
DHRS11	dehydrogenase/reductase (SDR family) member 11	0.796	0.000216	temporal cortex	cell membrane, multi-pass membrane protein, cell junction, gap junction	structural component of the gap junctions and the hemichannels

This result from both gene expression and genetic variation suggests that these six genes should play an important role in the etiology of ASD.

Identification of gene expression of ASD-related genes at single cell level

The above gene expression analysis from GEO microarray and GTEX RNA sequencing was based on bulk tissue samples which contained a wide variety of cells. The expression data represented an averaged effect of gene expression across thousands to millions of cells, which might obscure biologically relevant and critical differences between cells. Unlike these traditional methods, single cell RNA sequencing (scRNA-Seq) examines gene expression at single cell resolution, thus providing a better understanding of the gene function in different cell types in the context of tissue microenvironment. In order to determine the specific cell types in which the genes in Table 4 are expressed, a dataset from the UCSC cell browser was used (http://cells.ucsc.edu/?ds=autism). The dataset analyzed single cells in the cortex of ASD patients using single-nucleus RNA sequencing data to identify autism-associated transcriptomic changes in specific cell types [7].

As shown in Figure 4, genes *GGNBP2*, *TUBGCP5*, *ZDHHC8*, and *RABL2B* have similar expression profiles. All of these genes are highly expressed in excitatory neurons, cortico-cortical projection neurons, and somatostatin interneurons. Expression of these genes in endothelial cells, microglia, oligodendrocyte precursor cells (OPCs), and oligodendrocytes is relatively low. Excitatory neurons aid in the electoral transmission of neuronal signals. Cortico-cortical projection neurons communicate by sending action potentials that release glutamate. Somatostatin interneurons facilitate synapses. The results suggest these cell types should be directly involved in the pathogenesis of ASD.

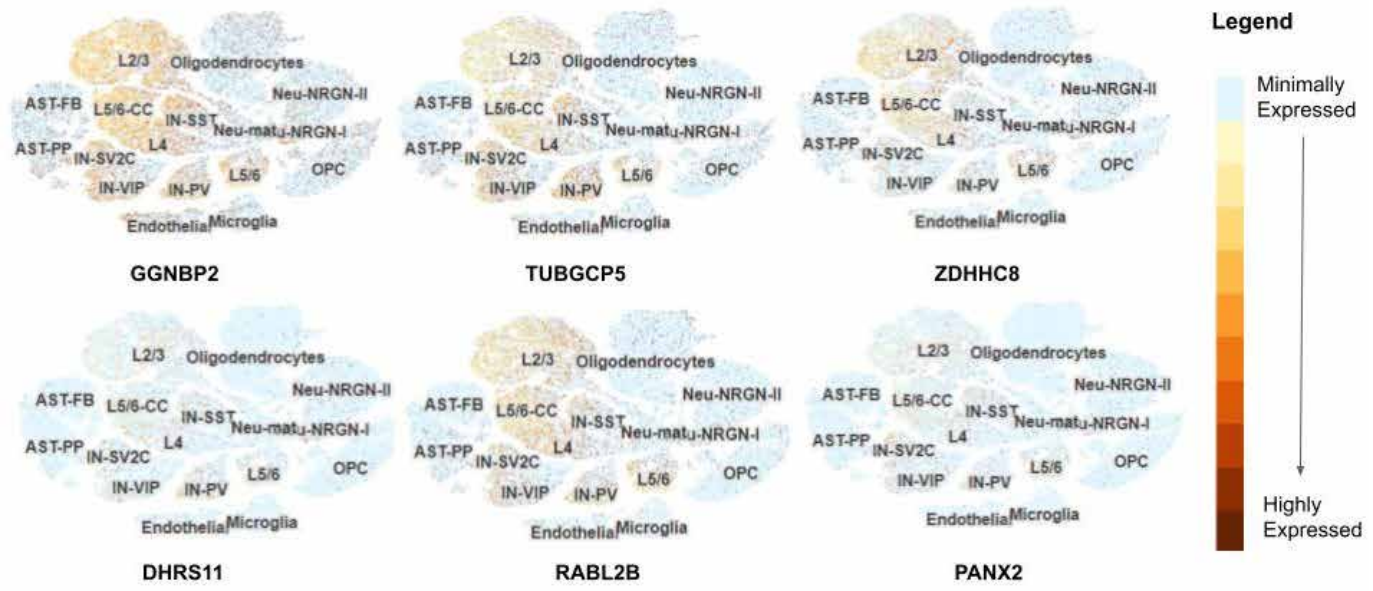

Figure 4. Expression profile of the six genes at single cell resolution in ASD brain tissue. Each dot corresponds to a single cell and each cluster is labeled with the cell type. The clusters include L2/3, IN-SST, IN-PV, IN-VIP and L2/3 represent excitatory neurons. L5/6 represents cortico-cortical projection neurons and IN-SST represents somatostatin interneurons

Discussion:

In the current study, we aimed to identify Autism Spectrum Disorder relevant genes using gene expression and genetic information. Evidences from both analyses would make the results more reliable. Under our original strict filter conditions to identify DEGs, there were no overlapped genes with simultaneous genetic change associated with ASD. When we used

a different strategy to see which genes were dysregulated in gene expression among all the genes with genetic association with ASD, 6 genes were identified to get both supports.

The data we used in this analysis were from bulk mRNAs, which were extracted from the whole tissues and represented a mixture of various cell types. We further used single cell data to identify the cell source of the final six genes and found that they could be expressed in neurons (data not shown).

The study reveals novel key genes that are tightly associated with ASD on genetic and RNA levels. Researchers have not studied in great detail the 6 identified DEGs and their influence in the pathogenesis of ASD. However, this study examines the brain regions and the exact cell types that express these genes.

To be noted, however, is that the data used to determine the specific cell types in which the genes are expressed come from PFC and ACC brain regions, whereas the genes studied are from the frontal cortex and temporal cortex.

Functional annotations of the 6 overlapped DEGs are provided in the results section. However, this study only seeks to identify the DEGs tightly associated with ASD, and the brain regions and cell types in which these DEGs are expressed. Future studies will be directed toward utilizing the annotations to understand the functional associations between these genes and the clinical symptoms of ASD.

The 6 genes identified may prove to be vital in animal research. Advanced knowledge about these genes and their pathways, along with technological advancements in genome engineering, can allow scientists to better understand the neurological basis of ASD and develop potential treatments using molecular-engineered animal models. For example, the zebrafish is a promising model for studying ASD, as it is highly social and well-characterized genetically. The model has the capacity to accomplish the dissection of molecular pathways related to synaptogenesis and therapeutic investigations. With the discovery of the above 6 genes, scientists will be able to better understand the neurobiology of ASD from the perspective of animal models and develop pharmacological interventions [8].

Future studies directed toward understanding the functional associations between these genes and the clinical symptoms of ASD will help shed light on the molecular mechanisms behind the occurrence of ASD and help find nutritional and medical interventions for ASD patients and mitigate the adverse effects resulting from ASD. Although controversial, the discovery of these genes may also be helpful in the field of molecular engineering, as these genes can be targeted in genetic modifying techniques, such as CRISPR, to prevent the development of ASD.

Conclusion:

In this study, statistical tools were used to analyze public databases in an effort to discover novel genes associated with autism by comparing DNA and RNA from autistic population and the general population. 31 down-regulated and up-regulated genes were identified in the cerebellum, frontal cortex, and temporal cortex which have a positive connection. Of these genes, 6 genes GGNBP2, TUBGCP5, ZDHHC8, DHRS11, RABL2B, and PANX2 have been identified to be tightly associated with ASD at RNA and genetic levels, and these genes may play a role in the pathogenesis of ASD.

Acknowledgements:

The author would like to thank Professor Pingzhang Wang of Peking University for guidance in this research.

References:

1. Yu X., Qiu Z., Zhang D. Recent Research Progress in Autism Spectrum Disorder // Neurosci. Bull.– No. 33(2). 2017.– P. 125–129.

2. Centers for Disease Control and Prevention, 2019. Treatment and Intervention Services for Autism Spectrum Disorder. URL: http://www.cdc.gov/ncbddd/autism/treatment.html.
3. Voineagu I., Wang X., Johnston P., Lowe J. K., Tian Y., Horvath S., Mill J., Cantor R. M., Blencowe B. J., Geschwind D. H. Transcriptomic analysis of autistic brain reveals convergent molecular pathology//Nature.– No. 474. 2011.– P. 380–384.
4. Dennis G. Jr., Sherman B. T., Hosack D. A., Yang J., Gao W., Lane H. C., Lempicki R. A. DAVID: Database for Annotation, Visualization, and Integrated Discovery // Genome Biol.– No. 4(5). 2003.– 60 p.
5. Lonsdale J., Thomas J., Salvatore M. et al. The Genotype-Tissue Expression (GTEx) project // Nat. Genet.– No. 45(6). 2013.– P. 580–585.
6. Landrum M. J., Chitipiralla S., Brown G. R., Chen C., Gu B., Hart J., Hoffman D., Jang W., Kaur K., Liu C. et al. ClinVar: improvements to accessing data // Nucleic Acids Res.– No. 48(D1). 2020.– P. D835-D844.
7. Velmeshev D., Schirmer L., Jung D., Haeussler M., Perez Y., Mayer S., Bhaduri A., Goyal N., Rowitch D. H., Kriegstein A. R. Single-cell genomics identifies cell type-specific molecular changes in autism // Science.– No. 364(6441). 2019.– P. 685–689.
8. Pardo C. A., Meffert M. K. Animal models in autism research: The legacy of Paul H. Patterson // Exp. Neurol.– No. 299(Pt A). 2018.– P. 197–198.

https://doi.org/10.29013/ELBLS-21-4-44-49

Tianrui Tan
The Experimental High School Attached
to Beijing Normal University
14 Erlong Road, Xicheng District, Beijing, China
E-mail: thomastianruitan@gmail.com

IMPACT OF HUMAN ACTIVITIES ON CORAL COVERAGE IN SANYA, CHINA

Abstract. The health condition of coral reefs has degraded seriously worldwide. Various factors account for the current decline of coverage of hard corals, including climate change, water pollution, spread of coral diseases, and an increase of natural predators. The development of tropical coastal regions has led to an increase in human activities, particularly in regions where coral reefs are present. Tourism, fishery, and aquaculture are potential human activities that can affect coral reef health. However, the impacts of such factors are still yet to be fully studied. To address this knowledge gap, this study developed a multiple linear regression model to quantify the impact of human activities, i.e., tourism, wild-capture fishery, and aquaculture, on coral coverage in Sanya, China. Annual overnight tourist number, wild-capture fishery production, and aquaculture production data in Sanya, China (2005~2018) were collected from official databases and reports. The results indicated a high correlation, R^2 of 0.832, and revealing that the number of tourist and fishery production have a negative and significant impact on the coverage rate of live hard corals, while the impact of aquaculture production is not significant. These results identify the serious threat of human activities on coral reef ecosystem in Sanya, and will raise public awareness of the impact of human activities on coral reef health, providing valuable insights for policy makers to the design of new coral reef protection strategies for the sustainability of the reef and marine ecosystem.

Keywords: Coral coverage, Human activities, Regression analysis, Indo-Pacific region, Sanya

Introduction

Coral reefs play a significant role in marine ecosystems and human life, maintaining biodiversity and energy throughput of tropical regions. Coral reefs, provide food resources, shelter, and spawning sites to an array of different marine organisms, accounting for almost 1/3 of the marine species in the world (1). The prolific marine organism resource also provided food, especially protein, for human. 10% of the world's wild-capture fishery production comes from coral reef regions (2). Plus, the calcium carbonate structure formed by hard corals strengthens and protects the shore line. During tropical storms, at least 70–90% of the energy of the wind-generated waves is absorbed by coral reef (3). Moreover, coral reef coral reefs are attracting tourists around the world for activities like scuba diving & snorkeling, supporting tourism in tropical coastal areas (4).

However, the health condition of coral reefs has degraded seriously throughout the world. Various factors account for the current decline of live hard coral coverage, including climate change, water pollution, spread of coral diseases, and increase of natural enemy population (4–7). In recent years, human activities have become increasingly prominent in tropical coastal areas with the development of

economy. Sanya, located on Hainan Island, a tropical island on the continental shelf of South China Sea, is a famous coastal tourist city in China. It is also on the north edge of the Indo-Pacific region — the hotspot of world's coral diversity — and have the most developed fringing reef in China (4, 8). Human activity in Indo-Pacific region is drastic and has affected the health of coral reef. Harvest of coral is the most direct way of harming the health of coral reef and has caused serious coral coverage decline in China in the 1980s (4). However, coral reserves have been established in some parts of the Indo-Pacific region, and destructive mass-harvest of coral for construction material rarely occurs currently (4). Pollutions caused by sewage dump also occurs in the Indo-Pacific region, but the seriousness of that problem can be reduced by the increasingly strict restriction of sewage discharge (4). Overfishing and tourist activities are becoming prominent in recent years (4). Although these two kinds of activities, except destructive fishing method like dynamite fishing, may not affect coral reef health through direct damage, changes of surrounding organisms and environment caused by fish catch or the disturbance of tourists cannot be ignored (5, 9).

Previous studies of coral reef degradation in Sanya and other parts of the Indo-Pacific region have focused on the major causes in different regions. Tito et al. (6) observed that global warming accounts for the decline of live coral cover rate in Bali, Indonesia. Increased water temperature caused coral bleaching in large scale. According to Guo et al. (7), water acidification caused death of corals in Great Barrier Reef, Australia by destructing the calcium carbonate skeleton of corals. It is also unignorable that the impact of natural enemies to live coral coverage can be drastic in a short period of time. Wu et al. (5) noticed that in Xisha Islands, China, the boost of population of crown-of-thorns starfish (*Acanthaster spp.*), a kind of native predator of coral polyps, has contributed to the dramatic drop of live coral coverage from 53.8% to 7.93% between 2007 and 2009. In mainland Asia, the most heavily populated area in the world, human impact is the major cause of coral reef degradation. Shi et al. (4) recorded 23 kinds human activities under 7 categories in Sanya, China and evaluated their impact level to coral reef health.

However, the previous studies about coral reef lack focus on quantitative analysis of co-relations between human activities and coral reefs, especially for newly emerged but rapidly developing activities such as recreations. Linear regression has been used to analyze the correlation between environmental factors and coral coverage. In the few existing quantitative analysis of human impacts on coral reef, a study of the impacts of recreation on coral reefs in Akumal, Mexico conducted by Gil et al. (9) used linear analysis to show the coral and algae coverage change under the disturbance of tourists.

A study using linear regression to quantify how serious the impact of human activities on the coral community in Sanya is can be influential. Apart from adding quantitative analysis of co-relations between human impacts and coral coverage, this study can also help people understand the leading factor causing coral reef degradation in certain areas and support the design of new coral reef protection measurements.

Methodology

The data in this study was originally collected in coral reefs along the coast of Sanya, China. The source of the data is "Report of the Situation of Chinese Coral Reef 2019"(10) and the Bureau of Statistic of Sanya (11).

This study focused on three determinants (independent variables), comprising tourism, wild-capture fishery, and aquaculture that affect the coral reef health in Sanya, China. The time range of data collected is 2005~2018.

In the study, tourism development was calculated from annual overnight tourist number of the regions. Wild-capture fishery was measured by annual marine wild-capture fishery production (tons). Plus, aquaculture was indicated by annual marine aquaculture production (tons). Finally, the coverage rate of live

hard coral (the dependent variable) was selected as the indicator of coral reef health.

Before analyzation, the data of annual overnight tourist number, annual marine wild-capture fishery production, and annual marine aquaculture production were normalized. The formula of this process is:

$$x_{normalized} = x / x_{\max}$$

In order to show the correlation between coral coverage and the human activities mentioned above, multiple linear regression models were developed. The formula is:

$$y = a_1 x_1 + a_2 x_2 + a_3 x_3 + e$$

y accounts for the dependent variable: live hard coral coverage rate. x_1 is annual overnight tourist number; x_2 annual marine wild-capture fishery production; x_3 annual marine aquaculture production. a is the estimated coefficient for each independent variable and e is the standard error.

Results and Discussions

Table 1. The Findings of Determinants of Live Hard Coral Coverage in Sanya, China

Variable	Estimated coefficients	Standard deviation	t-statistics	P-value
Constant	67.762	13.977	4.848	0.001
Tourist number (Overnight)	–37.423	5.905	–6.337	0.000
Wild-capture fishery production	–30.268	12.900	–2.346	0.041
Aquaculture production	6.667	7.983	0.835	0.423
Multiple R=0.912	R^2=0.832	Adjusted R^2=0.781		

The three factors analyzed account for about 83% of the decline in hard coral coverage (R^2 = 0.832) (Table 1). The number of tourists and fishery production are both significant ($P < 0.05$) while aquaculture production is not ($p = 0.42$). Hence, it is reasonable to conclude that tourism and wild-capture fishery are serious factors affecting the health of coral reef in Sanya.

Table 1 shows that tourist number are negatively correlated with the coverage of live hard coral in Sanya with the estimated coefficient of –37.423. The result shown above indicates that the influx of tourists every year impose significant pressure on the health of coral reef in Sanya.

Currently, tourism in Sanya negatively affects the health of coral reef in several direct or indirect ways. Firstly, scuba divers and snorkelers can cause direct physical harm to live corals. Although deliberately touching or breaking corals are banned, accidental contact with corals underwater can be frequently observed among divers or snorkelers and cause physical damage to live corals (12). For example, under strong underwater currents, it is easy for divers to grab or even bump into corals, which can damage soft tissues of polyps or ever crack calcium carbonate skeleton of corals (12). Plus, flippers of tourists can stir up seafloor sediments, which increase water turbidity and thus inhibit the growth of corals (12). Secondly, tourism can negatively influence the health of coral reef indirectly through pollution and the construction of tourism-related infrastructures. Hotels and restaurant built for tourists produce sewage and increase nutrient salt concentration of sea water, which cause eutrophication and inhibit coral growth (4, 13). Constructions related to tourism in coastal cities like Sanya often involve sea reclamation, which is disastrous to coral communities in shallow water along the coastline (4, 13)

In response to the problems caused by tourism, several actions should be considered. In order to relieve the pressure created by divers and involvers of other water sports, the number of tourist entry can be restricted. Diving spots like Wuzhizhou island in Sanya have already adopted a policy called diving-spot-rotation: opening different zones to tourists in different times of a year (12). Plus, setting higher sewage treatment standard ought to be considered when devising plans of coral reef preservation. Also,

the government should strictly control or ban sea reclamations in areas where coral reefs are present.

The next factor — wild-capture fishery production — is found to have negative correlation with coral coverage with the estimated coefficient of –30.268. This result indicates that fishery can also negatively affect the health of coral reef in Sanya.

According to previous studies, direct impact of fishery to coral reef health can be destructive. Practices like bomb fishing and electricity fishing used to be prevailed fishing methods in Indo-Pacific region and can still be observed frequently in developing countries in recent years (13). These destructive fishing methods can totally destroy coral reef ecosystem by decomposing reef structure and killing all the organisms living in the surrounding areas (14). After 1990s, destructive fishing method are banned by Chinese government and are greatly reduced in Sanya nowadays (5). In Sanya, fishery's most prominent impact on the health of coral reef is indirect. Although large-scale harvest of corals is rarely seen in Sanya after the national reserve of coral reef was established in the 1990s, overfishing of other marine organisms can be predicted to influence coral coverage. For example, *Charonia tritonis*, a kind of mollusk, is the major natural enemy of *Acanthaster cf. solaris*, which prey on coral polyps (15). A previous study has shown that overfishing of *Charonia tritonis* can cause the outbreak of *Acanthaster spp.*, threatening live coral communities (15). Sanya's coral reef has experienced the rapid increase of *Acanthaster spp.* population from 2006 to 2008, during which the live coral coverage declined significantly from 47% to 38% (10).

In order to minimize the impact to the health of coral reef of wild-capture fishery, fishery regulations should be carefully devised. Apart from banning destructive fishing method, time period and places in which commercial fishery is allowed should be considered. China has already set fishing-prohibit season in summer and has received positive feedback (16). Fishing-prohibit zone in places where coral reef is present has been shown effective in reducing harms of fishery to coral reef ecosystem in certain region like Wuzhizhou island, Sanya (12). Therefore, the policy of limiting or prohibiting the entry of commercial fishing vessels to certain coral reef zones can be added to the protection plan of coral reef in the scale of Sanya as a whole. Moreover, species which are important to the ecological equilibrium of coral reef ecosystem should be protected from overfishing. Catch share for species like large coral reef fish can be set to help the population of these species maintains stable.

According to the result listed in table 1, the correlation between aquaculture and live hard coral coverage is not significant. The estimated coefficient of this factor is only 6.667, and the P-value reaches 0.423 (exceeding 0.05), suggesting that aquaculture has a positive, but not significant, impact on coral reef health in Sanya.

Aquaculture can affect marine ecosystem both positively and negatively. Aquaculture can provide products to markets without catching individuals from the wild, which can relieve ecosystem's pressure created by overfishing (17). However, high-density aquaculture is able to cause pollution problems which are destructive to corals. The massive amount of feed, manure, and antibiotics released into water in aquaculture spots can cause eutrophication and inhibit coral growth (4, 18).In 2003, Shi et al. have recorded the decline of live coral coverage in places where aquaculture spots of algae and pearl shells were present in Luhuitou, Sanya (14).

In order to reduce the negative impact that aquaculture have on the health of coral reef and let aquaculture contribute to the protection of coral reef, scientific regulations are needed. The business conversion from fishery to aquaculture should be encouraged. But the density of individuals in an aquaculture spot should be limited. The use of antibiotics should be put under strict supervision. Sewage treatment technology need to be improved and the government ought to set up standard of sewage treatment.

Conclusion

This study identified the significant causes of coral reef degradation in Sanya, China by examining the correlation between human activities and live hard coral coverage with multiple linear regression. Human activities have a significant effect on the health of coral reefs in Sanya. Tourism and wild-capture fishery are major factors accounting for coral reef degradation in Sanya while the impact of aquaculture on coral reef health is slightly positive but not significant. When making policies of the protection of coral reef in Sanya, the scientific regulations of human activities should be considered as important parts. Because studies about impacts of human activities to coral reef health began relatively late in China, valid statistical data of specific tourist activities, fishery practices, and aquaculture practices in Sanya are not accessible yet. In order to further understand the mechanism of how tourism, fishery, and aquaculture affect the health of coral reef, future efforts can be paid on the collection of frequencies of more specific activities like scuba diving and the analysis of their correlations with coral coverage.

Reference:

1. Côté I.M., Reynolds J.D. Coral reef conservation. Cambridge University Press, UK, 2006.
2. Zhao M., Yu K., Zhang Q. Review on Coral Reefs Biodiversity and Ecological Function. Acta Ecologica Sinica, – 26. 2006. – P. 186–194.
3. Wells S., Ravilious C. In the front line: shoreline protection and other ecosystem services from mangroves and coral reefs. UNEP/Earthprint, 2006.
4. Shi Q., Zhao M., Huang L., Yan H., Zhang H. Human activities and Impacts on Coral reef at the Luhuitou Fringing Reef, Sanya. Tropical Geography, – 5. 2010. – P. 486–509.
5. Wu Z., Wang D., Tu Z., Li Y., Chen J., Zhang G. The Analysis on the Reason of Hermatypic Coral Degradation in Xisha. Acta Oceanologica Sinica, – 33. 2011. – P. 140-146.
6. Tito C.K., Ampou E.E. Coral reefs ecosystem degradation at Nusa Penida, Bali. IOP Conference Series: Earth and Environmental Science, – 429. 2020. – 012053 p.
7. Guo W., Bokade R., Cohen A.L., Mollica N.R., Leung M., Brainard R.E. Ocean acidification has impacted coral growth on the great barrier reef. Geophysical Research Letters, – 47. 2020.
8. Förderer M., Rödder D., Langer M.R. Patterns of species richness and the center of diversity in modern Indo-Pacific larger foraminifera. Sci Rep 8, – 81, 2018.
9. Gil M.A.., Renfro B., Figueroa-Zavala B., Penié I., Dunton K.H. Rapid tourism growth and declining coral reefs in Akumal, Mexico. Marine Biology, – 162. 2015. – P. 2225–2233.
10. Pacific Society of China, Branch of Coral Reef. Report of the Situation of Chinese Coral Reef 2019. 2020.
11. 统计年鉴_三亚市统计局. (n.d.). URL: http://www.sanya.gov.cn/tjjsite/tjnj/list2.shtml.
12. Zhang Y., Ren Y., Liu X., Zhu M., Wang A., Li X. A review of impact of diving tourism on coral reef ecosystem. Journal of Tropical Biology, – 12. 2021. – P. 261-270.
13. Peramunagama SSM, Ramanathan T. The Importance of Involving Community Organizations for Preventing Destructive Fishing Activities in Mannar, Sri Lanka. Advances in Technology, – 1. 2021. – P. 177–190.
14. Shi q, Zhao M., Zhang Q., Wang H., Wang L. Growth variation of scleratinan corals at Luhuitou Sanya Hainan Island and the impact from human activities. Acta Ecologica Sinca, – 27. 2007. – P. 3316–3323.
15. Hall M.R., Motti C., Kroon F. The potential role of the giant triton snail, Charonia tritonis (Gastropoda: Ranellidae) in mitigating populations of the crown-of-thorns starfish. Integrated Pest Management of Crown-of-Thorns Starfish, 2017.

16. Wu C., Zhang Y., Liu W., Zhao H., Chen M. Assessment of the impact of summer fishing moratorium in the offshore fishing grounds of Hainan Island based on landing survey. Journal of Fisheries Research, – 2. 2021. – P. 200–206.
17. Bu F., Dai G. The economic analysis on marine farming. Chinese Fisheries Economics, – 2. 2009. – P. 33–38.
18. Zeng R., Qi Z., Zhang T., Gong Y., Zhang Q., Wang H., Diao X. Characteristic of antibiotic pollution and ecological risk assessment in eastern Mariculture area of Hainan Province. Journal of Tropical Biology, – 12. 2021. – P. 41-48.

https://doi.org/10.29013/ELBLS-21-4-50-68

Yuan Bi,
The Webb School of California
High School Student
E-mail: andy13842823539@outlook.com

SYSTEMATIC ANALYSIS OF GENETIC VARIATIONS IN FGFR2 AND THE ASSOCIATION WITH HUMAN DISEASE

Abstract. Crouzon Syndrome (CS) and Jackson-Weiss Syndrome (JWS) are two types of craniosynostosis syndromes which are resulted from the premature fusion of fibrous tissue. The Phenotypes of CS and JWS are restricted growth of skull, brain and central nervous system. Genetic variants in the fibroblast growth factor receptor 2 (*FGFR2*) gene were reported to be related to CS and JWS. To our knowledge, a systematic analysis of all genetic variations in *FGFR2* has not been previously reported. We performed a genetic analysis on a total of 947 exonic variants in *FGFR2,* and concluded the variation pattern of *FGFR2* gene including variation distribution across different exons, multiple types of variants, and frequency of variations across human population groups. We then examined the relationship between *FGFR2* genetic variations and CS as well as JWS, and suggested gene therapy to treat the diseases. We analyzed mutations in *FGFR2* that cause different cancers and expression of *FGFR2* across different cancers. We also performed pathogenicity predictions on frequent *FGFR2* somatic mutations.

Keywords: Fibroblast Growth Factor Receptor 2, Crouzon Syndrome, Jackson-Weiss Syndrome, Mutations, Cancers, Pathogenicity Prediction.

1. Introduction

Crouzon Syndrome (CS) and Jackson-Weiss Syndrome (JWS) are two types of craniosynostosis syndrome, which has characteristics of premature fusion of fibrous joints and restricted growth of skull, brain and central nervous system. CS is the most common type of craniosynostosis syndrome [1]. CS has an approximate prevalence of 1 in 25,000 births in the world. 67% of the cases are familiar and 33–56% of the cases derive from spontaneous genetic variations [2].

CS has characteristics of abnormal growth of facial bones because of premature fusion of the fibrous tissue. The abnormal skull shapes formed include scaphocephaly (fusion of sagittal suture), oxycephaly (fusion of the lambdoid and coronal sutures), brachycephaly (fusion of coronal suture). Some craniofacial abnormalities such as prominent forehead and protrusion of eyeballs are associated with malformation of skulls [3]. CS's severity and patients' symptoms vary within different families [4].

JWS is another disease that is characterized by abnormal formations of facial structures and skulls. JWS is a rare disease, and the exact prevalence frequency of JWS is not reported yet. JWS is a disease of craniosynostosis and there are many clinical similarities between JWS and CS [5]. JWS presents limb abnormalities as people with JWS have toes with medial deviation, and its severity can vary [5, 6].

Studies have reported that both CS and JWS are caused by mutations in human fibroblast growth factor receptor 2 (*FGFR2*). *FGFR2* spanning about 119,744 bp (base pairs) of genomic sequence and residing on chromosome 10, encodes a receptor tyrosine kinase [7]. The full length of messenger RNA (mRNA) of *FGFR2* is 4,624 bp, which contains

a coding sequence of 2,466 bp and is further translated into FGFR2 protein with 821 amino acid residues [8,9]. FGFR2 protein belongs to the fibroblast growth factor receptor (FGFR) family, and members of the FGFR family are different from each other in tissue distribution and ligand affinities.

FGFR2 is composed of three regions: (i) an extracellular region; (ii) a transmembrane region; (iii) intracellular tyrosine kinase domains (TK1 and TK2) [10]. IgII, IgIII and link between these Ig-like domains interacts with the FGF ligands, which creates a cascade of downstream signals. Studies have shown that FGFR2 protein is essential in controlling and regulating cell proliferation, differentiation, migration, and apoptosis [11].

Genetic mutations of *FGFR2* increase the binding affinity while binding to fibroblast growth factor (FGF) ligands, disrupting cell differentiation and causing developmental defects [12,13]. Most of the sequence changes that cause craniosynostosis syndromes including CS and JWS are encoded in the extracellular ligand-binding portion, specifically between the IgII and the IgIII [14].

This *FGFR2* genetic research analyzed all the variants of the gene, and to our knowledge, a comprehensive analysis of genetic variations in *FGFR2* were not previously reported yet. The aim of this genetic research is to conduct a systematic analysis of *FGFR2* gene genetic variations using key information extracted from a human genome variation database. Examples of the key information extracted are types of variations, nucleotides change, exon sequencing, and amino acid changes. The analysis focuses on relationships between *FGFR2* variations and CS as well as JWS. In addition, we found that the genetic mutations of the *FGFR2* gene was associated with multiple types of cancer. Therefore, gene mutation and subsequent functional effects of *FGFR2* in human cancers were also investigated in the study.

2. Materials and Methods

This study uses a series of online tools and web sources to assist our bioinformatics analyses.

2.1 Single nucleotide polymorphism database

The Single Nucleotide Polymorphism Database (dbSNP) was established by the National Center for Biotechnology Information (NCBI) aiming to address large sampling designs [15]. After its establishment, dbSNP has served as a central repository of genetic variants for the public use purpose. dbSNP documents the following nucleotide sequence variations (i) single nucleotide substitutions; (ii) small insertion/deletion polymorphisms; (iii) sequence invariant sequence; (iv) microsatellite repeats; (v) named variants; (vi) uncharacterized heterozygous assays. Besides, dbSNP records information of population frequency, neutral polymorphisms, and disease-causing mutations [16]. All current known genetic variants in human genome are recorded in the database and can be downloaded freely. Therefore, human genetic variations in *FGFR2* gene were extracted from the online compressed file (ftp://ftp.ncbi.nlm.nih.gov/snp/organisms/human_9606/VCF/00-All.vcf.gz) of the Human Variation Sets File in VCF (Variant Call Format), and used for next steps of analysis.

2.2 Genetic variant annotation

In order to obtain the annotated Ensemble gene results, a VCF format file containing all SNP sites of *FGFR2* (FGFR2.vcf) was uploaded to wANNOVAR (http://wannovar.wglab.org/) [17]. wANNOVAR is the web server version of ANNOVAR, which researchers used to perform genetic variants functional annotations from the sequence data. Both "exome summary results" containing all variants in the exome and "genome summary results" including variants in the whole gene are outputted.

2.3 The Cancer Genome Atlas datasets

The Cancer Genome Atlas Project (TCGA), established by National Cancer Institute, includes data of at least 10,000 cases of more than 30 different tumor types. The processed data in TCGA contains genome sequence, exome sequence, RNA expression data, and clinical datasets [18]. Data of cancer studies in this *FGFR2* genetic research comes from

TCGA. We analyzed mutations in *FGFR2* that cause cancers and expression of *FGFR2* across different cancers.

2.4 Somatic gene mutation analysis

We used the online tool cBioPortal (https://www.cbioportal.org/) to perform FGFR2 gene mutations analysis. cBioPortal for Cancer Genomics was designed for users to have easy access to complicated gene datasets and facilitate the transition of raw genomic data into direct biological information. It provides an extensive set of tools for exploration and visualization of cancer genomics data involving large numbers. The data sets in cBioPortal contain studies from TCGA [19, 20]. We also obtained the visualizations of different cancers' alteration frequency in *FGFR2* gene using cBioPortal.

2.5 Differential expression analysis in cancers

In order to analyze genetic expression of FGFR2 across different cancers, we further used UALCAN (http://ualcan.path.uab.edu/). UALCAN is an online tool that used data from TCGA to give comparison of gene expression across tumor samples and normal samples. UALCAN is also used by researchers to identify over-expressed or under-expressed genes in different types of cancer [21]. This *FGFR2* genetic research uses UALCAN to obtain visualization of comparison between gene expression of normal samples and tumor samples.

3. Results

3.1 Research workflow

This study integrated a series of online tools and web sources to perform a systematic analysis of genetic variations in human *FGFR2* gene (Figure 1). Briefly, data information of the genetic variations was firstly extracted from the dbSNP database in variant call format (VCF). The VCF was then uploaded to wANNOVAR in order to obtain functional annotations result file genetic variants. The result file contains multiple columns representing different annotation tasks. We selected key columns that are significant to this research and performed analysis on these data. The cancer studies in this research came from TCGA and online tools including cBioPortal and UALCAN (Figure 1).

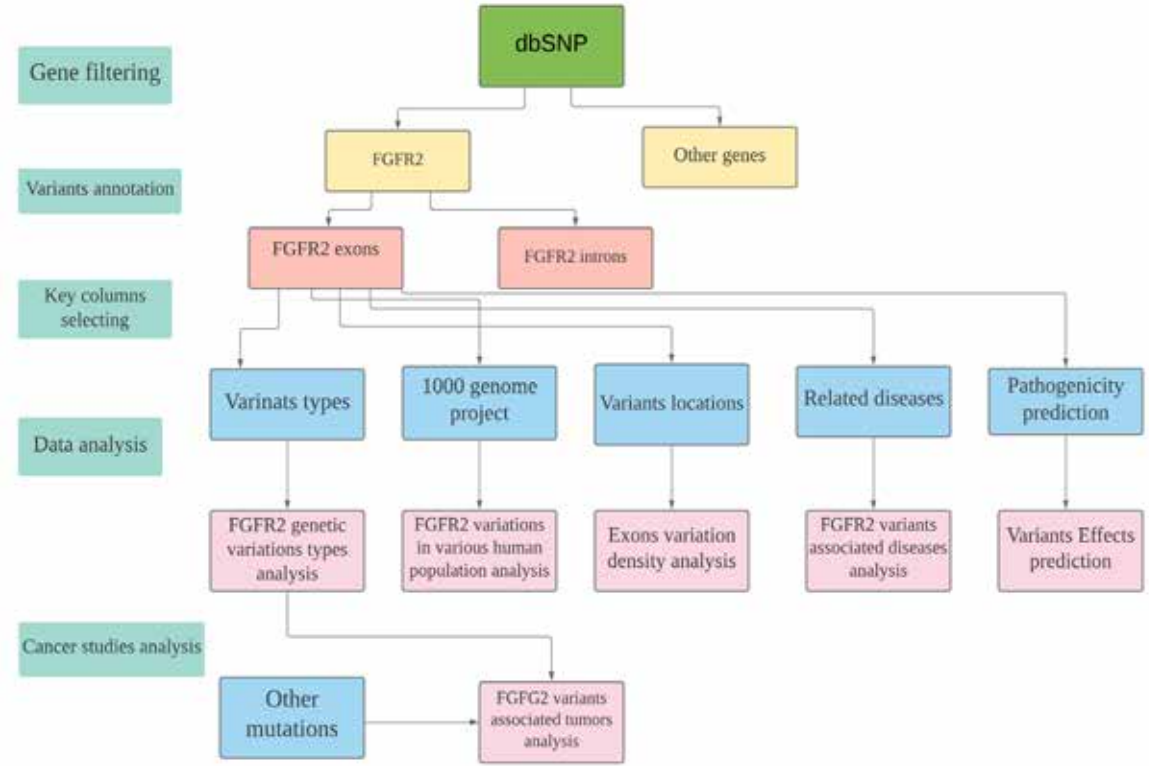

Figure 1. Research workflow

3.2 Brief information about FGFR2

Human *FGFR2* gene resides on chromosome 10. Ensembl provides comparative analysis at genomic and genic levels, and different transcripts can be compared [22]. The Ensemble gene ID of FGFR2 is ENSG00000066468, which has multiple transcripts from post-transcriptional processing mechanisms. The longest transcript has a transcript ID of ENST00000358487 and this transcript is 4,624 bp in length [23] (Figure 2).

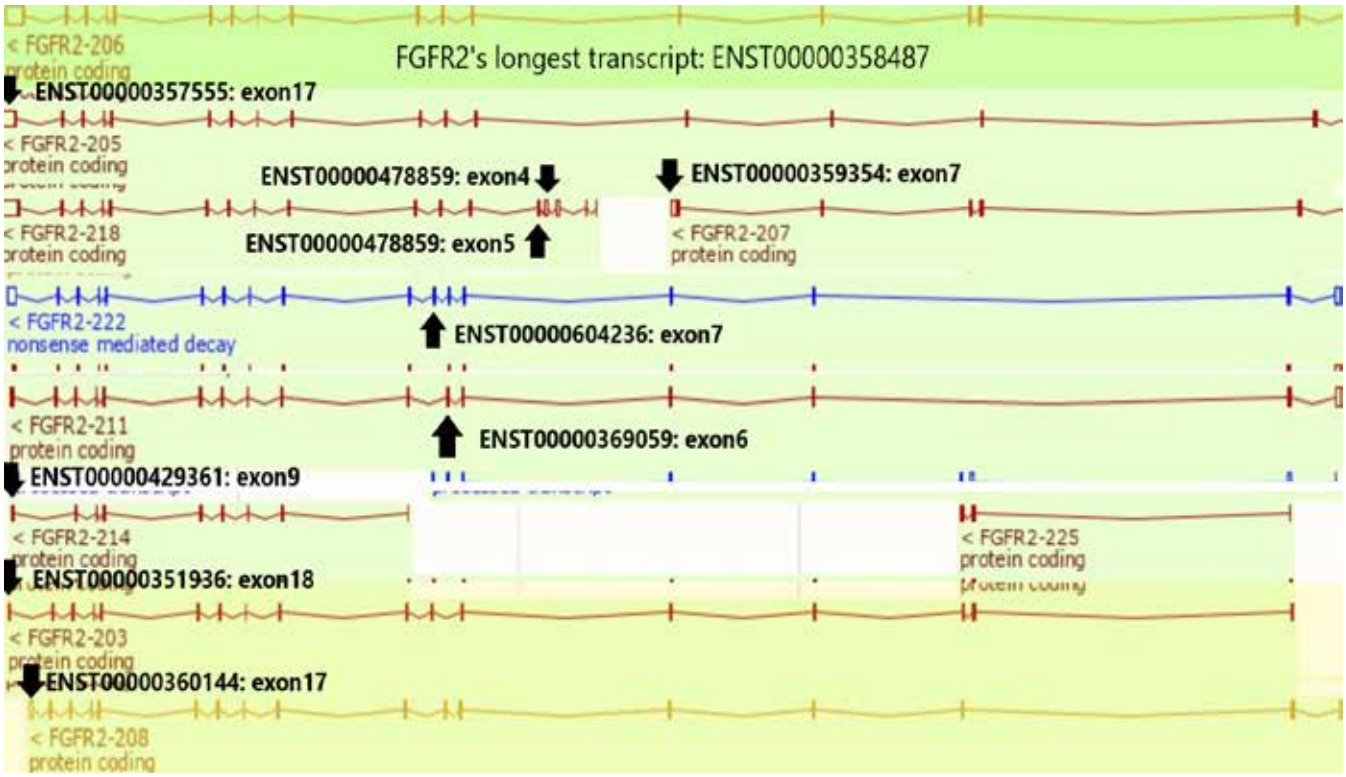

Figure 2. Gene structure of human *FGFR2*. We used arrows to indicate structures of exons and introns in all transcripts.

The longest transcript is ENST00000358487, which has the greatest number of exons out of all transcripts. In this research, we set exons locations on ENST00000358487 as reference standard to exons in other transcripts. However, there are variations on exons on other transcripts that do not accord with exons locations on transcript ENST00000358487. We mark these exons using arrows FGFR2 is a tyrosine-protein kinase that binds to ligands and activates signaling pathways [24]. The FGF family includes at least 22 known FGF ligands that bind to the extracellular ligand-binding region of the FGFR2 protein. FGFR2 interacts with the FGF1 ligand, while the spliced isomers of FGFR2 can interact with other members of the FGF family such as FGF1, FGF2, FGF3, and FGF4 [25, 26, 27].

FGFR2 activates several signaling pathways through binding to the FGF ligands (Figure 3). This pathway includes: (i) phosphoinositide 3-kinase (PI3k)/ protein kinase B (Akt); (ii) phospholipase C gamma 1 (PLCG1) and protein kinase C (PKC); (iii) mitogen-activated protein kinase (MAPK) and extracellular signal-related kinases 1 and 2 (ERK 1/2) [25, 26, 27]. The FGF/FGFR signaling is essential in biological process including bone formation and homeostasis. Mutations in *FGFR2* can cause unregulated FGF signaling and premature suture closure, as dysregulated downstream signaling including enhancement of pathways PLCG1, phosphoinositide 3-kinase (PI3K)/Akt, and RAS/RAF/MAPK [28].

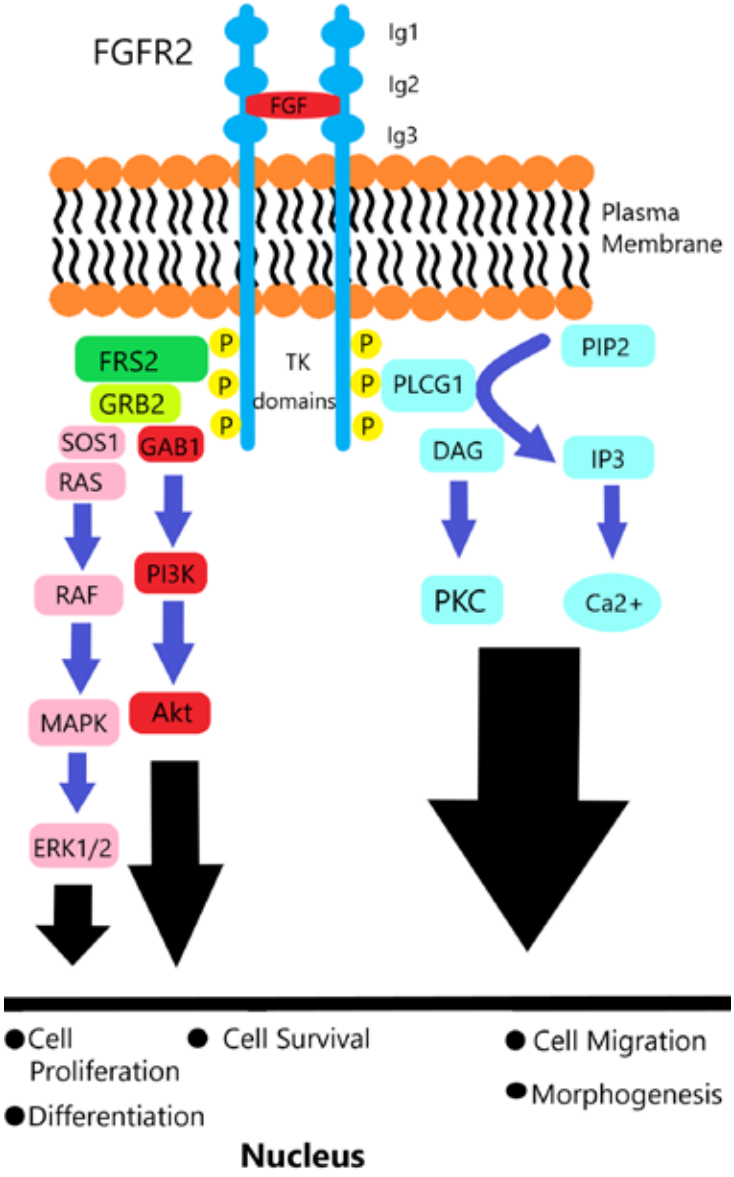

Figure 3. FGFR2's main signaling pathway. FGFR2 signaling pathways contain 3 main pathways.

Phosphorylation of PLCG1 leads to the production of cellular signaling molecules diacylglycerol (DAG) and inositol 1,4,5-trisphosphate (IP3). PKC is then activated by DAG, and calcium is released from IP3, which regulated cells migration and morphogenesis. Phosphorylation of FRS2 can recruit growth factor receptor-bound protein 2 (GRB2), GRB2-associated-binding protein (GAB1) and son of sevenless homolog 1 (SOS1), which in turn mediates the RAS/RAF/MAPK signaling pathway and PI3K/Akt pathway. The pathway can then activate ERK1/2, controlling cell proliferation and differentiation. The PI3K/Akt pathway regulates cells survival.

3.3 Genetic variations distribution

wANNOVAR outputted a total of 26,169 variants, and the variants occur in different regions. (Figure 4) The "genome summary results" contains all the variants, and "exome summary results" only contain variants occurring in exons, which are approximately 3.6% (947/26,169) of all the genetic variations. Intronic variants accounts for approximately 91% (23,824/26,169) of all genetic variations in *FGFR2* gene (Figure 4) This *FGFR2* genetic

research mainly focused on the "exome summary results" because genetic alterations occurring in exons can affect the proteins produced from gene.

wANNOVAR classifies all of the gene variants into following several categories: synonymous single nucleotide variation (SNV), nonsynonymous SNV, frameshift insertion, frameshift deletion, frameshift substitution, nonframeshift insertion, nonframeshift deletion, nonframeshift substitution, startloss, startgain, stoploss, stopgain [30].

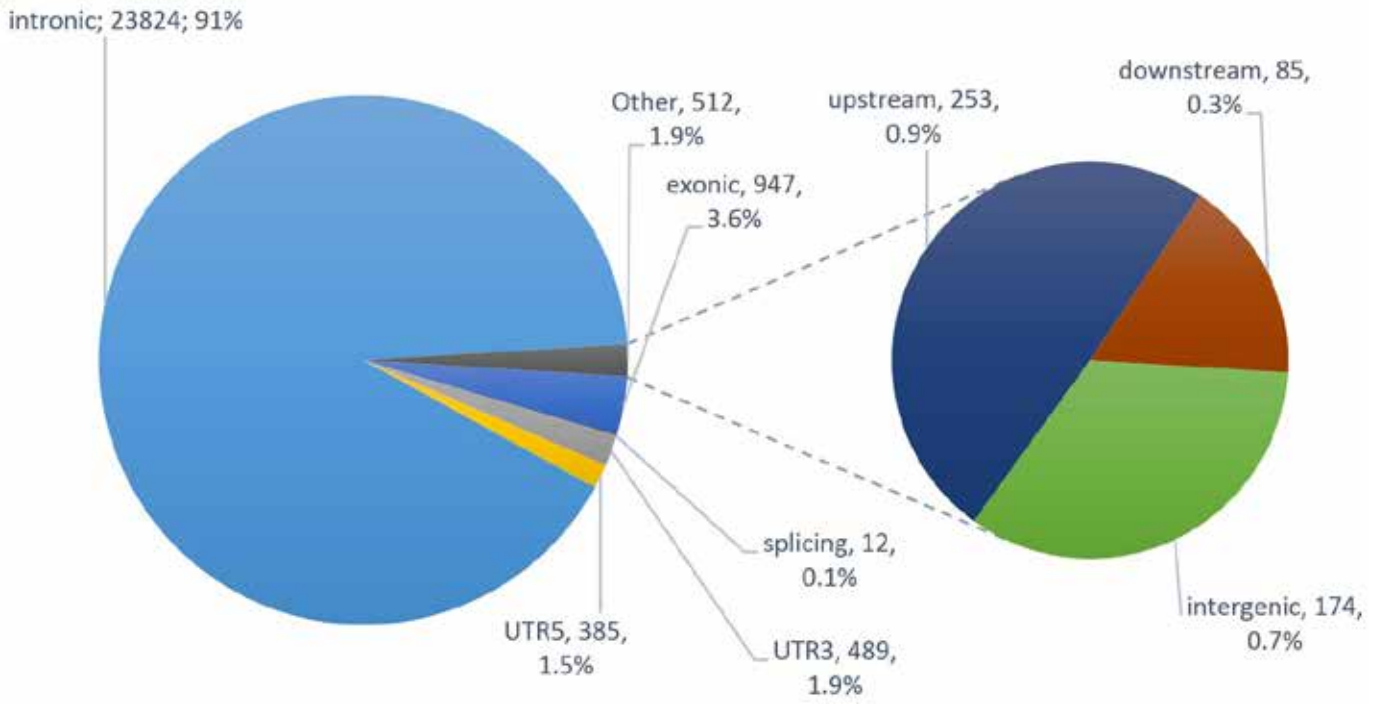

Figure 4. Distribution of genetic variants across different regions in *FGFR2*.

3'-untranslated regions (UTR3) and 5'-untranslated regions (UTR5) respectively refer to untranslated region found on 3 prime side or 5 prime side of the coding sequence Both upstream and downstream refer to relative positions of genetic code in DNA. Upstream is towards the 5-prime end of the coding sequence, while downstream is toward the 3-prime end. Splicing refers to the boundary of exons and introns. Intergenic region refers to the stretch of sequences located between successive genes. Different regions of *FGFR2* gene are marked with numbers of variants found within the regions and percentage to the total number of variants [29].

Among all 947 exonic variations in *FGFR2* gene, nonsynonymous SNV is the most frequent type of variation as it accounts for approximately 60% of all exonic genetic variations. The least frequent type of variant is nonframeshift insertion as it only accounts for 1% of all exonic variations in *FGFR2*. Frameshift substitution and startgain are not found in all of the exonic genetic variations in *FGFR2* (Table 1).

Table 1. – Counts and percentage of exonic variants types in *FGFR2* gene

Variation Types	Definition	Counts	Percentage
1	*2*	*3*	*4*
Synonymous SNV	Single Nucleotide Variation that causes no amino acid changes.	324	34%

1	*2*	*3*	*4*
Nonsynonymous SNV	Single Nucleotide Variation that causes amino acid changes.	574	60%
Frameshift Insertion	Insertion of nucleotides whose numbers are not divisible by three, disrupting the reading frames.	4	0.5%
Frameshift Deletion	Deletion of nucleotides whose numbers are not divisible by three, disrupting the reading frames	10	1%
Frameshift Substitution	Substitution of nucleotides that causes disruptions in reading frames.	0	0%
Nonframeshift Insertion	Insertion of nucleotides whose numbers are divisible by three, which does not disrupt the reading frame.	1	0.2%
Nonframeshift Deletion	Deletion of nucleotides whose numbers are divisible by three, which does not disrupt the reading frames.	7	0.9%
Nonframeshift Substitution	Substitution of nucleotides that disrupt no reading frames.	5	0.6%
Startloss	Variant that results in elimination of start codon.	2	0.3%
Startgain	Variant that results in creation of start codon.	16	2%
Stoploss	Variant that results in elimination of stop codon.	4	0.5%
Stopgain	Variant that results in creation of stop codon.	0	0%
Total		947	

Genetic variations were distributed in different exons. Ensemble provides the length of exons in FGFR2 gene in different transcripts. There are a total of 26 exons having genetic variations in the result file, and among all 26 exons, exon 18 in transcript ENST00000358487 is the longest with 1690 bp in length. Exon 5 in transcript ENST00000478859 is the shortest with 40 bp in length. We observed the numbers of genetic variants across different exons in the result file. Exon 3 in transcript ENST00000358487 has highest numbers of variations as there are 99 genetic variations occurring in this exon. Exon 7 of transcript ENST00000604236 and exon 7 of transcript ENST00000359354 have least genetic variations and each of them has 3 genetic variations. (Figure 5).

We then calculated the variation density of different exons by dividing variation numbers in the exon over exon length. Among the 26 exons, exon 7 of transcript ENST00000358487 has highest variation density of 0.43, followed by exon 8 of transcript ENST00000358487 with variation density of 0.41. Exon 1 of transcript ENST00000358487 has lowest variation density of 0, as there are no variants reported on this exon. Exon 7 of transcript ENST00000359354 has second lowest variation density of 0.006. (Figure 5).

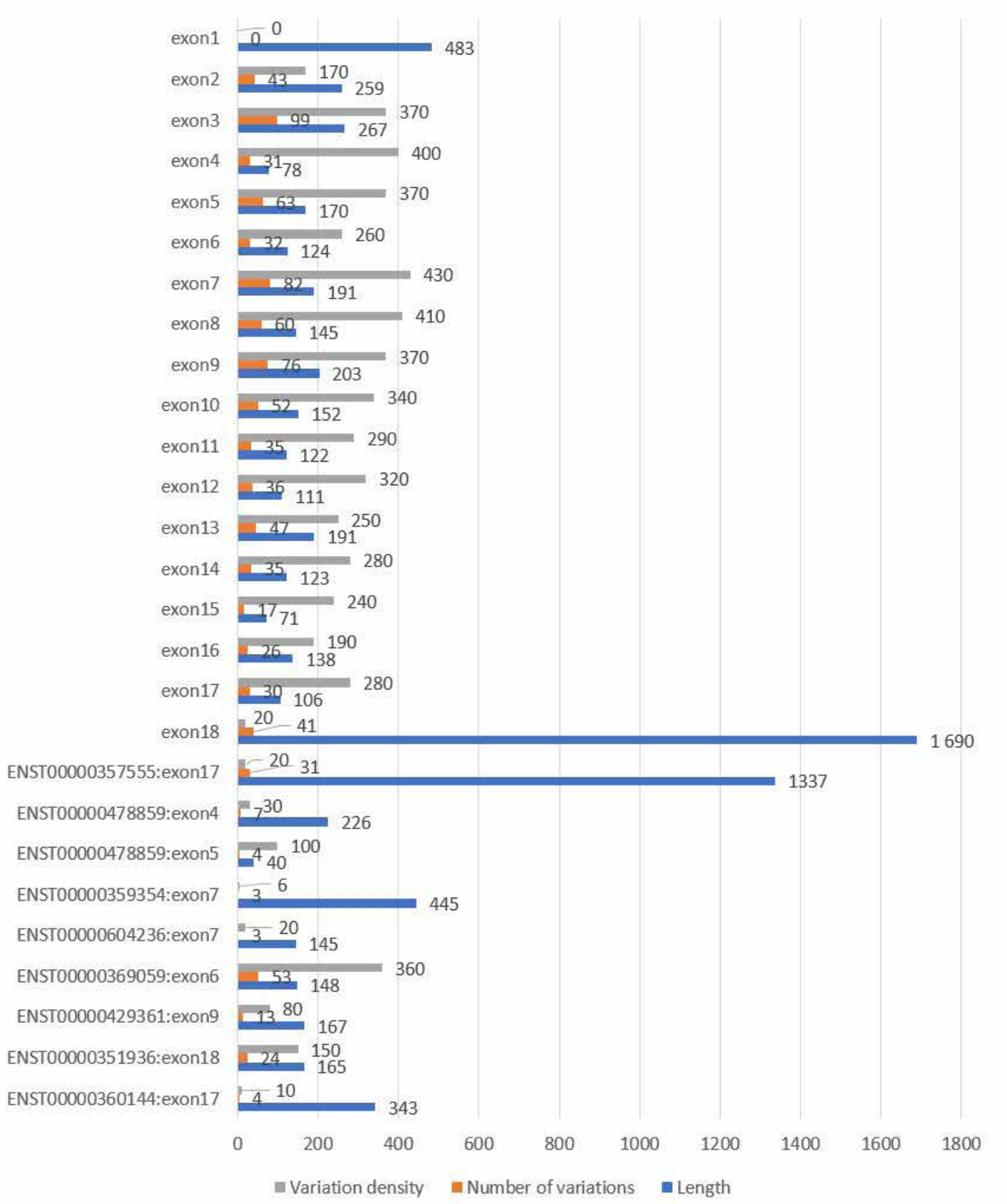

Figure 5. Exons' length and variations number across different exons. We multiplied each exon's variation density by 1000 in order to clearly visualize the comparisons

We set exons sequence on transcript ENST00000358487 as standard references to exons in other transcripts. For exons that are not on transcript ENST00000358487, we marked the transcripts they appear on and exon numbers according to different transcripts.

3.4 Exome annotation result

The file "exome summary results" contains 140 columns and 948 rows. Except for the first row containing column titles, each row represents a genetic variant in *FGFR2* exome. Each column describes an annotation task wANNOVAR performs on the *FGFR2* variants, and we extracted information from some columns (Table 2) in this *FGFR2* genetic research.

Table 2. – Selected columns from exome annotation file

Column Names	Column Descriptions
Chr	Chromosome that the gene locates on
Start	Start nucleotide number of the SNP
End	End nucleotide number of the SNP
Ref	Original nucleotides before the SNP
Alt	New nucleotides after the SNP
Func.ensGene	Regions where SNP occurs
Gene.ensGene	Ensemble ID of the gene
ExonicFunc.ensGene	Types of SNP
AAChange.ensGene	Change of amino acids because of gene variations
1000G (ALL, AFR, AMR, EAS, EUR, SAS)	Allele frequency in 1000 Genome Project. The population groups include the following categories: ALL, African, American, East Asian, European, South Asian.
ClinVar_SIG	Interpretation provided by ClinVar of relationships between genetic variations and diseases [31].
ClinVar_DIS	Diseases associated with the variations [30].
COSMIC_DIS	Effects of SNPs across human cancers
COSMIC_ID	ID identified by Catalogue of Somatic Mutations in Cancer (COSMIC) [32]
SIFT_score	Predicts the effects of amino acid substitutions on proteins. Ranges from 0.0 (deleterious) to 1.0 (tolerated)
SIFT_pred	Predicts the SNP to be D (deleterious) or T (tolerated)

The "exome summary results" contains various columns performing different annotation tasks on genetic variations, and users can select key columns to perform genetic alterations analysis.

Based on the annotation, 37 genetic variations in 25 genome positions are identified to be associated with CS and JWS (Table 3). In addition, there are 26 variations which are predicted to be pathogenic in term of the Five-Tier Terminology System [33] (Table 4).

Table 3. – This table includes all of the *FGFR2* genetic variants that are identified to be associated with CS or JWS. For exons that are not marked with transcripts, they are on transcript ENST00000358487

rsID	Exon located	Amino acid change	Diseases related	Relationship with diseases
rs3750819	Exon2	R6H	CS|JWS	benign|benign
rs3750819	Exon2	R6P	CS|JWS	benign|benign
rs56226109	Exon3	S57L	CS|JWS	likely benign|likely benign
rs755793	Exon5	M186T	CS	benign
rs121918505	Exon7	S267P	CS	pathogenic
.	Exon7	F276V	CS	pathogenic
.	Exon7	Y281C	CS	likely pathogenic
rs121918497	Exon7	Q289P	CS|JWS	pathogenic|pathogenic
rs121918501	Exon7	W290R	CS	pathogneic
rs121918501	Exon7	W290G	CS	pathogenic
.	Exon7	W290S	CS	pathogenic
rs121918500	Exon7	K292E	CS	pathogenic
.	Exon7	Y308C	CS	pathogenic
rs121918493	Exon8	Y328C	CS	pathogenic
.	Exon8	D336G	CS	pathogenic
rs387906676	Exon8	A337T	CS	pathogenic
rs387906676	Exon8	A337P	CS	pathogenic
.	Exon8	G338R	CS	pathogenic
.	Exon8	G338E	CS	pathogenic
rs121918489	Exon8	Y340H	CS	pathogenic
rs121918488	Exon8	C342S	JWS	pathogenic
rs121918488	Exon8	C342R	JWS	pathogenic
.	Exon8	C342G	JWS	pathogenic
rs121918487	Exon8	C342Y	JWS	pathogenic
.	Exon8	C342S	JWS	pathogenic
.	Exon8	C342F	JWS	pathogenic
rs121918496	Exon8	C342W	CS	pathogenic
rs121918492	Exon8	A344G	CS|JWS	pathogenic|pathogenic
rs121918494	Exon8	S347C	CS	pathogenic
rs121918490	Exon8	S354C	CS	pathogenic
rs121918507	Exon12	K526E	CS	pathogenic
.	Exon12	N549H	CS	likely pathogenic
rs141929882	Exon13	R592C	CS|JWS	likely pathogenic|likely pathogenic
rs558460047	ENST00000429361: Exon9	T362M	CS|JWS	likely benign|likely benign
rs748777325	ENST00000357555: Exon17	K682Rfs*38	CS|JWS	likely benign|likely benign
rs764959117	Exon18	E806K	CS|JWS	Uncertain Significance| Uncertain Significance
rs764959117	Exon18	E806Q	CS|JWS	Uncertain Significance| Uncertain Significance

Table 4. – Definition of terms used in the five-tier terminology system. The American College of Medical Genetics and Genomics established the five-tier terminology system to indicate the relationships between genetic variations and diseases.

Terms	Definition
Pathogenic	The genetic variant is disease-causing
Likely Pathogenic	The certainty that the genetic variant being diseasing-causing is greater than 90% [33]
Uncertain Significance	Unknown whether genetic variation is disease-causing
Benign	The genetic variation is not disease-causing
Likely Benign	The certainty that the genetic variant not being disease-causing is greater than 90% [33]

We examined the data to determine relationship between genetic variations and CS disease or relationship between genetic variations and JWS disease. We analyzed genetic variations (we did not include synonymous SNV because it does not change amino acids) across different exons and their associations with the diseases. For JWS, variants in exon 8 of transcript ENST00000358487 accounts for 87.5% (7/8) of pathogenic variations, and variants in exon 7 of transcript ENST00000358487 accounts for the rest 12.5% (1/8). For CS, exon 8 of transcript ENST00000358487 has 55% of all pathogenic variants, exon 7 of ENST00000358487 has 40%, and exon 12 of ENST00000358487 has 5% (Figure 6).

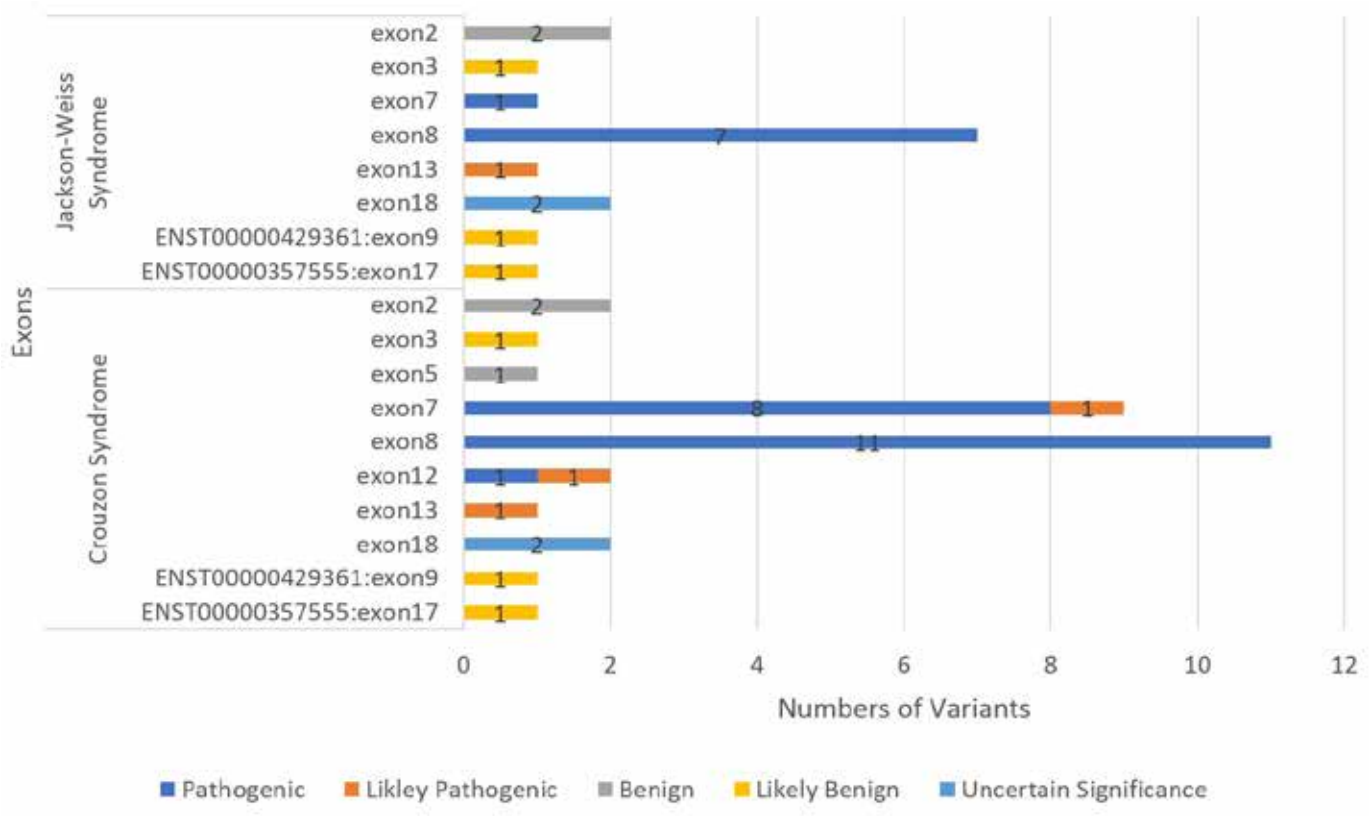

Figure 6. Distributions of FGFR2 genetic variants that have relationships with CS and JWS across different exons. For exons that are not marked with transcript ID, they belong to transcript ENST00000358487

We also analyzed different types of SNPs (including synonymous SNV) and their associations with CS as well as JWS. Most (95%) of the CS pathogenic variants are classified into nonsynonymous SNV. Interestingly, there is one synonymous SNV being pathogenic to CS even though synonymous SNV does not generally cause amino acid changes. All of the variants that are pathogenic to JWS belong to nonsynonymous SNV. There is one frameshift deletion variation analyzed to be likely benign to both CS and JWS. All other types of variations were not reported to have relationships with CS and JWS.

3.5 Genetic variations across human population groups

One of the annotation tasks performed by wANNOVAR is giving gene's Human 1000 Genome Project data. The aim of the 1000 Genome Project is to present a comprehensive description of genetic variations of human through sequencing individuals' genomes [34]. The 1000 Genome Project classifies populations into the following 5 major categories: African, American, European, East Asian, and South Asian [35]. In *FGFR2* gene, we analyzed 5 variants to have distinctively different variation frequency in different human population groups.

Among the five genetic variations, four are classified into synonymous SNV, and one of the variants is nonsynonymous SNV. We focused on the analysis of the nonsynonymous SNV variant because synonymous SNV does not have functional consequence to the protein encoded. This nonsynonymous SNV is ENSG00000066468: ENST00000358487: exon5: c.T557C: p.M186T and the rsID is rs755793. This variant has a frequency of 0.36 in African population, 0.11 in American population, 0.065 in Eastern Asian population, 0.007 in European population, and 0.002 in Southern Asian population.

3.6 *FGFR2* exonic alterations and associations with tumors

FGFR2 genetic variants are related to different types of cancer. Deregulation of FGFR2 protein caused by *FGFR2* alterations has been reported to contribute to tumor progression, and alterations in *FGFR2* are found in several types of cancer [36].

cBioPortal provides mutations analysis of different types of tumors using studies from TCGA. In this *FGFR2* genetic research, we analyzed data from 30 published cancer studies from TCGA and 4 extra published cancer studies in the cBioPortal database. A total of 11305 samples from 11255 patients were included in the cancer analysis (Table 5) [37, 38].

Table 5. – Cancer studies and number of samples in each study

Cancer Studies	Number of Samples
1	*2*
Acute Myeloid Leukemia (TCGA, PanCancer Atlas)	200
Adrenocortical Carcinoma (TCGA, PanCancer Atlas)	92
Bladder Urothelial Carcinoma (TCGA, PanCancer Atlas)	411
Brain Lower Grade Glioma (TCGA, PanCancer Atlas)	514
Breast Invasive Carcinoma (TCGA, PanCancer Atlas)	1084
Cervical Squamous Cell Carcinoma (TCGA, PanCancer Atlas)	297
Cholangiocarcinoma (TCGA, PanCancer Atlas)	36
Colorectal Adenocarcinoma (TCGA, PanCancer Atlas)	594
Diffuse Large B-Cell Lymphoma (TCGA, PanCancer Atlas)	48
Esophageal Adenocarcinoma (TCGA, PanCancer Atlas)	182
Glioblastoma Multiforme (TCGA, PanCancer Atlas)	592
Head and Neck Squamous Cell Carcinoma (TCGA, PanCancer Atlas)	523
Kidney Renal Clear Cell Carcinoma (TCGA, PanCancer Atlas)	512
Liver Hepatocellular Carcinoma (TCGA, PanCancer Atlas)	372

1	*2*
Lung Adenocarcinoma (TCGA, PanCancer Atlas)	566
Lung Squamous Cell Carcinoma (TCGA, PanCancer Atlas)	487
Mesothelioma (TCGA, PanCancer Atlas)	87
Ovarian Serous Cystadenocarcinoma (TCGA, PanCancer Atlas)	585
Pancreatic Adenocarcinoma (TCGA, PanCancer Atlas)	184
Pheochromocytoma and Paraganglioma (TCGA, PanCancer Atlas)	178
Prostate Adenocarcinoma (TCGA, PanCancer Atlas)	494
Sarcoma (TCGA, PanCancer Atlas)	255
Skin Cutaneous Melanoma (TCGA, PanCancer Atlas)	448
Stomach Adenocarcinoma (TCGA, PanCancer Atlas)	440
Testicular Germ Cell Tumors (TCGA, PanCancer Atlas)	149
Thymoma (TCGA, PanCancer Atlas)	123
Thyroid Carcinoma (TCGA, PanCancer Atlas)	500
Uterine Carcinosarcoma (TCGA, PanCancer Atlas)	57
Uterine Corpus Endometrial Carcinoma (TCGA, PanCancer Atlas)	529
Uveal Melanoma (TCGA, PanCancer Atlas)	80
Ampullary Carcinoma (Baylor College of Medicine, Cell Reports 2016)	160
Metastatic Melanoma (DFCI, Science 2015)	110
Non-Small Cell Lung Cancer (MSK, Cancer Cell 2018)	75
Metastatic Esophagogastric Cancer (MSKCC, Cancer Discovery 2017)	341

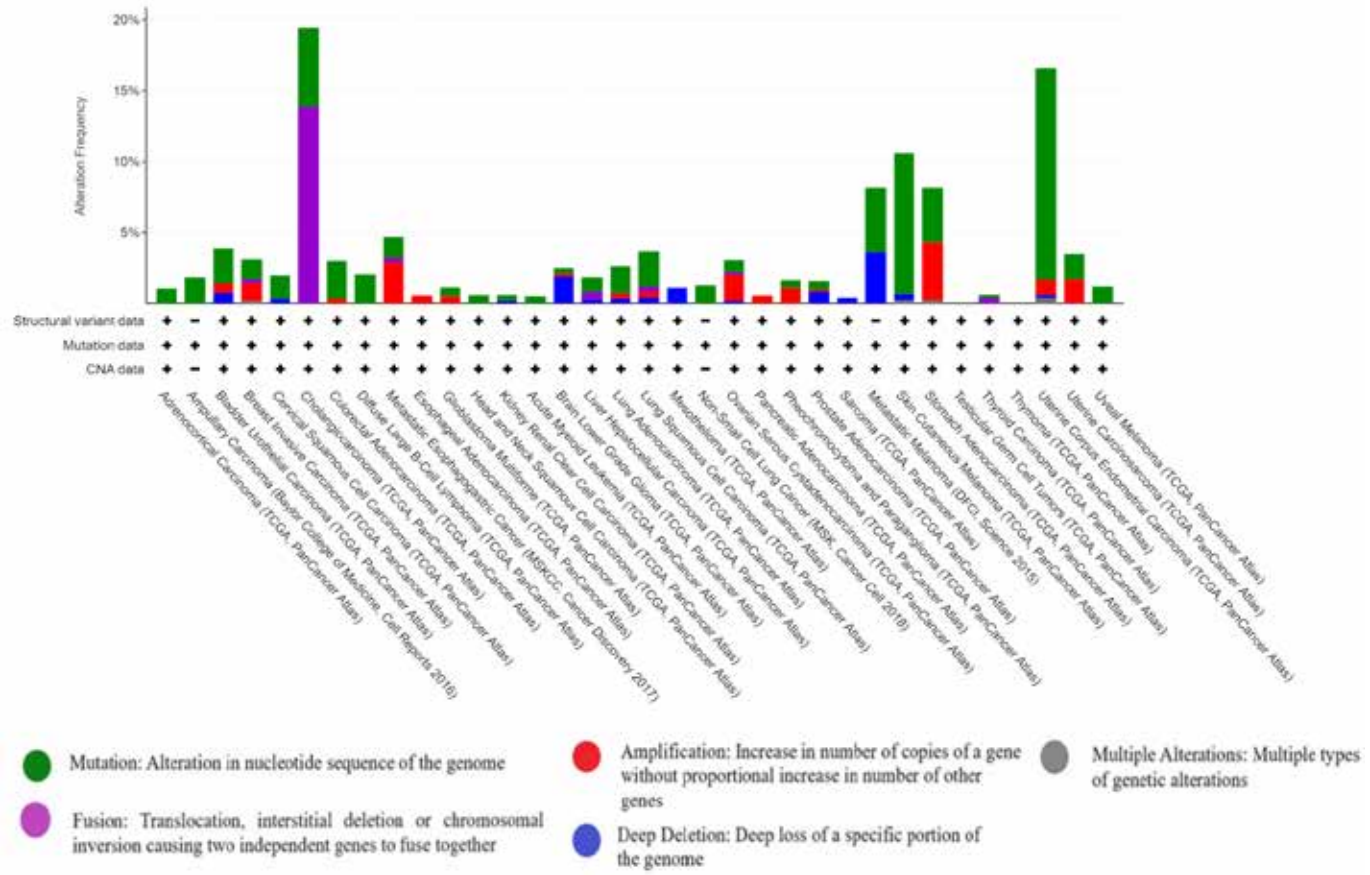

Figure 7. Alteration frequency in different types of cancer caused by *FGFR2* variants

cBioPortal presents the alteration frequencies of cancers. Among all types of cancers, Cholangiocarcinoma has the highest alteration frequency of 19.44%. In Cholangiocarcinoma's 19.44% alteration frequency, Fusion has a frequency of 13.89% and mutation's frequency is 5.56%. Uterine Corpus Endometrial Carcinoma has second highest alteration frequency of 16.64%, and Skin Cutaneous Melanoma has the third highest alteration frequency of 10.59%. In Uterine Corpus Endometrial Carcinoma's 16.64% alteration frequency, mutation accounts for 14.93%, amplification accounts for 1.13%, deep deletion accounts for 0.19%, and multiple alteration accounts for 0.38%. For Skin Cutaneous Melanoma's 10.59% frequency, mutation has 9.91%, deep deletion has 0.45%, and multiple alterations has 0.23% (Figure 7).

3.7 *FGFR2* gene expression across different cancers

UALCAN provides analysis of gene expression across different cancers using cancer studies from TCGA. The comparisons between normal FGFR2 varies across all the cancers. Out of 24 types of cancers, 19 types have *FGFR2* gene expression lower than normal, indicating for loss of function mutation in *FGFR2*. Interestingly, Cholangiocarcinoma, the type of cancer with highest genetic alteration frequency, has *FGFR2* gene expression higher than normal. This implies that gain of function mutations causes Cholangiocarcinoma (Figure 8) [39, 40].

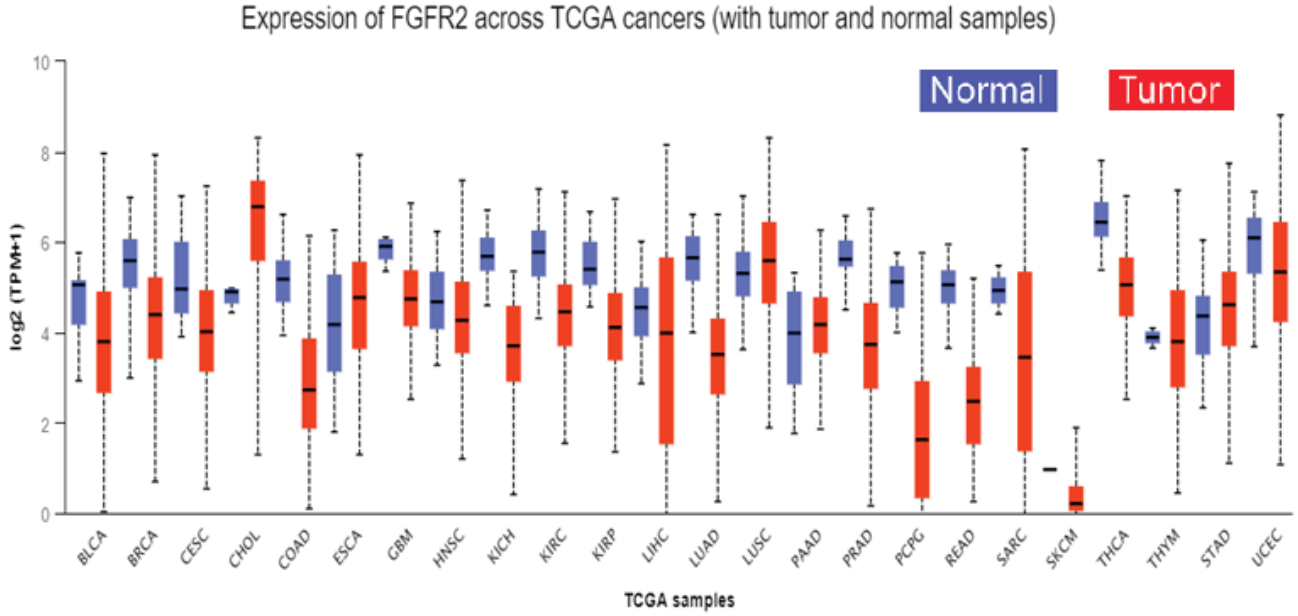

Figure 8. FGFR2 gene expression across normal samples and tumor samples

3.8 FGFR2 mutations pathogenicity prediction

In order to predict frequent *FGFR2* somatic mutations' pathogenicity, we analyzed mutation data from the National Cancer Institute Genomic Data Commons (GDC). GDC stores genomic and clinical data information from patients with cancer, and the aim of this system is to allow public access to genomic data [41].

The Sorting Intolerant from Tolerant (SIFT) is an algorithm that is able to predict the effects of genetic variations on proteins. It can help users to identify whether genetic variants are disease-causing or tolerated. The underlying theory behind the SIFT algorithm is that evolutionary conserved regions are less tolerant to genetic variants. SIFT examines the composition of amino acids and calculates the SIFT score, which indicates the normalized probability of observing amino acid changes at the position. SIFT scores range from 0 to 1. Variants with score less than 0.05 are deleterious (disease-

causing), while variants with score greater or equal to 0.05 are tolerated (benign) [42].

We extracted *FGFR2* exonic mutation data and utilized SIFT to predict the pathogenicity of common mutations (Figure 9).

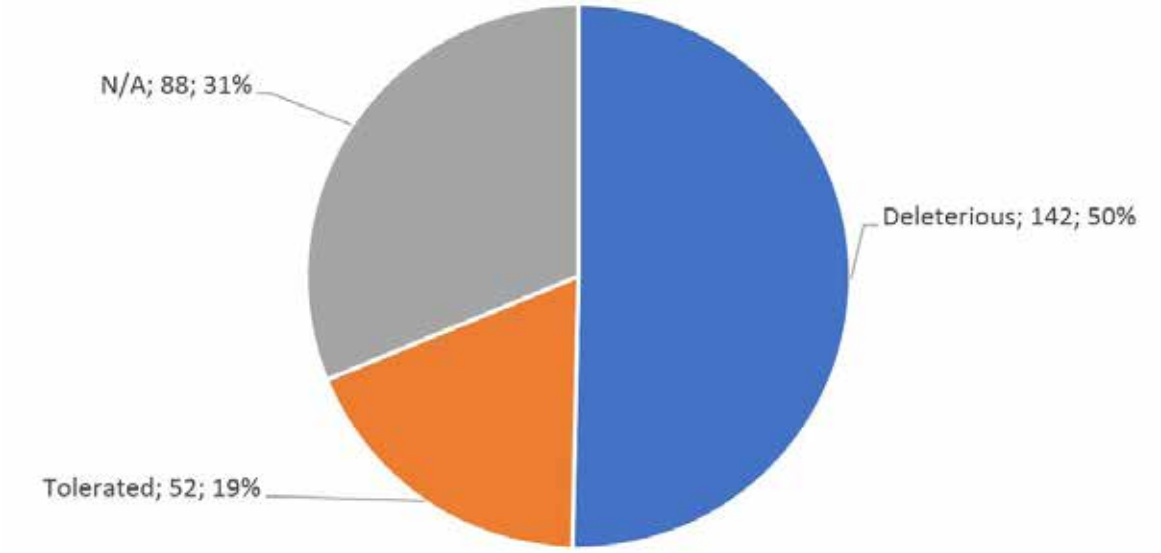

Figure 9. Prediction of effects of FGFR2 exonic mutations. Among a total of 282 most frequent exonic mutations, 50% (142/282) are deleterious, 19% (52/282) are tolerated

4. Discussion

The FGF/FGFR2 signaling pathway is essential to bone development and homeostasis, and mutations in *FGFR2* would lead to unregulated FGF signaling and premature suture closure. Besides from CS and JWS, other types of Craniosynostosis syndromes, such as Apert Syndrome, Pfeiffer Syndrome, and Seathre-Chotzen-like Syndrome, are all caused by *FGFR2* genetic mutations [43]. Currently, the only treatment for Craniosynostosis Syndrome is surgery in the first year of life, which expands the intercranial volume to prevent the buildup of pressure on the brain, and restores the cosmetic appearance [44].

Mutation in *FGFR2* gene increases the binding affinity with FGF ligands and enhances the downstream signaling, leading to premature suture fusion. Therefore, it would be promising to to inhibit the downstream signaling pathway RAS/RAF/MAPK to prevent cells from proliferate prematurely and minimize the phenotypes of CS and JWS. However, these signaling pathways are significant to human growth in other aspects including mitosis and meiosis [45]. Inhibiting the downstream signaling pathway might bring various potential risks, so it is important to consider other treatment methods for the diseases. For Crouzon Syndrome and Jackson-Weiss Syndrome, gene therapy can be a potential treatment as normal versions of *FGFR2* gene can be introduced into cells containing faulty *FGFR2* gene.

This *FGFR2* gene research provides an analysis of all genetic variations in human *FGFR2* exome. To our knowledge, research regarding all the genetic variations in human *FGFR2* has not been yet reported. Among all 947 exonic variations, nonsynonymous SNV and Synonymous SNV accounts for respectively 60% and 34% of all types of variations. Considering numbers of variations reported and length of different exons, exon 7 of transcript ENST00000358487 has the highest variation density of 0.43, followed by exon 8 in the same transcript with variation frequency of 0.41. We found that a specific nonsynonymous SNV, rs755793, has its variation frequency distinctively different human populations. Its variation frequency in African population is 0.36, while in Southern Asian population,

the frequency is 0.002. We examined most frequent somatic mutations in *FGFR2* exome and predicted whether the variants are deleterious. According to the prediction, 50% of the frequent exonic mutations in *FGFR2* are deleterious, which increases individual's susceptibility to diseases. However, 31% of the total number of *FGFR2* mutations cannot be calculated to obtain SIFT scores because of missing information, so the SIFT prediction does not give a comprehensive analysis of all *FGFR2* mutations. Still, the SIFT prediction can show that at least half of the mutations in *FGFR2* are disease-causing and harmful to human bodies.

The current database contains genetic variations information from individuals that are not merely limited to CS or JWS patients, so the total data is not a perfect representation of patients with either of these two types of diseases. According to our current data, the only pathogenic genetic variations for CS are only found on exon 7, exon 8 and exon 12 of transcript ENST00000358487, and JWS pathogenic genetic variations are only reported on exon7 and exon 8 of the same transcript. Most of the variants causing CS and JWS overlap in exon 8, encoding for extracellular IgIII domain. In fact, a lot of phenotypes of these two diseases overlap as they are both types of Craniosynostosis syndromes. Interestingly, we found one synonymous SNV with the rsID of rs121918491 to be pathogenic to CS. One possible explanation of this is that although the variants do not cause amino acid changes, the substrate specificity of tRNA to the altered codons can affect the timing of translation, which then affect the folding of protein. As a result, phenotypes of proteins encoded might be influenced by synonymous SNV.

Gene therapy should target exon 8 of transcript ENST00000358487 to deal with CS and JWS, and CRISPR/Cas 9 can be a potential technique to perform gene editing for *FGFR2*. CRISPR/Cas 9 technique can be used to replace the faulty gene segments with healthy copies of the *FGFR2* gene. RNA editing is another promising treatment method for CS and JWS.

This *FGFR2* genetic variations research also contains analysis of different types of cancers caused by the variations. Mutations in *FGFR2* gene have often been related to multiple types of tumor progressions. According to visualizations and our analysis using cBioPortal, the most common types of cancers caused by *FGFR2* alterations is Cholangiocarcinoma. The visualization derived from analysis of 11305 patients and 11255 samples in a total of 34 studies shows that Cholangiocarcinoma has an alteration frequency of 19.44%. Most of the tumors can be caused by loss of function mutations, but the one with highest alteration frequency, Cholangiocarcinoma, is caused by gain of function mutations. Overexpression, which is initially caused by genetic translocations, of *FGFR2* fusion proteins leads to increased sensitivity to FGFR inhibitors [46]. Hromas and his colleagues did research on preventing the chromosomal translocations, and from the research they came up with the conclusion that poly-adenosine diphosphate ribose polymerase 1 (PARP1) inhibitors can prevent the formation of chromosomal translocations [47]. It would be promising to run experiment method of using PARP1 inhibitors to treat Cholangiocarcinoma caused by *FGFR2* mutations.

5. Conclusion

In conclusion, to our knowledge, this is the first systematic analysis of all exonic variants in *FGFR2*, so the study provides important information for people to understand this gene. This study shows that nonsynonymous SNV is the most frequent variant as it accounts for 60% of all 947 exonic variants. Exon 7 has the highest variation density of 0.43. Most of the variants that are pathogenic to CS and JWS are in exon 7 and exon 8. Exon 7 and exon 8 encode for IgIII and the space between IgII and IgIII, and these regions directly bind with the FGF ligands. The study also suggests that *FGFR2* variants are associated with certain types of cancers, and possible treatment methods were discussed.

Reference:

1. Houssaint E., Blanquet P.R., Champion-Arnaud P., Gesnel M.C., Torriglia A., Courtois Y. & Breathnach R. Related fibroblast growth factor receptor genes exist in the human genome. Proceedings of the National Academy of Sciences of the United States of America, – 87(20). 1990. – P. 8180–8184.
2. Samatha Y., Vardhan T.H., Kiran A.R., Sankar A.J. & Ramakrishna B. Familial Crouzon syndrome. Contemporary clinical dentistry, – 1(4). 2010. – P. 277–280.
3. Gupta S., Prasad A., Sinha U., Singh R. & Gupta G. Crouzon Syndrome in a Ten-week-old Infant: A Case Report. Saudi journal of medicine & medical sciences, – 8(2). 2020. – P. 146–150.
4. Graul-Neumann L.M., Klopocki E., Adolphs N., Mensah M.A. & Kress W. Mutation c.943G>T (p. Ala315Ser) in FGFR2 Causing a Mild Phenotype of Crouzon Craniofacial Dysostosis in a Three-Generation Family. Molecular syndromology, – 8(2). 2017. – P. 93–97.
5. Van Herwerden L., Rose C.S., Reardon W., Brueton L.A., Weissenbach J., Malcolm S. & Winter R.M. Evidence for locus heterogeneity in acrocephalosyndactyly: a refined localization for the Saethre-Chotzen syndrome locus on distal chromosome 7 p- and exclusion of Jackson-Weiss syndrome from craniosynostosis loci on 7 p and 5q. American journal of human genetics, – 54(4). 1994. – P. 669–674.
6. Wilkie A.O. Craniosynostosis: Genes and mechanisms. Hum Mol Genet. – 6. 1997. – P. 1647–1656. Doi: 10.1093/hmg/6.10.1647.
7. USCS Genome Browser, Homo sapiens fibroblast growth factor receptor 2 (FGFR2), transcript variant 1, mRNA; July 2020. Available from: URL: https://genome.ucsc.edu/cgi-bin/hgGateway
8. The UniProt Consortium, UniProt: a worldwide hub of protein knowledge. Nucleic Acids Res. 47: D506-515. FGFR2 Human, 2019. Available from: URL: https://www.uniprot.org/.
9. Nucleotide. Bethesda: National Library of Medicine, National Center for Biotechnology Information; Accession No. NM_000141.5. Homo sapiens fibroblast growth factor receptor 2 (FGFR2), transcript variant 1, mRNA; July, 2020. Available from: URL: https://www.ncbi.nlm.nih.gov/nuccore/NM_000141.
10. Gene. Bethesda: National Library of Medicine, National Center for Biotechnology Information; July, 2020. Available from: URL: https://www.ncbi.nlm.nih.gov/gene/2263.
11. Al-Namnam N.M., Hariri F., Thong M.K. & Rahman Z.A. Crouzon syndrome: Genetic and intervention review. Journal of oral biology and craniofacial research, – 9(1). 2019. – P. 37–39.
12. Lin Y., Ai S., Chen C., Liu X., Luo L., Ye S., Liang X., Zhu Y., Yang H. & Liu Y. Ala344Pro mutation in the FGFR2 gene and related clinical findings in one Chinese family with Crouzon syndrome. Molecular vision, – 18. 2012. – P. 1278–1282.
13. Lin Y., Liang X., Ai S., Chen C., Liu X., Luo L., Ye S., Li B., Liu Y. & Yang H. FGFR2 molecular analysis and related clinical findings in one Chinese family with Crouzon syndrome. Molecular vision, – 18. 2012. – P. 449–454.
14. Oldridge M., Lunt P.W., Zackai E.H., McDonald-McGinn D.M., Muenke M., Moloney D.M., Twigg S.R., Heath J.K., Howard T.D., Hoganson G. Genotype-phenotype correlation for nucleotide substitutions in the IgII-IgIII linker of FGFR2. Hum Mol Genet. – 6. 1997. – P. 137–143.
15. dbSNP. 2020. Available from: URL:https://www.ncbi.nlm.nih.gov/snp/.
16. Sherry S.T., Ward M.H., Kholodov M., Baker J., Phan L., Smigielski E.M. & Sirotkin K. dbSNP: the NCBI database of genetic variation. Nucleic acids research, – 29(1). 2001. – P. 308–311.
17. Lab W.G. wANNOVAR. 2021. Available from: URL:http://wannovar.wglab.org/.

18. Chandran U.R., Medvedeva O.P., Barmada M.M., Blood P.D., Chakka A., Luthra S., Ferreira A., Wong K.F., Lee A.V., Zhang Z., Budden R., Scott J.R., Berndt A., Berg J.M. & Jacobson R.S. TCGA Expedition: A Data Acquisition and Management System for TCGA Data. PloS one, – 11(10). 2016. – e0165395.
19. Buechner P., Hinderer M., Unberath P., Metzger P., Boeker M., Acker T., Haller F., Mack E., Nowak D., Paret C., Schanze D., von Bubnoff N., Wagner S., Busch H., Boerries M. & Christoph J. Requirements Analysis and Specification for a Molecular Tumor Board Platform Based on cBioPortal. Diagnostics (Basel, Switzerland), – 10(2). 2020. – 93 p.
20. Gao J., Aksoy B.A., Dogrusoz U., Dresdner G., Gross B., Sumer S.O., Sun Y., Jacobsen A., Sinha R., Larsson E., Cerami E., Sander C. & Schultz N. Integrative analysis of complex cancer genomics and clinical profiles using the cBioPortal. Science signaling, – 6(269). 2013. – l1 p.
21. Chandrashekar D.S., Bashel B., Balasubramanya S., Creighton C.J., Ponce-Rodriguez I., Chakravarthi B. & Varambally S. UALCAN: A Portal for Facilitating Tumor Subgroup Gene Expression and Survival Analyses. Neoplasia (New York, N.Y.), – 19(8). 2017. – P. 649–658.
22. Herrero J., Muffato M., Beal K., Fitzgerald S., Gordon L., Pignatelli M., Vilella A.J., Searle S.M., Amode R., Brent S., Spooner W., Kulesha E., Yates A. & Flicek P. Ensembl comparative genomics resources. Database: the journal of biological databases and curation, 2016. bav096.
23. Institute, E.M.B.L.s.E.B. FGFR2 ENSR00000358487 Transcripts. July 2020. Available from: URL: https://asia.ensembl.org/Homo_sapiens/Gene/Summary?db=core;g=ENSG00000066468;r=10:121479072-121598458;t=ENST00000358487.
24. Ornitz D.M. & Marie P.J. Fibroblast growth factor signaling in skeletal development and disease. Genes & development, – 29(14). 2015. – P. 1463–1486.
25. Seto M.L., Hing A.V., Chang J., Hu M., Kapp-Simon K.A., Patel P.K. et al. Isolated sagittal and coronal craniosynostosis associated with TWIST box mutations. Am J Med Genet Part A. – 143(7). 2007. – P. 678–86.
26. Lei H., Deng C-X. Fibroblast growth factor receptor 2 signaling in breast cancer. Int J Biol Sci. In press.
27. Robin N.H. FGFR-Related Craniosynostosis Syndromes. Gene Reviews. 2007. – P. 1–30.
28. Azoury S.C., Reddy S., Shukla V. & Deng C.X. Fibroblast Growth Factor Receptor 2 (FGFR2) Mutation Related Syndromic Craniosynostosis. International journal of biological sciences, – 13(12). 2017. – P. 1479–1488.
29. Notari D.L., Molin A., Davanzo V., Picolotto D., Ribeiro H.G. & Silva S. IntergenicDB: a database for intergenic sequences. Bioinformation, – 10(6). 2014. – P. 381–383.
30. Li Q. & Wang K. InterVar: Clinical Interpretation of Genetic Variants by the 2015 ACMG-AMP Guidelines. American journal of human genetics, – 100(2). 2017. – P. 267–280.
31. Landrum M.J., Chitipiralla S., Brown G.R., Chen C., Gu B., Hart J., Hoffman D., Jang W., Kaur K., Liu C., Lyoshin V., Maddipatla Z., Maiti R., Mitchell J., O'Leary N., Riley G. R., Shi W., Zhou G., Schneider V., Maglott D., … Kattman B.L. ClinVar: improvements to accessing data. Nucleic acids research, – 48(D1). 2020. – P. D835–D844.
32. Forbes S.A., Bhamra G., Bamford S., Dawson E., Kok C., Clements J., Menzies A., Teague J.W., Futreal P.A. & Stratton M.R. The Catalogue of Somatic Mutations in Cancer (COSMIC). Current protocols in human genetics, Chapter – 10. Unit–10.11. 2008.
33. van Rooij J., Arp P., Broer L., Verlouw J., van Rooij F., Kraaij R., Uitterlinden, A. & Verkerk A. Reduced penetrance of pathogenic ACMG variants in a deeply phenotyped cohort study and evaluation of Clin-

Var classification over time. Genetics in medicine: official journal of the American College of Medical Genetics, – 22(11). 2020. – P. 1812–1820.
34. Altshuler D.L., et al. A map of human genome variation from population-scale sequencing. Nature.
35. Belsare S., Levy-Sakin M., Mostovoy Y. et al. Evaluating the quality of the 1000 genomes project data. BMC Genomics – 20. 2019. – P. 620.
36. Szybowska P., Kostas M., Wesche J., Wiedlocha A. & Haugsten E.M. Cancer Mutations in FGFR2 Prevent a Negative Feedback Loop Mediated by the ERK1/2 Pathway. Cells, – 8(6). 2019. – 518 p.
37. Cerami et al. The cBio Cancer Genomics Portal: An Open Platform for Exploring Multidimensional Cancer Genomics Data. Cancer Discovery. May, – 2. 2012. – 401 p.
38. cBioPortal for Cancer Genomics. 2021. Available from: URL: https://www.cbioportal.org.
39. Chandrashekar D.S., Bashel B., Balasubramanya S., Creighton C.J., Ponce-Rodriguez I., Chakravarthi B. & Varambally S. UALCAN: A Portal for Facilitating Tumor Subgroup Gene Expression and Survival Analyses. Neoplasia (New York, N.Y.), – 19(8). 2017. – P. 649–658.
40. UALCAN. 2021. Available from: URL:http://ualcan.path.uab.edu/.
41. Jensen M.A., Ferretti V., Grossman R.L. & Staudt L.M. (). The NCI Genomic Data Commons as an engine for precision medicine. Blood, – 130(4). 2017. – P. 453–459.
42. Sim N.L., Kumar P., Hu J., Henikoff S., Schneider G. & Ng P.C. SIFT web server: predicting effects of amino acid substitutions on proteins. Nucleic acids research, 40(Web Server issue), 2012. – W452–W457.
43. Agochukwu N.B., Solomon B.D. & Muenke M. Impact of genetics on the diagnosis and clinical management of syndromic craniosynostoses. Child's nervous system: ChNS: official journal of the International Society for Pediatric Neurosurgery, – 28(9). 2012. – P. 1447–1463.
44. Lattanzi W., Barba M., Di Pietro L. & Boyadjiev S.A. Genetic advances in craniosynostosis. American journal of medical genetics. Part A, – 173(5). 2017. – P. 1406–1429.
45. Kalous J., Tetkova A., Kubelka M. & Susor A. Importance of ERK1/2 in Regulation of Protein Translation during Oocyte Meiosis. International journal of molecular sciences, – 19(3). 2018. – 698 p.
46. Wang J., Xing X., Li Q., Zhang G., Wang T., Pan H. & Li D. Targeting the FGFR signaling pathway in cholangiocarcinoma: promise or delusion? Therapeutic advances in medical oncology, – 12. 2020. 1758835920940948.
47. Hromas R., Williamson E., Lee S. H. & Nickoloff J. Preventing The Chromosomal Translocations That Cause Cancer. Transactions of the American Clinical and Climatological Association, – 127. 2016. – P. 176–195.

Section 4. Physiology

https://doi.org/10.29013/ELBLS-21-4-69-73

Dr. Pano Genti,
Faculty of Rehabilitation Sciences,
Department of Biomedical and Human Disciplines,
Sports University of Tirana, Albania
E-mail: gpano@ust.edu.al

Prof. Assoc. Arben Kaçurri
Sport Sciences Research Institute,
Department of Physical Activity and Health,
Sports University of Tirana, Albania
E-mail: akacurri@ust.edu.al

EVALUATION OF BODY POSTURE IN FEMALE ALBANIAN NATIONAL VOLLEYBALL TEAM

Abstract. In many sports, including team games, disproportional body mass and muscle strength, spine statics disorders and/or trunk asymmetries are often noted; these may result from non-uniform loads applied to the spine and/or sport-specific unilateral muscle work [1–3].

The aim of this paper was to evaluate body posture in male and female Albanian national volleyball players and compare them between each other. 19 males and 13 female national team volleyball players aged 18–32 years. Zebris System software Win Spine 2.3 was used to examine the body posture. Posture analysis in upright standing sagittal projection, upright standing frontal projection and upright standing transversal projection showed postural asymmetries. Overhead athletes as volleyball players need adequate range of motion to obtain high enough velocity to hit the ball and a good posture plays an important role but it needs a lot of practice and awareness to obtain. Further studies need to be conducted in all group ages teams, focusing in the prevention of postural problems which are specific for this game. Also, coaches, physical therapists, physio-therapists have an important role in the improvement of training specific exercises aiming in the prevention of overall postural problems in volleyball players.

Keywords: Body posture, Female, Volleyball players.

Introduction

In many sports, including team games, disproportional body mass and muscle strength, spine statics disorders and/or trunk asymmetries are often noted; these may result from non-uniform loads applied to the spine and/or sport-specific unilateral muscle work [1–3]. Asymmetric tilt and shift patterns in the shoulder girdle cause muscle imbalance and weakness, thus increasing the risk of shoulder injuries [4], which might, in turn, contribute to

spine asymmetry. Postural status is the result of earlier growth and development, but also of dominant physical activity or a sport and individual practices [5]. According to Zetou et al. [6], athletes who have had a previous history of pain or shoulder injury are more likely to have a postural position where the shoulders have come forward, thus increasing the probability of their injury. Volleyball players playing the position of the striker has resulted in a high risk for shoulder pain and in most have a postural position where the shoulders have come forward [6]. Sports that apply specific body positions, such as apologists, rowing, weightlifting, gymnastics or figure skating, cause major spinal overload, which affects the shape of the vertebral column, increases the risk of musculoskeletal disorders and hinders development [7]. Articulation mobility disorder in undamaged volleyball players is muscle imbalance, defined by Janda [8] as shortness or weakness in muscle function. The relatively high incidence of muscle imbalance in young volleyball athletes has been confirmed by Voralek [9]. The most frequent incidence of contactless injuries is caused by undue landing or fall after a dance. Females are more prone to injury compared to males because they have weaker m. quadriceps and hamstring, related to a greater lack of proprioceptive abilities and cinematics or biomechanics of landing or decline [10; 11].

Objectives

The aim of this paper was to evaluate body posture in female Albanian national volleyball team.

Methods

13 female of Albanian national team volleyball players aged 18–32 years undergone anthropometrical measurements (height, weight, BMI) and posture analysis using "Zebris WinSpine Pointer 2.3". Cobb Angle" was used to classify scoliosis, both in the anterior and posterior plan [12]. The classification and evaluation defined by the researcher Mejia [13], was used for the kyphosis classification, and for lordosis was used the classification from Tuzun [14].

Results

Table 1.– Anthropometric measurement results

Nr	Weight (kg)	Height (cm)	BMI
1	53	165	19.5
2	48	164	17.8
3	53	170	18.3
4	64	173	21.4
5	69	168	24.4
6	57	158	22.8
7	70	174	23.1
8	88	188	24.9
9	64	173	21.4
10	53	170	24.5
11	48	165	19.5
12	53	164	17.8
13	64	170	18.3
Mean	**62.8**	**170**	**21.5**

The results of BMI = Weight (kg)/length m^2 show that the subjects on average have a normal BMI.

Table 2.– Upright standing, Sagittal Projection results

Nr	Total Length (mm)	Thoracic length (mm)	Lumbar length (mm)	Pelvic torsion°
1	496	295	148	3.5
2	424	180	180	5.5
3	502	283	161	12.5
4	509	282	167	4.5
5	452	301	11	0.4
6	498	201	153	3.2
7	491	277	158	6.9
8	473	324	110	3.6
9	459	282	130	3.5
10	515	291	166	5.7
11	470	275	143	3
12	461	270	141	3.8
13	482	277	151	1.4
Mean	**479.38**	**272.15**	**139.92**	**4.42**

The results of the Upright standing, Sagittal Projection averages show a pelvic torsion average result in normal ranges, "4.42°".

Table 3.– Upright standing, Sagittal Projection results

Nr	Thoracal kyphosis°	Lumbar lordosis°	Total trunk arch°	Sacral angle°
1	43.4	13.5	3	7.1
2	55.3	3.7	5.4	1.1
3	62	21.7	0.5	2.4
4	49.3	33.9	6.2	24.8
5	53.2	29.2	4.5	14.5
6	41	7.5	0.4	
7	56.4		1.1	38.9
8	52.1	37.6	2	17.5
9	45.4	28.5	1.3	
10	51.8	45.3	4.8	32.4
11	48.4	24	1	11
12	38.3	15.4	0.6	2.4
13	67.6		6.5	40.2
Mean	**51.09**	**23.6**	**2.8**	**17.4**

Results of the Upright standing position in the Sagittal Projection, show an average of 51.09° in the thoracal part (Thoracal kyphosis).

Table 4.– Upright standing, Frontal Projection results

Nr	Pelvis Obliquity	Pelvic/Shoulder Obliquity°	Right Scapula distance (mm)	Left Scapula distance (mm)	Scapula distance difference (mm)
1	***2***	***3***	***4***	***5***	***6***
1	1.6	0.1	52	57	5
2	1.6	1.6	78	78	0
3	0	0.4	76	63	12
4	2.2	1.5	64	63	1
5	0.7	0.4	58	47	10
6	3.4	1.7	63	66	2
7	0.2	2.5	61	68	7
8	0.5	3	61	78	17
9	1	0.5	61	69	8
10	2.5	1.7	50	37	13
11	1	1.3	46	50	3
12	1.8	2	54	44	9
13	4.2	2	51	63	12
Mean	**1.59**	**1.43**	**59.61**	**60.23**	**7.61**

Table 5.— Upright standing, Transversal Projection results

Nr	Pelvis/Shoulder Rotation°
1	0.8
2	4.3
3	10.6
4	2
5	1.1
6	1.7
7	1.8
8	7
9	3.3
10	0.1
11	1.8
12	5
13	5.6
Mean	**3.46**

The results of the study in terms of general posture assessment give a normal situation without many differences or deviations of the vertebral column in all its segments. Posture analysis in upright standing sagittal projection, upright standing frontal projection and upright standing transversal projection did not show any significant postural problems. A slight non-significant lumbar lordosis thoracic kyphosis was observed. Also, all subjects had a tendency of shoulder rotation especially in the playing arm.

Discussion

Overhead athletes as volleyball players need adequate range of motion to obtain high enough velocity to hit the ball and a good posture plays an important role but it needs a lot of practice and awareness to

obtain. It requires adequate amount of mobility and stability to be able to achieve ideal posture. Also, unilateral asymmetries due to unilateral training loads and progressing thoracic curves urge a specific intervention training including functional training and core training exercises especially in younger adolescent female but also male volleyball players.

Conclusions

Further studies need to be conducted in all group ages teams, focusing in the prevention of postural problems and aiming the improvement of overall training specifics postural exercises in order for the players to use them throughout their sports careers. It would also be very positive for these types of studies to be extended in time and systematically with the aim of creating a database for all children, young people and adults who practice volleyball sport. Also, coaches, physical therapists, physio-therapists have an important role in the improvement of training specific exercises aiming in the prevention of overall postural problems in volleyball players.

It would be of great value if all volleyball coaches, especially those who deal with age groups, had information about different types of postural training exercises and including it in their training programs with the aim of preventing and improving physical and functional parameters including posture problems.

References:

1. Barczyk K., Skolimowski T., Hawrylak A., Biec E. Sagittal spinal configuration in persons practicing selected sport disciplines (Engl. abstr.). Pol. J. Sports Med.– 21. 2005.– P. 395–400.
2. Hawrylak A., Skolimowski T., Barczyk K., Biec E. Assymetry of trunk in athletes of different kind of sport. (Engl. abstr.) Pol.J.Sports Med.,– 17. 2001.– P. 232–235.
3. Starosta W. Ksztalt kr^goslupa z punktu widzenia motoryki czlowieka i motoryki sportowej. (Engl. abstr.) Po-stqpy Rehabilitacji,– 7. 1993.– P. 19–32.
4. Wang H. K., Cochrane T. Mobility impairment, muscle imbalance, muscle weakness, scapular asymmetry and shoulder injury in elite volleyball athletes. J Sport Med Phys Fit.– 41. 2001.– P. 403–410.
5. Shumway-Cook A., Woollacott M. Attentional demands and postural control: the effect of sensory context. J Gerontol a Biol Sci Med Sci,– 55. 2000.– M10–6.
6. Zetou E., Malliou P., Lola A., Tsigganos G. & Godolias G. Factors related to the incidence of injuries' appearance to volleyball players. Journal of Back and Musculoskeletal Rehabilitation,– 19(4). 2006.– P. 129–134. URL: https://doi.org/10.3233/BMR-2006–19404
7. Baranto A., Hellström M., Cederlund C., Nyman R., Sward L. Back pain and MRI changes in the thoracolumbar spine of top athletes in four different sports: a 15-year follow-up study. Knee Surg Sports Traumatol Arthrosc.– 17. 2009.– P. 1125–1134. URL: https://doi.org/10.1007/s00167–009–0767–3
8. Janda V. Muscle Function Testing, London, Butterworths, 1983.
9. Voralek R., Süss V., Parkanova M. Poruchy pohybového aparátu a svalové dysbalance u hráček volejbalu ve věku 15–19 let (The locomotion disorders and muscular disbalance in volleyball players aged 15–19 years). Rehabilitacia,– 44(1). 2007.– P. 14–21.
10. Bahr R., Bahr I. A. Incidence of acute volleyball injuries: a prospective cohort study of injury mechanisms and risk factors. Scand J Med Sci Sports,– 7. 1997.– P. 166–171. [Medline] [CrossRef]. URL: https://doi.org/10.1111/j.1600–0838.1997.tb00134.x
11. Renstrom P., Ljungqvist A., Arendt E., et al. Non-contact ACL injuries in female athletes: an International Olympic Committee current concepts statement. Br J Sports Med,– 42. 2008.– P. 394–412. [Medline] [CrossRef] URL: https://doi.org/10.1136/bjsm.2008.048934

12. Cobb J. R. Outline for the study of scoliosis. In: Instructional course lectures for the American Academy of Orthopaedic Surgeons,– Vol. 5. JW Edwards, Ann Arbor, 1948.– P. 261–275.
13. Mejia E. A., Hennrikus W. L., Schwend R. M., Emans J. B. A prospective evaluation of idiopathic left thoracic scoliosis with MRI. Journal of Pediatric Orthopedics.– 16. 1996.– P. 354–358. URL: https://doi.org/10.1097/00004694–199605000–00012
14. Tuzun C., Yorulmaz I., Cindas A., Vatan S. Low back pain and posture. Clinical Rheumatology – 18. 1999.– P. 308–312. URL: https://doi.org/10.1007/s100670050107

Contents